SEDIMENT YIELD MODELLING IN THE MZIMVUBU RIVER CATCHMENT

Report to the
WATER RESEARCH COMMISSION

by

JJ Le Roux, CH Barker
Department of Geography, University of the Free State

HL Weepener, EC Van den Berg & SN Pretorius
Agricultural Research Council – Institute for Soil, Climate and Water

WRC Report No. 2243/1/15
ISBN 978-1-4312-0667-4

April 2015

Obtainable from

Water Research Commission
Private Bag X03
Gezina, 0031

orders@wrc.org.za or download from www.wrc.org.za

EXECUTIVE SUMMARY

INTRODUCTION

The Department of Water and Sanitation is planning water resource development in the Mzimvubu River Catchment, which is on record the only large river network in South Africa without a dam. Recent soil erosion mapping and modelling studies, however, indicate that large parts of the catchment consist of highly erodible soils with widespread soil erosion evident. These studies, nonetheless, provide no information about where material moves to or about the sediment yield because a significant part of the eroded soil will deposit again before reaching a river channel or catchment outlet. The mean total sediment produced in a catchment usually differs from sediment yield at a catchment outlet, depending on the complex spatial configuration of topographical variables and land use-cover interactions. Furthermore, most regional studies across the globe emphasize the sheet and rill aspects of the erosion cycle, but few map and/or model gully erosion at large spatial scales. Modelling the sediment yield contribution from gully erosion at a large catchment scale has not been performed in South Africa. However, gully erosion processes cannot be disregarded in the Mzimvubu River Catchment because it will lead to the underestimation of soil losses in the catchment where gullies are prominent.

This study models the major soil erosion processes in the catchment, as well as the sediment yield contribution from sheet-rill and gully erosion for the whole study area. Understanding these processes will enable area-specific management intervention and erosion control measures that are currently planned for the future dam site at Ntabelanga on the Tsitsa River. Thus, the study will aid in the allocation of scarce conservation resources. In terms of outcomes and expected impacts, modelling the flow and sediment yield in the catchment makes it possible to estimate the dam life expectancy for the future dam (that could aid dam design). The study will furthermore describe methodology that can be applied and extended on data that are available for the entire country.

AIMS AND OBJECTIVES

The aim of the study is to assess the sediment yield contribution from sheet-rill and gully erosion in the Mzimvubu River Catchment. The aim will be achieved through meeting the following objectives:

- Model the sediment yield contribution from sheet and rill erosion using the Soil and Water Assessment Tool (SWAT) in a GIS;
- Model the sediment yield contribution from gully erosion using remote sensing and integrated GIS techniques.

Special attention will be given to the future dam site at Ntabelanga on the Tsitsa River, including the estimation of the dam’s life expectancy (without proper siltation prevention or design measures).

METHODOLOGY

In order to provide a comprehensive overview of sediment yield in the Mzimvubu River Catchment, two approaches were implemented. These include (1) Model the sediment yield contribution from sheet-rill erosion using ArcSWAT, a graphical user interface for SWAT and ArcMap® software, and (2) Modelling the sediment yield contribution from gully erosion using remote sensing techniques in an integrated GIS approach. The integrated GIS approach include gully digitizing, segmentation of SPOT 5 imagery, gully change detection, and developing a rule-based gully sediment yield model in a GIS. Both approaches were conducted over the same 5 year timeframe between 2007 and 2012 for which the most recent multi-temporal and high resolution imagery is available.

RESULTS AND DISCUSSION

Integration of the sheet-rill and gully results produced a total sediment yield map (shown in the figure below) of the Mzimvubu River Catchment, with an average of 5.0 t/ha·yr. In the Ntabelanga Dam Catchment the sediment yield range between 1 t/ha·yr upstream to 22.5 t/ha·yr at the future dam outlet. The annual average sediment output in the Ntabelanga Dam Catchment range between a quarter million t/yr upstream to nearly 10 million t/yr at the future dam outlet. Gully erosion feed massive amounts of sediment into the river network, contributing approximately 20 times more to the sediment output than sheet-rill erosion.

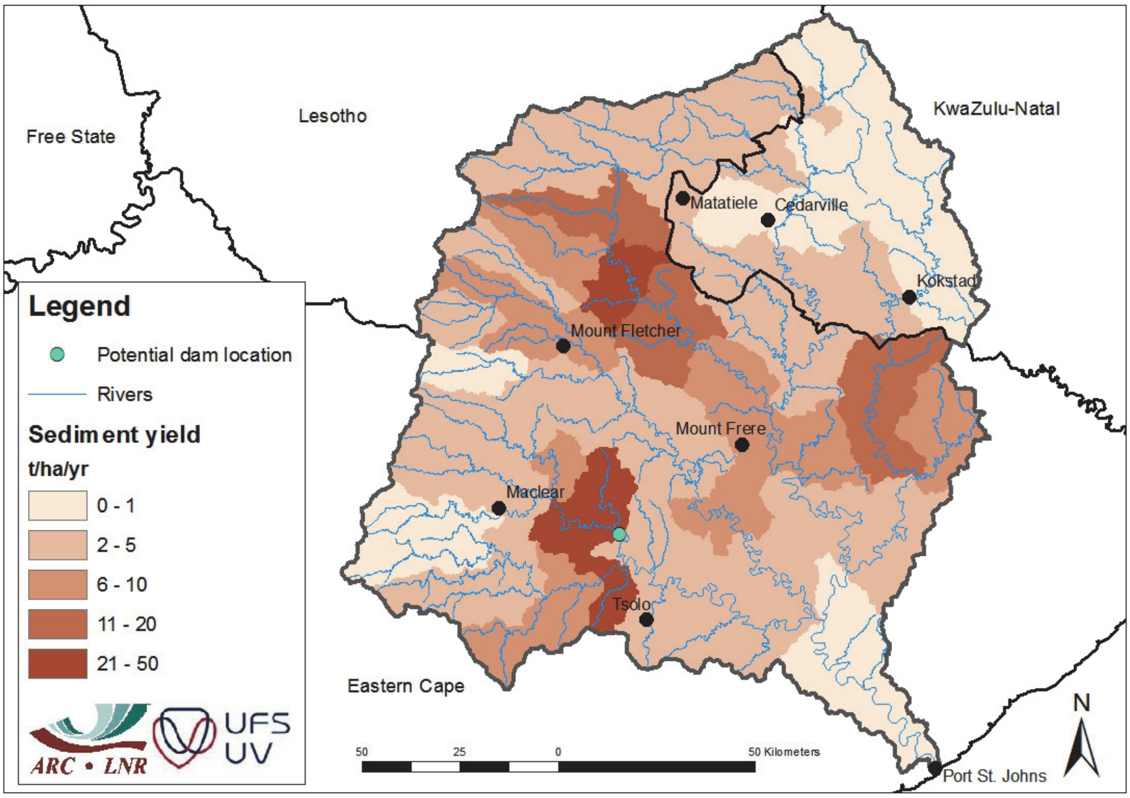

Total sediment yield map of the Mzimvubu River Catchment.

The sediment output and sediment yield contribution from sheet-rill erosion for sub-catchments in the Mzimvubu River Catchment is approximately 80,000 t/yr and 1.0 t/ha·yr respectively. The average sediment output and sediment yield contribution from sheet-rill erosion in the sub-catchment where the future dam will be built is approximately 50,000 t/yr and 0.1 t/ha·yr respectively. ArcSWAT utilizes the Modified USLE that models only sheet and rill processes and disregards gully erosion in the central part of the catchment. Thus, ArcSWAT underestimates soil losses and subsequent sediment yield in the Mzimvubu River Catchment where gullies are prominent.

Gullied areas increased substantially since 2007 with 37 out of the 52 sub-catchments having a positive active/non-active gully ratio. The sediment yield and sediment output contribution from gully erosion for sub-catchments in the Mzimvubu River Catchment is high, averaging approximately 5.0 t/ha·yr and 1 787 500 t/yr respectively. The average sediment output and sediment yield contribution from gully erosion in the sub-catchment where the future dam will be built is approximately 9.8 million t/yr and 22.4 t/ha·yr respectively.

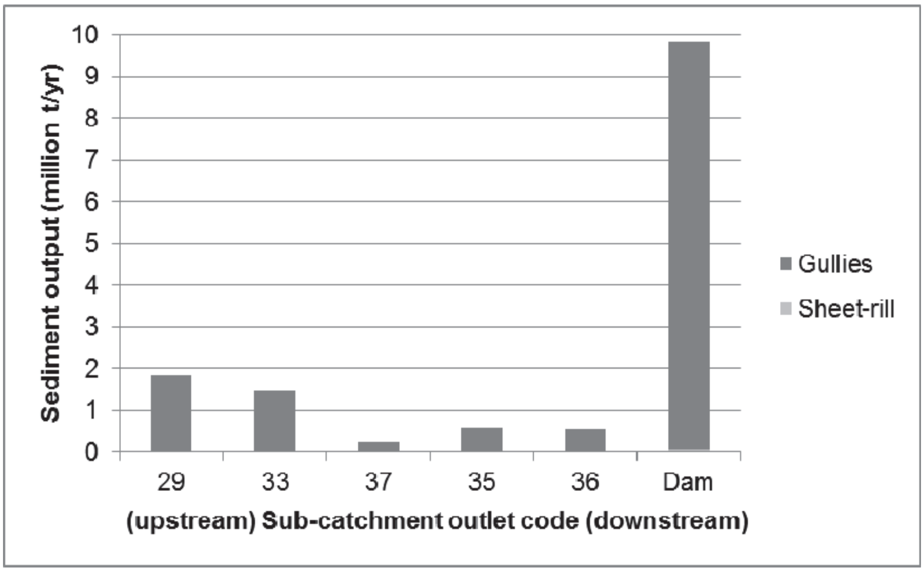

Total annual average sediment output at 6 sub-catchment outlets of the future dam catchment.

CONCLUSIONS

Although each sub-catchment has different processes and factors contributing to the sediment yield dynamics, gully erosion is the dominant process and sediment yield contributor in the Mzimvubu River Catchment. Based on sediment yield results and digital elevation data in a GIS, the life expectancy of the dam could be between 34 and 49 years without proper siltation prevention or design measures. The future dam at Ntabelanga could therefore experience a similar fate as the Welbedacht Dam near Dewetsdorp in the Free State where the storage capacity reduced by more than 80% in just twenty years after completion. However, the results should not be interpreted as absolute values. The fact that soil erosion is naturally highly variable needs to be recognized, as well as the fact that results will vary by altering certain parameters. Furthermore, the sediment yield and dam life expectancy is based on a 5 year timeframe between 2007 and 2012 for which the most recent multi-temporal and high resolution imagery is available. The sediment yield prior and after this timeframe remains uncertain. Nevertheless, modelling the flow and sediment yield in the catchment made it possible to identify major soil erosion processes and sediment generating areas. In terms of institutional development, the results developed in this study will be useful to the Department of Water and Sanitation, as well as the Department of Environmental Affairs. Understanding these processes and factors will enable area-specific management intervention and erosion control measures, and could aid in dam design. Results will also aid in area-specific rehabilitation of gullies and the allocation of scarce conservation resources.

RECOMMENDATIONS FOR FUTURE RESEARCH

To prevent siltation of the future dam at Ntabelanga, it is recommended to identify vegetated and/or gully-free areas susceptible to gully development. The main reason that susceptible areas need to be identified and protected is because it is not financially feasible to rehabilitate large gullies with expensive structures at a catchment scale. Since prevention is better than cure, area-specific management and erosion control measures will be needed to prevent sedimentation of the future dam. Therefore, the next step will be to identify or map/model areas that are intrinsically susceptible to erosion before being extrinsically triggered or accelerated by land use and human-induced reduction of the vegetation cover.

It is further recommended to assess by means of scenario analysis how much sediment will be yielded from the susceptible areas (currently gully-free) if gully development should take place. In future it will also be useful to determine the relative impact of different land use and management scenarios, as well as scenarios under climate change. It is often argued that climate change will increase future erosion rates, especially where increased rainfall intensity and/or extreme event frequency are predicted. However, certain land use changes causing a reduction in the vegetation cover are likely to have greater impact on the erosion risk than any likely climate change.

Before gully susceptible areas and scenario analysis can be achieved, it is recommended to first determine gully factor dominance including topographical variables, parent material-soils interactions, rainfall erosivity and cover management. The manner in which event driven processes influence sediment generation in the catchment needs to be researched. This study indicates that nearly 80% of the average annual streamflow and 85% of the annual sediment output contribution from sheet-rill erosion are concentrated in the rainy season. However, the manner in which event driven processes influence gully development and sediment generation still needs to be researched in the Mzimvubu River Catchment.

It is recommended to increase efforts of continuous long-term monitoring of discharge and sediment load in South Africa. There is a need for datasets comprising spatially distributed data of recorded flow and sedimentation, especially for calibration and validation. Nevertheless, this study remains useful as a comparative tool for planning. This study indicated that the proposed location for the Ntabelanga Dam is located in an area where sedimentation will be a huge risk. It is therefore important to take precautions such as the following:

- Design the dam in such a way that sediment will bypass the main dam;
- Include silt traps upstream of the dam;
- Manage catchment processes upstream of the dam to reduce erosion (this may include manage land use practices such as grazing, erect sediment fences below disturbed areas, establish vegetation communities to reduce runoff, create wetlands to reduce the speed of flow in drainage canals/rivers, rehabilitate eroded areas and gullies where possible – keeping in mind that the soils are susceptible to pipe forming and that the normal rehabilitation practices might not be sufficient/successful.
- Conduct a pilot study to find the best mitigation measures applicable to the larger area.

ACKNOWLEDGEMENTS

Thanks to the Water Research Commission (WRC) for funding the research project. Special thanks to Mr W Nomquphu at the WRC for managerial and administrative support, as well for his advice and sharing knowledge on the study area. The authors would like to also thank him for accompanying us in the field in November 2013. The project benefited greatly from advice given by the Reference Group including:

Ms T Germishuyse	Golder Associates Africa (Pty) Ltd
Dr N Njovanovic	Council for Scientific and Industrial Research
Prof PD Sumner	University of Pretoria
Dr GM Van Zijl	University of the Free State

Numerous colleagues at the Agricultural Research Council – Institute for Soil, Climate and Water (ARC-ISCW) have assisted the research efforts. Dr G Paterson gave valuable advice and assistance regarding soils in the area, and Mrs M Van der Walt assisted with the retrieval and interpretation of spatial soil data. Thanks to Mr R Tswai and to Mr P Beukes who assisted with the remote sensing part of the project. The authors would like to thank Mr J Malherbe for providing advice and climatic data required for application in the study. Editing of the final report by Dr TP Fyfield is very much appreciated.

TABLE OF CONTENTS

List of Figures

List of Tables

1. INTRODUCTION

The Department of Water and Sanitation is planning water resource development in the Mzimvubu River Catchment, which is on record the only large river network in South Africa without a dam (DWA, 2012). Development will include an irrigation dam and a smaller hydroelectric dam at Ntabelanga on the Tsitsa River. Recent soil erosion mapping and modelling studies, however, indicate that large parts of the uMzimvubu River Catchment, as well as the Tsitsa River Catchment consist of highly erodible soils with widespread soil erosion evident. Soil erosion not only involves the loss of fertile topsoil and reduction of soil productivity, but is also coupled with serious off-site impacts related to pollution and sedimentation due to suspended sediment concentrations in streams. For example, due to siltation, the storage capacity of the Welbedacht Dam near Dewetsdorp in the Free State reduced rapidly from the original 115 to approximately 16 million cubic metres within twenty years since completion in 1973 (DWA, 2011). The soil erosion/sedimentation problem may get worse in the future due to population growth and potential climatic changes.

The most recent erosion study produced a gully location map of SA by means of visual interpretation and vectorization from SPOT 5 satellite imagery acquired in 2007 (Mararakanye and Le Roux, 2012). Results indicate that over 18 000 gullies occur in the Mzimvubu River Catchment, directly affecting an area of approximately 22 600 ha. The gully mapping study was preceded by the production of a water erosion prediction map of SA by simplifying and interfacing the Universal Soil Loss Equation (USLE) into a GIS (Le Roux *et al*., 2008). From the USLE assessment it was found that one third (538 381 ha) of the Mzimvubu River Catchment is exposed to high erosion risk and that the average erosion rate predicted is excessive at 33 t/ha·yr with over 10 million t of soil eroding annually. These studies, nonetheless, provide no information about where material moves to or about the sediment yield because a significant part of the eroded soil will deposit again before reaching a river channel or catchment outlet. A third study worth mentioning is the revised sediment yield map of SA that was produced using latest reservoir sediment deposition data and mathematical modelling (Msadala *et al*., 2010). Results indicate that the Mzimvubu River Catchment consists of some of the highest sediment yielding areas in SA. Due to the absence of a dam with sediment deposition data, the study of Msadala *et al*. (2010), however, relies heavily on results from above-mentioned USLE assessment of Le Roux *et al*. (2008) that predicts the mean total sediment produced in a catchment.

The mean total sediment produced in a catchment usually differs from sediment yield at a catchment outlet, depending on the complex spatial configuration of topographical variables and land use-cover interactions (De Vente *et al*., 2007). Furthermore, the USLE assessment emphasizes the sheet and rill aspects of the erosion cycle but disregards gully erosion thus underestimating soil losses in catchments such as the Mzimvubu where gullies are prominent. It is therefore fair to say that none of the studies mentioned above provide sufficient information about the sediment yield dynamics in the Mzimvubu River Catchment.

At the catchment-scale, sediment dynamics are driven by complex physical processes that involve interaction of a large number of spatial and temporal factors that cannot be monitored directly (Bracken and Croke, 2007). Assessments in large catchments are usually carried out by means of a spatially-distributed sediment modelling approach by integrating 2D-routing of sediment fluxes in a GIS (Lenhart *et al*., 2005). Sediment yield models that are routinely coupled within a GIS offer unprecedented flexibility in the representation and organization of spatial data (Chen and Mackay, 2004). Furthermore, the advent of developments in remotely sensed data and digital elevation data offers considerable potential for improved sediment modelling.

The problem is most regional studies across the globe emphasize the sheet and rill aspects of the erosion cycle, but few map and/or model gully erosion at large spatial scales (e.g. Vrieling *et al*., 2007; Ndomba *et al*., 2009; Eustace *et al*., 2011; Le Roux and Sumner, 2012; Van Zijl *et al*., 2013). Perspectives on gully factors and sediment contribution have typically been obtained from field scale (<10-1 km^2) studies and are confined to local conditions (e.g. Grellier *et al*., 2012). Modelling the sediment yield contribution from gully erosion at a large catchment scale has not been achieved in South Africa. This study models the major soil erosion processes in the catchment including sheet-rill and gully erosion, as well as the sediment yield contribution from sheet-rill and gully erosion for the whole study area.

In terms of outcomes and expected impacts, modelling the flow and sediment yield in the catchment makes it possible to estimate the dam life expectancy for the future irrigation dam site at Ntabelanga on the Tsitsa River (that could aid dam design). The study also identifies major soil erosion processes and sediment generating areas, as well as the influence of different contributing factors. Understanding these processes and factors will enable area-specific management intervention and erosion control measures that are currently planned for the future dam catchment. For example, due to limited financial resources it will not be feasible to rehabilitate all gullies with expensive structures at the catchment scale, but it is imperative to minimize current expansion of active gullies with site-specific rehabilitation. Thus, the study will aid in the allocation of scarce conservation resources. Area-specific management and control measures will not only prevent soil loss within the catchment, but will also prevent sedimentation and increase the life span of the future dam. Sediment yield modelling also requires well-structured input and output datasets including information on a large number of spatial and temporal catchment processes. Such a database for the Mzimvubu River Catchment will provide a better understanding of catchment processes which is essential to prevent sedimentation and pollution of water resources. The study will furthermore describe methodology that can be applied and extended on data that are available for the entire country.

1.1 Aims and objectives

The aim of the study is to assess the sediment yield contribution from sheet-rill and gully erosion in the Mzimvubu River Catchment. The aim will be achieved through meeting the following objectives:

- Model the sediment yield contribution from sheet and rill erosion using the Soil and Water Assessment Tool (SWAT) in a GIS;
- Model the sediment yield contribution from gully erosion using remote sensing and integrated GIS techniques.

Both approaches will be conducted over the same 5 year timeframe between 2007 and 2012 for which the most recent multi-temporal and high resolution imagery is available. Special attention will be given to the future dam site at Ntabelanga on the Tsitsa River, including the estimation of the dam's life expectancy (without proper siltation prevention or design measures). Modelling the sediment yield contribution from gully erosion at a large catchment scale has not been achieved in South Africa, and few studies map and/or model gully erosion at large spatial scales. This study models the major soil erosion processes in the catchment including sheet-rill and gully erosion, as well as the sediment yield contribution from sheet-rill and gully erosion for the whole study area.

1.2 Project report outline

After the Introduction Section, Chapter 2 presents a literature review that outlines different soil erosion models followed by remote sensing techniques available for assessing soil erosion at a regional scale. Chapter 3 provides a site description of the Mzimvubu River Catchment followed by the methodology for determining the sediment yield in this study in Chapter 4. Chapter 5 displays and discusses a set of maps and statistics presenting the results of the study. Finally, a summary given in Chapter 6 concludes the study report, including future needs and recommendations for sediment yield assessment at a regional scale.

2. LITERATURE REVIEW

Although erosion control measures need to be implemented at the field or hillslope scale, allocation of scarce conservation resources and development of policies require erosion assessment at a regional scale (Vrieling, 2006). Sediment yield models and remote sensing techniques applied within GIS play an important role in the assessment of sediment yield in large areas.

2.1 Literature review on erosion and sediment yield models

A wide variety of models are available for sediment yield assessment and various aspects of sediment yield modelling have been reviewed in the literature (e.g. Merritt *et al*., 2003; Jetten *et al*., 2003; Van Zyl, 2007; Parsons, 2012). Differentiation between classes of models is usually based on the level of complexity used to present the soil erosion processes, as well as the spatial and temporal resolution of the model. Merrit *et al*. (2003) analyzed specific models based on model input-output, model structure, runoff, erosion/transport and water quality modelling, and accuracy and limitation of the model.

According to Jetten *et al*. (2003), models evolved from rainfall-based erosion predictions using Curve-Number-based runoff estimations, to physically-based water balance approaches. In this context, models fall into three main categories: (2.1.1) empirical, (2.1.2) conceptual and (2.1.3) physically-based models (Merritt *et al*., 2003). Table 1 summarizes the models that are mentioned in Section 2.1 in terms of their classification and scales of application, including model acronyms and names.

Table 1: Summary table of models mentioned in text.

Abbre-viation	**Name**	**Developed by**	**Aim**	**Time step and partition**
ACRU	Agricultural Catchment Research Model	Univ. of Natal – Dept. of Agricultural Engineering (Schulze, 1995)	Sub-catchment modelling	Daily Sub-catchment
KINEROS	Kinematic Runoff and Erosion model	US Dept. of Agriculture – Agricultural Research Service (Woolhiser *et al*., 1990)	Event-oriented, physically-based model describing the processes of interception, infiltration, surface runoff and erosion from small agricultural and urban watersheds.	Event Field
LISEM	Limburg Soil Erosion Model	Department of Physical Geography at Utrecht University and Soil Physics Division at Winard Staring Centre (De Roo and Jetten, 1999)	Spatially distributed physics-based hydrological and soil erosion model, based on EUROSEM	Event Catchments up to 100 km^2
MUSLE	Modified Universal Soil Loss Equation	(Williams and Brendt, 1977)	Prediction of daily, monthly and annual sediment yield for basins	Daily Sub-catchment
(R)USLE	(Revised) Universal Soil Loss Equation	US Dept. of Agriculture (Wischmeier and Smith, 1978; Renard *et al*., 1994)	Lumped empirical models that estimates annual rill and interill erosion based on main soil erosion factors	Annual Hillslope
SWAT	Soil and Water Assessment Tool	US Dept. of Agriculture – Agricultural Research Service (Arnold *et al*., 1994)	Prediction of the effects of management decisions on water sediment yields for ungauged rural basins	Daily Event Sub-catchment
WEPP	Water Erosion Prediction Project	US Dept. of Agriculture – Agricultural Research Service (Nearing *et al*., 1989)	Soil and water conservation planning and assessment	Breakpoint Continuous Channel Hillslope

2.1.1 Empirical models

Empirical models are generally easier to use compared to other model types because they are based primarily on the analysis of observations (Merritt *et al*., 2003). These models have relatively low input data requirements and associated levels of uncertainty in predictions. The most well-known and implemented empirical model for estimating soil loss is the USLE developed in the 1970s by the United States Department of Agriculture (USDA), and its upgraded version the Revised USLE. The (R)USLE is based on the main factors causing soil erosion, including long-term rainfall, an estimate of soil erodibility, land cover information and topographic information. Although developed for application to hill-slopes, (R)USLE and its derivatives have been incorporated into many regional scale erosion studies across the globe (e.g. Lu *et al*., 2003; Le Roux *et al*., 2008). The main attribute of empirical models is their high level of spatial and temporal aggregation and their incorporation of a relatively small number of variables (Jakeman *et al*., 1999). However, empirical models do not take connectivity aspects into account and therefore more complex models are required to simulate sediment yield at the catchment scale. Conceptual models are usually preferred above empirical models for sediment yield modelling. The main reason is that sediment yield is the integrated result of all erosion processes operating in a catchment, including sediment transfer and deposition (Vanmaercke *et al*., 2011; Parsons, 2012).

2.1.2 Conceptual models

The main feature that distinguishes conceptual models from empirical models is that they lump or aggregate representative processes over the scale at which outputs are simulated (Wheater *et al*., 1993), but incorporate important transfer mechanisms of sediment and runoff generation in their structure (Merritt *et al*., 2003). Conceptual models primarily use simplified deterministic representations of the processes governing erosion and delivery (Van Zyl, 2007) including a hydrological module, an empirical sediment module, and in most cases a contaminant module that use loading functions (Pegram and Görgens, 2001). Several conceptual models draw on the Modified USLE where sediment yield is computed using surface runoff and peak flow rate together with the widely used USLE factors mentioned above. In many cases these models are continuous simulation models in order to simulate long periods of time with a time step of 1 day e.g. SWAT. The foundational strength of semi-distributed models such as SWAT is that it partitions the catchment of interest into homogeneous morphological units while considering most significant connectivity aspects, including factors controlling upland sediment generation, channel transport and deposition into sinks (Gassman *et al*., 2007). The ACRU model is an example of such a model that has been developed and applied successfully in SA (Schulze, 1995; Dickinson and Collins, 1998; Van Zyl and Lorentz, 2003; Le Roux *et al*., 2013). A major limitation to the use of conceptual models, however, is the lack of recorded flow and/or sediment data required for calibration and validation (Van Zyl, 2007).

2.1.3 Physically-based models

Physically-based models have a much more sophisticated model structure than empirical or conceptual models. They are based on the solution of fundamental physical equations describing the conservation of mass and momentum of streamflow and sediment transport on a hillslope or in a catchment (Merrit *et al*., 2003). Physically-based models are in many cases spatially distributed and event-based in order to estimate the response of the modelled area to single storm events e.g. KINEROS and LISEM. The model time-step is of the order of minutes or hours for each event. Another process-based model worth mentioning is the WEPP that simulates climate, infiltration, water balance, plant growth and residue decomposition, tillage and consolidation to predict surface runoff, soil loss, deposition, and sediment delivery (Nearing, *et al*., 1989). Unfortunately, a large number of parameters have to be determined and as such these models are limited to areas for which there has been intensive data collection (Van Zyl, 2007). This prevents the application of physically-based models, such as WEPP and KINEROS in the Mzimvubu River Catchment. Gully erosion modelling in particular requires large datasets related to topography, lithology, soils, rainfall, land use and vegetation cover (e.g. Multivariate Adaptive Regression Splines by Gómez Gutiérrez *et al*., 2009). Semi-distributed or semi-lumped conceptual models are often preferred above fully-distributed or physically-based models, since the latter lead to additional errors and uncertainty resulting from more parameters and input data requirements in large catchments (Lenhart *et al*., 2005; Medeiros *et al*., 2010). The combination of conceptual models and remote sensing techniques within a GIS framework is commonly utilized for sediment yield assessment at a catchment scale (Gau, 2008).

2.1.4 Temporal and spatial interfacing of models in a GIS

GIS is a useful tool that offers unprecedented flexibility in the representation and organization of spatial data, as well as in terms of time distribution of data. Therefore, numerous models are interfaced into a GIS to streamline access to key databases and facilitate the preparation of input datasets. ArcSWAT is a graphical user interface for SWAT and ArcMap® software. It is a large catchment scale, semi-distributed and continuous time model operating on a daily time-step. The foundational strength of semi-distributed models such as ArcSWAT is that they partition the catchment of interest into homogeneous morphological units thus, allowing to certain extents, the spatial variation of topography and land use to be accounted for in a GIS (Lenhart *et al*., 2005; Gassman *et al*., 2007). Furthermore, ArcSWAT considers most connectivity aspects into one simulation package in a GIS, including factors controlling upland sediment generation, channel transport and deposition into sinks (Gassman *et al*., 2007). In terms of sediment yield, connectivity aspects from hillslopes to channels, as well as channel connectivity downstream needs to be considered in a GIS. Relatively recent advances in GIS science, also known as GIScience, offer considerable potential in this regard. Bishop *et al*. (2012) reviews some advances in GIScience, including new sensor technology, data sources, and information extraction technologies and capabilities, and examples of geomorphological applications. The following section briefly reviews remote sensing techniques available for mapping erosion features at a regional scale.

2.2 Literature review on remote sensing of erosion features

Remote sensing techniques have been widely used to map eroded areas, the assessment of off-site impacts and erosion controlling factors, as well as for data integration for erosion modelling (Vrieling, 2006). Various techniques have been used ranging from simple visual interpretation of images to complex image manipulation (Smith and Pain, 2009). Sensors are carried by aircraft or satellites and are mostly identical in terms of primary output data, but the lower altitude at which airborne systems function allows higher spatial resolutions (Smith and Pain, 2009).

2.2.1 Airborne systems

Airborne systems have been widely used to account for and map the heterogeneity of soil erosion features including photogrammetric methods using stereo images (Flügel *et al*., 2003), synthetic aperture radar interferometry (Hochschild and Herold, 2001), and airborne laser altimetry (Ritchie, 2000). Until now, most remote sensing studies are based on the use of airphoto interpretation and photogrammetry to map erosion features such as gullies (Martinez-Casasnovas, 2003; Casalí *et al*., 2009). Recent elevation products such as LiDAR (Light Detection and Ranging) and IfSAR (Interferometric Synthetic Aperture Radar) are capable of volumetric measurements of individual gullies (Johansen *et al*., 2012). These products are derived from pulsed laser systems that generate millions of 3D point measurements (point clouds), manipulated directly or interpolated to create a high resolution grid based DEM (Smith and Pain, 2009). Although airborne systems are useful for direct identification of erosion, the disadvantage of aerial photography is that it does not provide repeatable coverage over large areas that are needed for assessment of large areas for which satellite imagery is better adapted (Vrieling, 2006). Fortunately, colour digital aerial imagery at 0.5 m can now be acquired at a national scale from National Geospatial Information (NGI) between 2008 and 2012 (post 2012 imagery will be available in 2015).

2.2.2 Satellite imagery

Satellite images generally provide broad coverage and long time series of data. For example, Landsat MSS and TM imagery remains a significant data source since the early 70's due to its satisfactory repeat coverage for monitoring, large scene size and low cost of entry (imagery dating back to 1972 now freely available) (Smith and Pain, 2009). The Landsat-8 carrying Operational Land Imager (OLI) was launched in February 2013 and began normal operations in May 2013. However, its potential to assess erosion and sediment yield have not been tested in peer-reviewed studies yet. Techniques frequently used include visual interpretation (Dwivedi *et al*., 1997), correlation between spectral reflectance values (Price, 1993), automatic extraction/classification techniques (Servenay and Prat, 2003), change detection methods (Lu *et al*. 2004) and imaging radar instruments (Metternicht and Zinck, 1998). Until recently, however, coarse spatial resolutions offered by satellite imagery made it difficult to detect erosion features with required accuracy (King *et al*., 2005). Vrieling (2006) states that most studies that have applied satellite imagery concentrate on the assessment of erosion risk factors, especially vegetal attributes (e.g. Symeonakis and Drake, 2004). In terms of erosion features, previous remote sensing studies essentially mapped large eroded areas suffering from extensive erosion. According to Hochschild *et al*. (2003), space-borne data is difficult to relate to particular processes due to the heterogeneity of the object itself as well as the environment. The spectral reflectance between individual erosion features such as gullies varies significantly over large areas and depends on vegetation cover, as well as several soil properties such as soil organic matter and soil moisture content (King *et al*. 2005, Stroosnijder 2005). An important difficulty when monitoring soil erosion by satellite is the influence of canopy cover, especially dense tree canopy concealing poor ground cover and erosion processes in temperate and humid areas.

Le Roux and Sumner (2012) based gully erosion mapping in the Tsitsa River Catchment in the Eastern Cape Province on analysis of SPOT 5 imagery acquired in 2007/8. In order to speed up the processing of data and to exclude subjectivity of manual interpretation, the study first considered different techniques of classification. However, classification techniques could not express individual gullies with acquired accuracy due to their spectral complexity, especially over such a large area. Other regional studies that utilized classification techniques in semi-arid regions of SA confirm this trend, i.e. could not rapidly, nor accurately, define individual gullies from bare soil at a large catchment scale (e.g. Mararkanye and Le Roux *et al*., 2012). Taruvinga (2008) demonstrated that classification techniques (i.e. support vector machine applied on SPOT 5 imagery) mainly identifies large (>3.5 ha) prominent gullies (continuous), omitting small intermittent gullies (discontinuous) near Utrecht in KwaZulu-Natal. Another study worth mentioning is the study of Mararakanye and Nethengwe (2012) that investigated object-based modeling (i.e. Imagine Objective) on SPOT 5 imagery for gully features extraction in a small catchment of the Capricorn District Municipality in the Limpopo Province. Although the study obtained an overall classification accuracy of 76% and a kappa statistic of only 0.52, Mararakanye and Nethengwe (2012) postulates that higher accuracy will be possible using imagery with higher spatial resolution. Fortunately, with the development in sensor technology, space-borne data with improved spatial, spectral and temporal resolution is now available including IKONOS, Quickbird, WorldView and GeoEye (Smith and Pain, 2009). The use of imagery with high spatial resolution in object-based modelling techniques is particularly promising in this regard. Object-based modelling, also referred to as object-based image analysis, is an important trend in remote sensing and GIScience (Blaschke, 2010).

2.2.3 Object-based modelling

Object-based modelling first requires segmentation to generate objects with unique spectral and spatial characteristics. Segmentation can be defined as a process of partitioning an image into homogenous segments or image-objects on the basis of both spectral and spatial characteristics (Blaschke, 2010; Dey *et al*., 2010). Segmentation is superior to conventional pixel-based classification, which is solely spectral (Benz *et al*., 2004). After segmentation, objects can be classified into homogenous groups which involve computing the attributes of the object such as its location, size, shape, and its contextual relationships such as distance and direction to all other objects on the landscape across multiple scales (Bishop *et al*., 2012). Therefore, object-based modelling, as opposed to individual pixels is more appropriate to address the aforementioned heterogeneity of erosion features (Shruthi *et al*., 2011).

Although object-based modelling has considerable potential to improve classification accuracies, its potential to map erosion features have only been minimally tested in peer-reviewed studies. Knight *et al*. (2007) mapped alluvial gullies using ASTER imagery in the Mitchell River Catchment in the northern Australian tropics. However, Knight *et al*. (2007) only obtained accuracies for the gully class of approximately 50%. Shruthi *et al*. (2011) researched the use of object-based modelling to extract gully erosion features from IKONOS and GEOEYE-1 imagery in the Sehoul commune region of Morocco, using a combination of topographic, spectral, shape and contextual information. The study successfully identified gully related edges within the complex gully systems with negligible overestimations (0.03% and 1.77%) between the reference area and the modelled area in two small sub-catchments. The study of Wang *et al*. (2014) successfully mapped gully extent, as well as gully volumes, but this was only achieved for two gullies in Beiyanzikou catchment of Qixia, China. To assess detailed spatial information on gully volume, LiDAR data are required (Johansen *et al*., 2012).

Eustace *et al*. (2011) used a semi-automated object oriented classification method to detect and map gully extent and volume within the Fitzroy Catchment of Queensland, Australia. This has been achieved by (*i*) using fine-resolution LiDAR transects to derive DEMs at twenty sites (limited due to cost), (*ii*) carrying out object-oriented classification to derive gully extent from the LiDAR transects, (*iii*) statistically model the relationship between gully presence, soil, topography and vegetation status, and (*iv*) extrapolating the model across the study area with an area of over 140,000 km^2 at the scale of 25 m pixels. Cross-validation indicated a moderate predictive ability, with an average area under the receiver operating characteristic curve of 0.62. The reasons for the modest result include the limited number of twenty LiDAR transects, the low resolution of the soil map leading to the exclusion of soil erodibility as an important causal factor in the model, and the fact that gullies may be caused by different processes at different locations (Eustace *et al*., 2011). Other limitations include the absence of field measurements to verify the volumetric gully estimates and not assessing how gullies change through time. One of the most recent trends is to use object-based modelling for change detection (Blaschke, 2010).

2.2.4 Change detection with object-based modelling

A great variety of methods for change detection from satellite imagery exists including (Lu *et al*. 2004; Blaschke, 2010): albedo and spectral image differencing, principal component analysis, spectral change vector analysis, post-classification comparison, repeat-pass SAR interferometry, DEM extraction and slight deformation measurements. Change detection techniques by means of object-based modelling have become an important technique for mapping gully erosion activity/stability and rates. As mentioned above, however, object-based modelling have not been widely applied and tested in peer-reviewed studies, especially as a tool to detect changes of erosion features over time. Wiegand *et al*. (2013) applied object-based modelling on orthophotos over 10 years to detect changes in extent of shallow erosion features in the inner Schmirn Valley, Austria. Johansen *et al*. (2012) extended the research of Eustace *et al*. (2011) by expanding the object-based modelling routine to include the volume estimation and assessment of multi-temporal change for three selected study sites in the Fitzroy Catchment of Queensland, Australia. This was achieved by developing an object-based approach for monitoring gully extent and gully volume based on multi-temporal LiDAR data captured in 2007 and 2010, and assessing changes in extent and volume of gullies of the three study sites. Gully extent and volume were effectively assessed, although only the gully extent mapped from the 2010 LiDAR data was validated based on high spatial resolution orthophotos (with an overall accuracy of 92%).

The following section presents the general environmental setting for the Mzimvubu River Catchment. Descriptions include location, landforms, climate, vegetation, land use, geology and soils.

3. SITE DESCRIPTION

This section presents the general environmental setting for the Mzimvubu River Catchment located largely in the Eastern Cape Province and partially KwaZulu-Natal Province (see Figure 1). Descriptions include location, landforms, climate, vegetation, land use, geology and soils.

The Mzimvubu River Catchment is classified as a primary catchment that lies between 29º 54' 51'' and 31º 38' 35'' south and 27º 55' 56'' and 29º 39' 14'' east. It has a drainage area of 19 826 km^2 and a flow length of approximately 350 km from north to south. The Mzimvubu River takes its source from the Drakensberg and is fed by mainly 5 tertiary rivers/catchments namely the Tsitsa, Tina, Kinira, Mzimvubu and Mzintlava, from west to east respectively. After a flow length of approximately 200 km, the Tsitsa River flows into the Tina River, which flows into to Mzimvubu River less than 5 km downstream from abovementioned confluence. The Kinira River flows into the Mzimvubu after a flow length of approximately 150 km, whereas the Mzintlava River flows into the Mzimvubu River after a flow length of approximately 200 km. Approximately 50 km northwest from Port St Johns, the Mzimvubu River continues to meander through several deep gorges until reaching the main catchment outlet in the ocean at Port St Johns. Connectivity of the main rivers mentioned above is not influenced by large dams, but several small dams occur in their tributaries along the axial valleys. A total of 104 relatively large farm dams and reservoirs, ranging between ≤0.1 and 80 ha, have been mapped from SPOT 5 imagery (see Methodology in Section 4.1). The three largest dams in the catchment are Crystal Springs in T32C, Roodeberg Dam in T32B and Mountain Dam in T33A with capacities of just over 1 million m^3 (Midgley *et al*., 1990). Approximately 198 wetlands occur in the upper catchment area, ranging between relatively small (≤8 ha) isolated wetlands to large (3 400 ha) networks. Figure 3 in the Methodology Section shows the location of these dams and wetlands, as well as the future dam site at Ntabelanga on the Tsitsa River.

Elevation ranges from sea level at the catchment outlet in the southeast to approximately 3 000 m in the Drakensberg Mountains bordering Lesotho. Landforms are complex, ranging from very steep mountain slopes (40%) of the Drakensberg to gently undulating footslopes (2%) and nearly level valley floors. The catchment is characterised by three prominent/steep escarpment areas including the Drakensberg Mountains also known as the Great Escarpment, followed by mountain ranges that separates the Highlands from the mid-slopes, and a third relatively steep drop in elevation approximately 50 km inland from the coast.

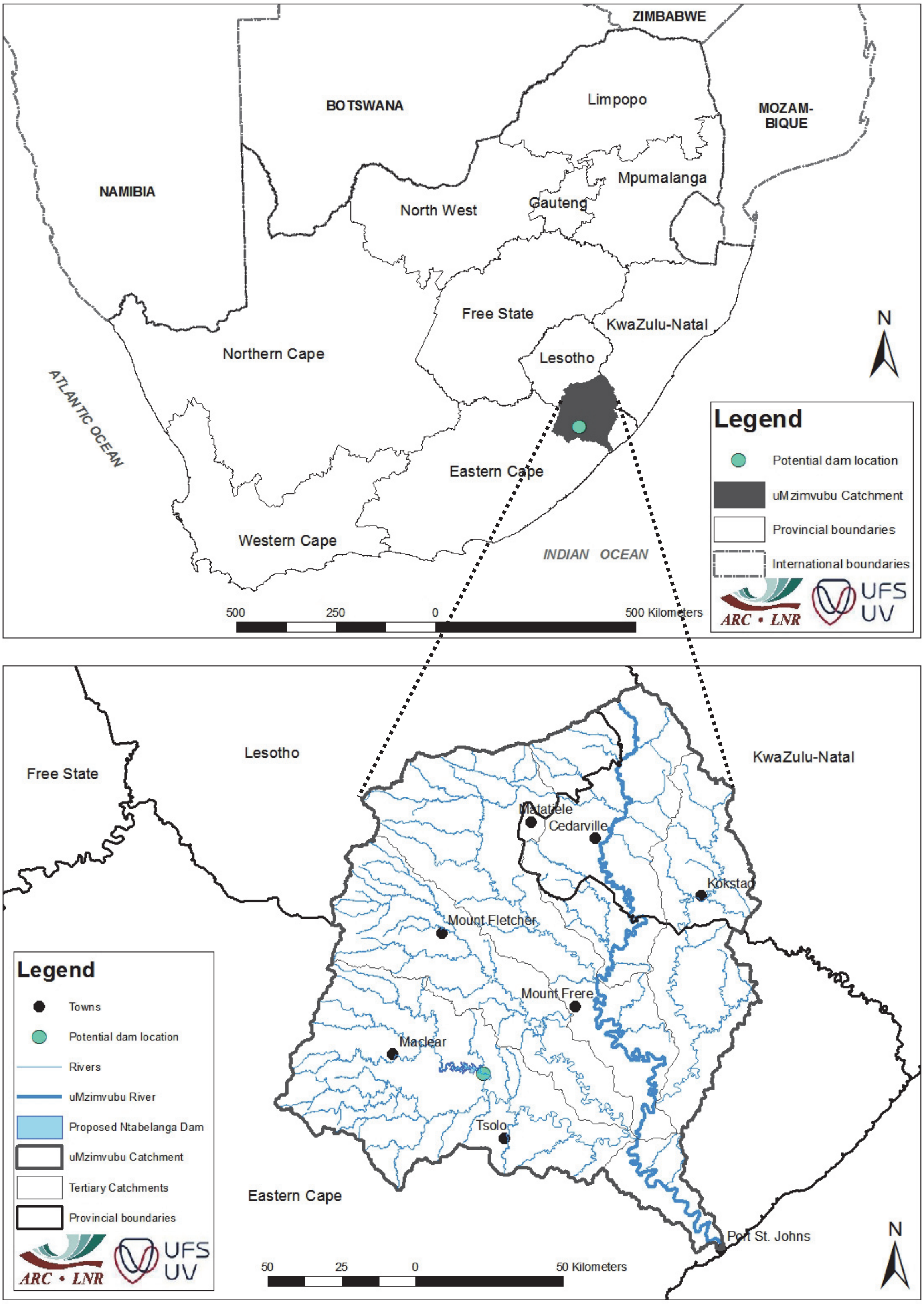

Figure 1: **Location map of the Mzimvubu River Catchment.**

The climate is characterized as sub-humid with the mean annual rainfall ranging from 625 mm in the lower inland plains to 1 415 mm in the mountain chains of which around 80% is recorded in the summer season extending from October to March (Climatology Staff, 1978-2012). Maximum rainfall occurs in summer months of November to February (averaging 123 mm in December), whereas minimum rainfall occurs in winter months of June to August (averaging 17 mm in July). Mean temperatures range between 6.6 and 20.3 ºC, with monthly means of daily minima and maxima, respectively -4.5 and 10.7 ºC in winter (July) and 17.1 and 29.8 ºC in summer (January). The mean annual potential evaporation is 1 573 mm (AGES, 2009).

The Mzimvubu River Catchment mainly falls within the Grassland biome, with narrow bands of Eastern Valley Bushveld (where acacias and euphorbias dominate) along the river networks in the lower part of the catchment (Mucina and Rutherford, 2006). Natural vegetation is largely influenced by altitude, as well as burning. Small pockets of Afromontane Forest occur along drainage lines or ravines where they are protected against fire. From high to low altitude the Grassland biome is further classified into the following belts: The Lesotho Highland Basalt Grassland in the highest part of the catchment, Southern Drakensberg Highland Grassland at a slightly lower elevation, East Griqualand Grassland on the lower slopes, followed by Drakensberg Foothill Moist Grassland (Mucina and Rutherford, 2006). According to the National Land Cover (2000), natural vegetation exceeds 14 300 km^2 (72%) of the catchment area, including grassland (65%), thicket (5%), forest (2%) and shrubland/fynbos (0.1%). The lower slopes are mainly used for grazing and agricultural practices. The main land use is degraded or unimproved grassland used for subsistence grazing (1 300 km^2, 7% of the catchment) with minority land uses including commercial agriculture (3%) and forest plantations (2%). Relatively large waterbodies such as farm dams and wetlands occupy roughly 400 km^2 (2%) of the catchment area. Urban areas cover the remaining 700 km^2 (4%) of the catchment area of which 3% is classified as townships and 0.3% as formal built-up areas. Some of the major towns are Maclear, Tsolo, Mount Fletcher, Mount Frere, Matatiele and Kokstad.

The geology consists of a succession of sedimentary layers of the Quaternary age (Council for Geoscience, 2007). The coastal region is dominated by Table Mountain sandstone with steep sea cliffs characteristic of the Wild Coast. A major fault, caused by the breakup of Gondwanaland approximately 130 million years ago, separates the sandstone cliffs and a section of shale rich units of the Ecca series further inland. Approximately 10 km inland from the outlet, is another geological fault worth mentioning. This fault consists of a large Karoo dolerite sill that protrudes through the catchment, separating the southern section of shale units of the Ecca series and a northern section of Diamictite of the Dwyka series (polymictic clasts, set in a poorly sorted, fine-grained matrix). Further inland, the oldest materials are Adelaide mudrock with subordinate sandstone. The latter is succeeded by various layers of sedimentary deposits including mudstones of the Tarkastad, Molteno and Elliot Formations. The next layer consists of fine-grained sandstone and siltstone of the Clarens Formation capped by Drakensberg basaltic lava in the most upper catchment area. Formations are all characterized by Karoo dolerite injections appearing as sills, sheets and dykes. In addition to alongside river valleys, a large patch of alluvium deposits occur just north of Cedarville.

Soils in the catchment vary significantly but most prominent soil forms include poorly drained and shallow to moderately deep loams usually with minimal development on hard or weathering rock (e.g. Mispah and Glenrosa soil forms) (Land Type Survey Staff, 1972-2012). Moderately deep to deep sandy loams with good permeability and relative stability (e.g. Hutton soil form) are less prominent. Soils from the Tarkastad, Molteno Elliot Formations in the central part of the catchment are associated with duplex soils with a non-reddish colour that are highly erodible with widespread gully erosion evident. The most prominent feature of these soils is the marked increase in clay content from the topsoil to subsoil horizon, with an abrupt transition between the topsoil and the subsoil with respect to texture, structure and consistence (Samadi *et al*., 2005). These soils are usually associated with vertic, melanic and/or plinthic soils. As a result, these soils inhibit root growth and limit infiltration, which leads to increased runoff and erosion. A large central section of the catchment is affected by dense and deep gully networks. Gullies vary in shape (V- to U-shaped) and size; from 0.5 m to 30 m deep and 0.5 m to 300 m wide.

The following section explains the methodology followed for assessing the sediment yield in the Mzimvubu River Catchment.

4. METHODOLOGY

In order to provide a comprehensive overview of sediment yield in the Mzimvubu River Catchment, two approaches were implemented. These include (1) Model the sediment yield contribution from sheet-rill erosion using ArcSWAT, a graphical user interface for SWAT and ArcMap® software, and (2) Modelling the sediment yield contribution from gully erosion using remote sensing techniques in an integrated GIS approach. Both approaches were conducted over the same 5 year timeframe between 2007 and 2012 for which the most recent multi-temporal and high resolution imagery is available.

The initial database for erosion assessment consisted of:

- Hydrologically corrected SRTM DEM at 90 m resolution (Weepener *et al*., 2012);
- A river network developed by (Weepener *et al*., 2014) from 1:50,000 topographic maps with river lines prepared by NGI (2013);
- Daily rainfall and temperature data for the period 1 January 1982 to 31 December 2012 (Climatology Staff, 1978-2012);
- Land Type Inventories at 1:250,000 scale (Land Type Survey Staff, 1972-2012);
- Terrain units derived from abovementioned DEM of 90 m resolution and resampled to 30 m resolution (unpublished);
- SPOT 5 imagery with 3 bands at 10 m resolution with various acquisition dates from 2006 to 2012 (unpublished);
- Ground truthing data during two field visits in 2013 and one in 2014.

4.1 Sediment yield modelling using SWAT

SWAT is a large catchment scale model that was developed at the US Department of Agriculture (USDA) Agricultural Research Service (ARS) (Arnold *et al*., 1998). It is a semi-distributed, catchment-scale and continuous time model operating on a daily time-step to simulate water, sediment and chemical fluxes in large catchments with varying climatic conditions, soil properties, stream channel characteristics, land use and management practices (Arnold *et al*., 1998; Srinivasan *et al*., 1998). ArcSWAT which is a graphical user interface for SWAT and ArcMap® software will be used to model the sediment yield contribution from sheet-rill erosion in the Mzimvubu River Catchment. ArcSWAT was selected because the model offers unprecedented flexibility in the representation and organization of spatial data (Chen and Mackay, 2004). Semi-distributed models such as ArcSWAT are preferred above fully-distributed models in large catchments, since the application of the latter in large catchments lead to additional errors and uncertainty resulting from more parameters and input data requirements (Medeiros *et al*., 2010). The foundational strength of ArcSWAT is that it partitions the catchment of interest into homogeneous morphological units thus, allowing to certain extents, the spatial variation of topography and land use to be accounted for (Lenhart *et al*., 2005; Gassman *et al*., 2007). ArcSWAT has gained international acceptance and has been applied to support various large catchment (10 to 10,000 km^2) modelling studies across the world with minimal or no calibration effort (e.g. Srinivasan *et al*., 2010).

First, the hydrologic cycle is based on the water balance equation. Surface runoff volume is computed using the SCS curve number method which is empirically based and relates runoff potential to land use and soil characteristics (USDA SCS, 1972). Peak runoff rate is estimated with a modification of the rational method: where runoff rate is a function of daily surface runoff volume and a proportion of rainfall occurring until the time of concentration (Neitsch *et al*., 2011). The time of concentration is estimated using Manning's formula considering both overland and channel flow. Sediment yield caused by rainfall and runoff is computed with the Modified USLE (Williams, 1975) using surface runoff and peak flow rate together with the widely used USLE factors (Wischmeier and Smith, 1978). These factors include slope length and steepness, soil erodibility, crop cover management and erosion control practice.

Once the loadings of water, sediment, nutrients and pesticides have been determined, SWAT (applied in a GIS: ArcSWAT) routes them through the stream network of the catchment (Neitsch *et al*., 2011). Flow is routed through the channel using a variable storage coefficient method developed by Williams (1969), including transmission losses leaching through the streambed (USDA SCS, 1972) and return flow or base flow originating from groundwater (Arnold *et al*., 1993). Sediment is routed by means of a simplified stream power theory where the maximum amount of sediment that can be transported from a reach segment is a function of the peak channel velocity (Arnold *et al*., 1995). The methodological flowchart of the procedures followed in this study is outlined in Figure 2.

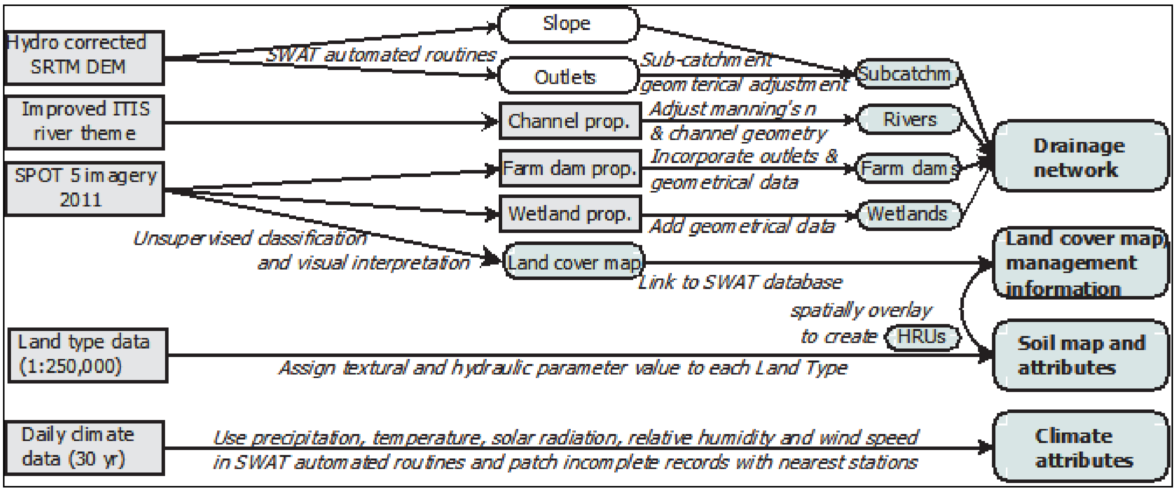

Figure 2: **Methodology flow chart for modeling sediment yield using ArcSWAT.**

4.1.1 Topographic-drainage-network variables

Topographic and drainage network data were prepared from the hydrologically improved DEM of Weepener *et al*. (2012) and the national 1:50,000 topographic maps with river lines prepared by NGI (2013) and Weepener *et al*. (2014). The ArcSWAT river theme represents all the relevant tributaries and main rivers; whereas sub-catchment numbers shapes and sizes are similar to quaternary catchments (see Figure 3). Furthermore, sub-catchment outlet points spatially overlay with flow monitoring points for calibration of model simulations with flow measurements. In addition one outlet was incorporated to represent the exit from the future irrigation dam site at Ntabelanga on the Tsitsa River. Existing sediment sinks including the 3 largest farm dams (i.e. Crystal Springs in T32C, Roodeberg Dam in T32B and Mountain Dam in T33A) were incorporated to receive loadings. Wetlands were also included as a land cover type in the model input database.

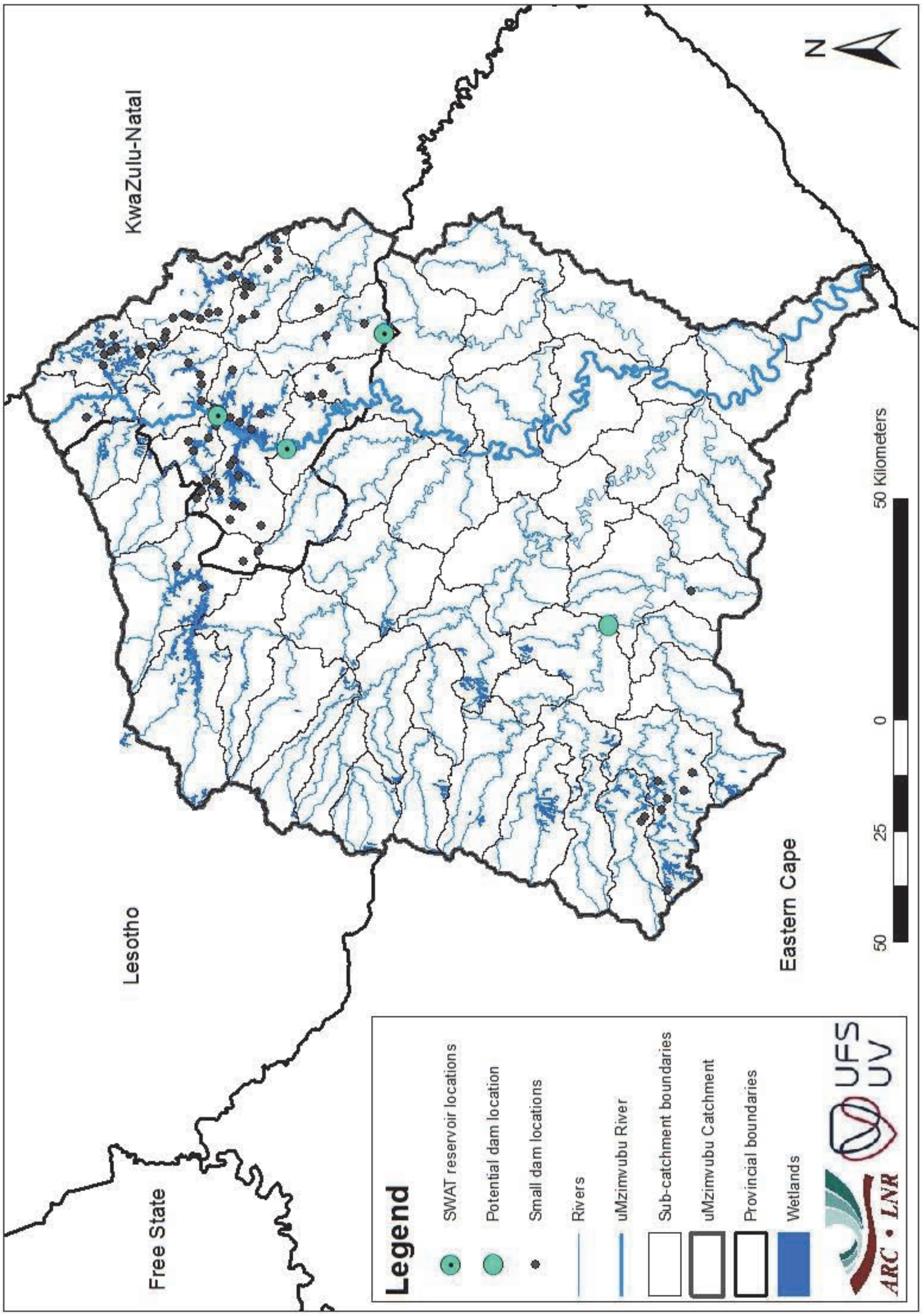

Figure 3: **Drainage network map of the Mzimvubu River Catchment.**

4.1.2 Land cover mapping

Of all hazard factors the cover management code and land use is the most important soil erosion factor which can rapidly change as a result of human activities. The most recent available spatial data in this regard is the National Land Cover (2000) database of SA derived from Landsat TM imagery prior the year 2000 and grid cell resolution of 30 m. It is therefore fair to say that National Land Cover (2000) does not adequately represent current land cover/use in the catchment. Hence, a new improved land cover map was created from SPOT 5 imagery acquired in 2011. Each image contains four bands with a resolution of 10 m and one pancromatic band with a resolution of 2.5 m. This study used the pan sharpened multispectral product with 2.5 m resolution. Four full scenes and ten partial scenes were used to cover the study area.

First, image classification was performed. In general, image classification is defined as the process of extracting different land cover classes or themes from remotely sensed satellite data (Aplin, 2004). A traditional ISODATA method was used for the classification of the satellite images. An unsupervised classification approach is often used in thematic mapping such as for vegetation and land cover mapping from imagery. Unsupervised classification is easy to apply and widely available in image processing and statistical software packages. The method is purely relying on spectrally pixel-based statistics and incorporates no prior knowledge of the characteristics of the classes being studied. A benefit of applying unsupervised classification is that it automatically converts raw image data into useful information. In this study, each unsupervised classification consisted of 200 classes. These classes were subjectively merged into 9 primary land cover classes using expert knowledge and information obtained from 104 field observations during ground truthing in November 2013 (see Figure 1 and Table 1 in Appendix 1). However, as expected, some features spectrally have the same signatures for different land cover classes including cultivated land and degraded grassland, bare soil and urban areas, and plantations and indigenous forests. Therefore, a second classification was necessary to more accurately classify these classes. This was achieved by manual interpretation and editing ‘areas of interests’. Urban-built-up classes and other spectrally heterogeneous classes were digitized manually. A script was used to integrate all classification layers.

Next, edge matching and filtering received high priority. Edge matching includes proper closing of feature boundaries from adjacent classifications and ensures a seamless transition in land cover pattern between classifications. The land cover map was finalized as a digital GIS-compatible raster file (see Figure 4), suitable for use at a scale of 1:25 000 (or coarser). The preliminary product contains 8 land cover classes, whereas the final product contains 12 classes (see Table 2).

Finally, the new land cover map/classes were linked to the land cover types in the ArcSWAT database. Due to the lack of data on these parameters and land use/operations, phenological plant development was based on daily accumulated heat units and several plant growth parameters in the ArcSWAT database.

Table 2: Land cover classes for the Mzimvubu River Catchment.

Class number	Primary land cover class	Secondary land cover class
1	Open water	Open water
2	Wetlands	Wetlands
3	Bushland/woodland/forest	Bushland/forest
4	Grassland	Natural grassland
5		Degraded grassland
6	Forest/Plantations	Plantations
7		Clear-felled plantations
8	Bare soil/rock	Bare soil/rock
9	Urban	Urban – high density
10		Urban – low density (rural)
11	Cultivation	Cultivation subsistence
12		Cultivation commercial
13	Clouds	-

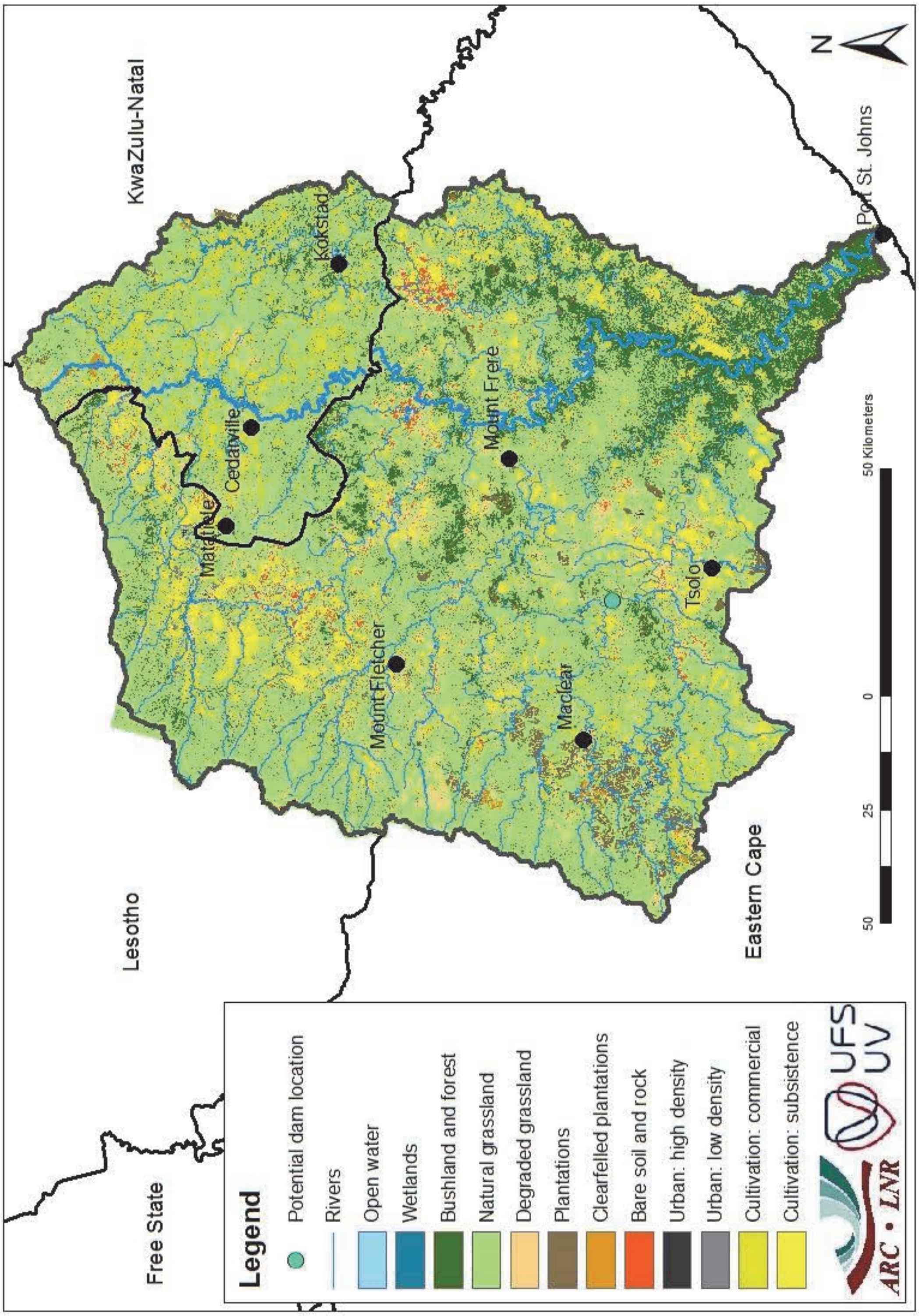

Figure 4: **Land cover map of the Mzimvubu River Catchment.**

4.1.3 Soil data

SWAT requires that each sub-catchment be characterized according to soil parameters which can be divided into physical and chemical characteristics. Information on chemical properties is optional, while the physical properties are required. In order to represent the variable soils in the catchment, textural and soil hydraulic parameter values were assigned to Land Types (Land Type Survey Staff, 1972-2012) according to descriptions given by soil profile descriptions and available soil maps usable at a scale of 1:250,000. Table 3 briefly describes the definition/description and methodology/reasoning behind the assignment of the required parameter values to Land Types in the catchment. Figure 5 illustrates the soil layer of the Mzimvubu River Catchment.

Table 3: Definition/description and methodology/reasoning used to assign soil parameter values to Land Types in the catchment.

Parameter name	Definition/description	Methodology/reasoning
Number of layers in the soil	---	One soil layer/horizon was incorporated into each soil component.
Depth from soil surface to bottom of layer (mm)	Depth of each individual soil layer.	Depth descriptions/classes in the Land Type database of SA were used to assign depth to each Land Type in catchment (Land Type Survey Staff, 1972-2012).
Maximum rooting depth of soil profile (mm)	If no depth is specified, the model assumes the roots can develop throughout the entire depth of the soil profile.	As above.
Soil Hydrologic Group (A,B,C,D)	The U.S. Natural Resource Conservation Service (NRCS) classifies soils into four hydrologic groups based on infiltration characteristics of the soils. In term of runoff potential, Soil Group A = low, B = moderately low, C = moderately high, D = high.	Used the hydrological classes given in Schulze (2007) for each Land Type.
Available water capacity of the soil layer (mm H_2O/mm soil)	The plant available water, also referred to as the available water capacity, is calculated by subtracting the fraction of water present at permanent wilting point from that present at field capacity, AWC = FC – WP where AWC is the plant available water content, FC is the water content at field capacity, and WP is the water content at permanent wilting point.	Used the total profile available water given in Schulze (2007) for each Land Type.
Saturated hydraulic conductivity (mm/hr)	The saturated hydraulic conductivity, K_{sat}, relates soil water flow rate (flux density) to the hydraulic gradient and is a measure of the ease of water movement through the soil. K_{sat} is the reciprocal of the resistance of the soil matrix to water flow.	Values were derived from SWAT look-up tables based on the soil texture classes of each soil series in the Land Type database of SA (Land Type Survey Staff, 1972-2012) – to spatially assign a conductivity value to each Land Type polygon, the values related to each soil series were weighted according to the area occupied by that soil within the polygon; therefore, the final values

		are an area weighted average for a Land Type.
Moist bulk density (Mg/m^3 or g/cm^3)	The soil bulk density expresses the ratio of the mass of solid particles to the total volume of the soil, $\rho b = M_S / V_T$. In moist bulk density determinations, the mass of the soil is the oven dry weight and the total volume of the soil is determined when the soil is at or near field capacity. Bulk density values should fall between 1.1 and 1.9 Mg/m^3.	An average value of 1.6 g/cm^3 was assigned to all Land Types due to the lack of data at this scale.
Moist soil albedo (non-dimensional value between 0 and 1)	The ratio of the amount of solar radiation reflected by a body to the amount incident upon it, expressed as a fraction. The value for albedo should be reported when the soil is at or near field capacity.	Albedo values were assigned to each soil series in the Land Type database of SA (Land Type Survey Staff, 1972-2012) as follows: sands = 0.25 (coded in Land Type database as soil forms Ah, Ai, Ha and Hb); clays (soil forms coded Ea) = 0.7; remaining textures = 0.5.
Texture of soil layer [optional]	This data is not processed by the model and the line may be left blank.	Assigned using clay classes given to each soil form in the Land Type database of SA (Land Type Survey Staff, 1972-2012).
Clay content (% soil weight)	The percent of soil particles which are < 0.002 mm in equivalent diameter.	Assigned using the average topsoil clay classes given to each soil form in the Land Type database of SA (Land Type Survey Staff, 1972-2012).
Silt content (% soil weight)	The percentage of soil particles which have an equivalent diameter between 0.05 and 0.002 mm.	Due to the lack of data, silt content was assigned values between 10-22.5%, increasing with increase in clay as follows: percentage of Land Type with <= 6% clay = 10% silt; 6.1-15% clay = 15% silt; 15.1-25% clay = 17.5% silt; 25.1-35% clay = 20% silt; 35.1-55% clay = 22.5% silt.
Sand content (% soil weight)	The percentage of soil particles which have a diameter between 2.0 and 0.05 mm.	Sand = 100% – (%clay + %silt + %rock + %carbon).
Rock fragment content (% soil weight)	The percent of the sample which has a particle diameter > 2 mm, i.e. the percent of the sample which does not pass through a 2 mm sieve.	Used agricultural restriction/rock (MB) classes in Land Type database of SA (Land Type Survey Staff, 1972-2012) as follows: MB0=0%; MB1=20%; MB2=50%; MB3=20%; MB4=100% (no soil).
Organic carbon content (% soil weight)	When defining by soil weight, the soil is the portion of the sample that passes through a 2 mm sieve.	An unpublished Carbon map of SA (derived from soil profile data and Land Type Database of SA) was used to assign carbon values to each Land Type in the catchment.
(K) factor in SI units t/ha per unit 'erosivity'	USLE equation soil erodibility described by Wischmeier and Smith (1978); and Neitsch *et al*. (2011).	Using the SLEMSA model of Elwell (1976), erodibility units were established and used as a guide to the assignment of USLE (Wischmeier and Smith, 1978) K-factors to Land Types (Le Roux *et al*., 2008).

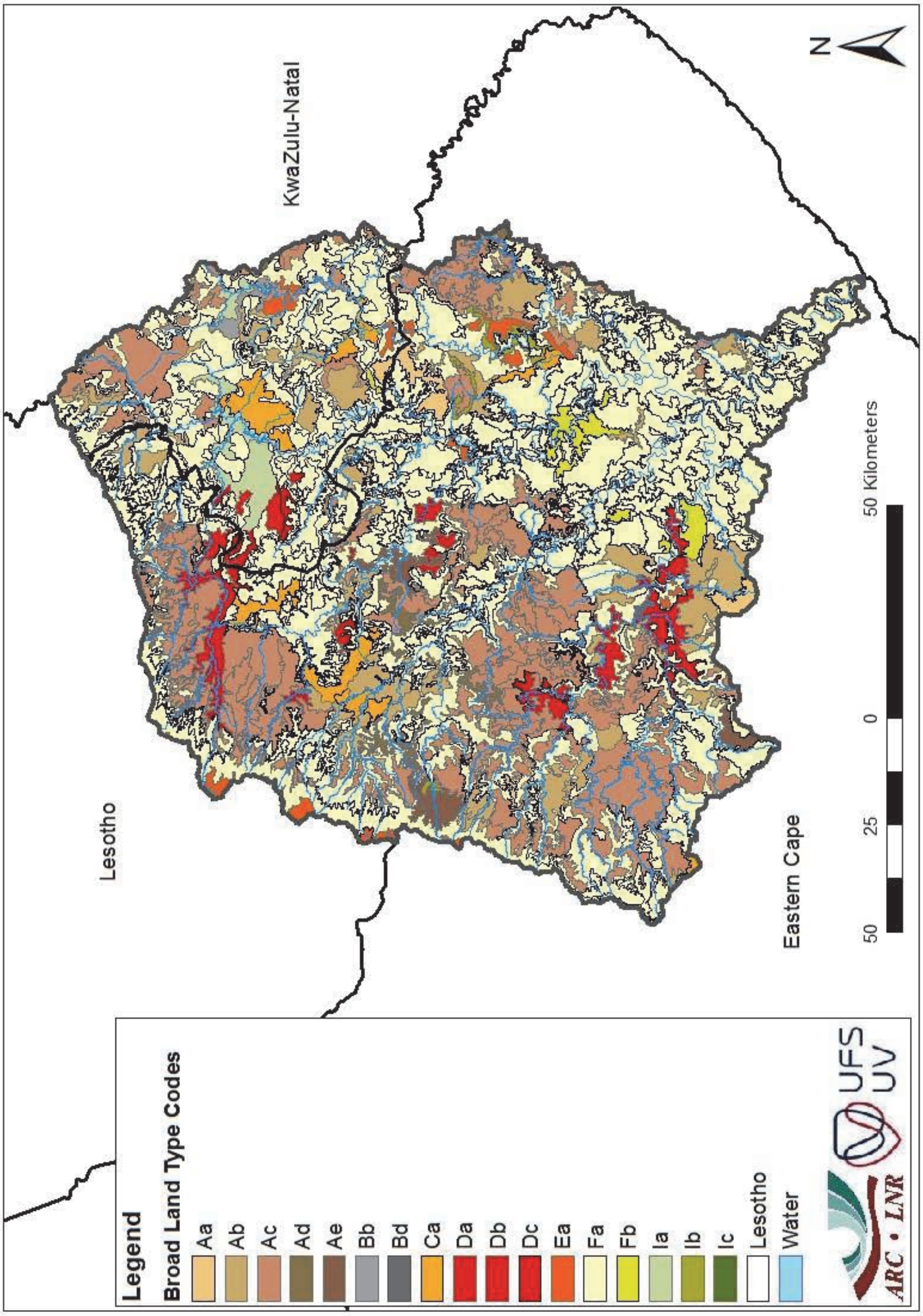

Figure 5: Soil layer of the Mzimvubu River Catchment.

4.1.4 Climate data

ArcSWAT also requires data for several climate parameters including precipitation, temperature, solar radiation, relative humidity and wind speed. Long term data are required to create a so-called weather-generator file in ArcSWAT. These were calculated from daily values over a 30 year period (1978 to 2007) from 2 stations within the Tsitsa River Catchment boundary near Maclear and Tsolo (Climatology Staff, 1978-2012) (see Figure 6). Since not all the stations have full records of the required parameters, incomplete records were patched with the most complete and closest stations. In total, 8 stations within or adjacent to the Mzimvubu River Catchment were utilized to extract rainfall and temperature data from 2006 to 2012. Data from several stations were interpolated (Thiessen Polygon analysis) in ArcSWAT to generate a spatial representation of the rainfall.

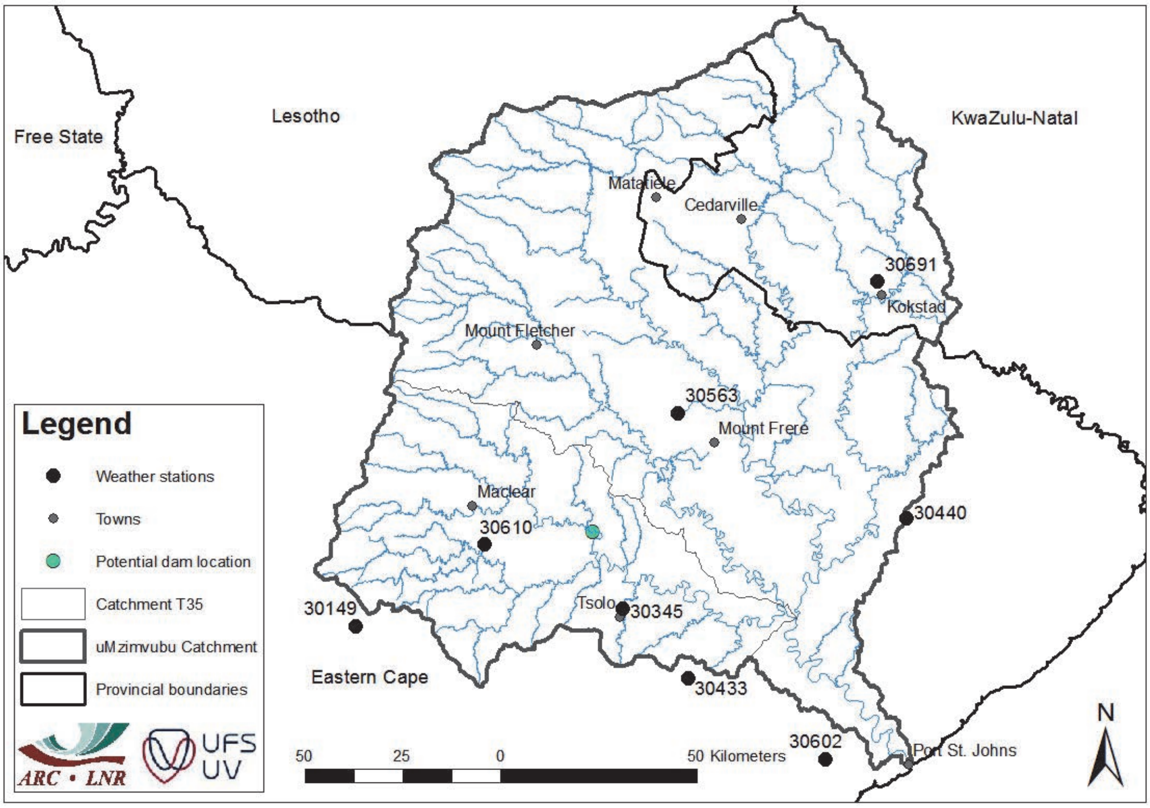

Figure 6: **Weather station locations in the Mzimvubu River Catchment.**

4.1.5 Management practices

In ArcSWAT, the HRU management file includes input data for planting, harvest, irrigation applications, nutrient applications, pesticide applications, and tillage operations. Due to the lack of data and scale of simulation, parameter values were assigned according to values provided in the SWAT database. Importantly, due to the lack of data on the crop rotation systems and timing of agricultural operations such as planting dates, phenological plant development is based on daily accumulated heat units. Detailed descriptions of the parameters are given in Neitsch *et al*., 2011).

4.1.6 Model simulation, calibration and validation

Model simulation was conducted over a period of 5 years (2008 to 2012) preceded by a one-year model “warm-up” initialization period. Calibration and validation were restricted to flow measurements from 7 stations from the Department of Water and Sanitation (see Figure 7). Due to the absence of data on sediment loads, calibration of ArcSWAT focused only on the hydrological part of the model on a monthly time-step adjusting the most sensitive model parameters similar to other studies (e.g. Tibebe and Bewket, 2011). The hydrological component was calibrated by modifying the curve number and base-flow coefficients, whereas the erosion component was calibrated by adjusting the USLE soil erodibility and support management factors. Model performance was improved by sequentially optimizing the widely used coefficient of efficiency (E) of Nash and Sutcliffe (1970), as well as the coefficient of determination (r^2). As a measure of goodness-of-fit between simulated and observed loads, a simple per cent deviation method of Martinec and Rango (1989) was used; given as:

$$D_v = [V - V' / V] \times 100 \qquad (1)$$

where, V is the measured runoff volume and V' is the simulated volume. D_v will be zero for a perfect fit and the smaller the value the more accurate are the simulated results. Comparison of the simulated results with the measured values of the station (coded T3H006) nearest to the future dam is illustrated in Figure 8. ArcSWAT over-predicted discharge by 14% as determined by D_v. The goodness of fit expressed by E was 75% and r^2 was 88%, indicating a relatively close relationship between the observed and simulated discharge.

During ground truthing in October 2013 (see Figure 1 and Tables 2 and 3 in Appendix 1), two grab-samples were taken near the Mzimvubu River mouth, as well as two samples at the Tsitsa-Tina River confluence (one sample on the Tstitsa side and one sample on the Tina side). Another five grab-samples were taken during ground truthing in June 2014: three at Tsitsa Bridge near the future dam site and two at the Tsitsa-Tina River confluence. The grab-samples indicate that the suspended sediment load is much higher in summer than in winter and that the load is thus related to increased (event) discharge. However, the grab-samples could not be used to validate the model since the sample size was too limited and since the samples were taken after 2012 outside the timeframe of the study. Unfortunately, a major limitation to the use of continuous time models such as ArcSWAT in developing countries is the lack of recorded flow and sediment data for calibration and validation (Van Zyl, 2007).

Since ArcSWAT computes sediment yield with Modified USLE that emphasizes the sheet and rill aspects of the erosion cycle, soil losses in the Mzimvubu River Catchment where gullies are prominent will be underestimated. The second approach was aimed at supplementing the ArcSWAT results by modelling the sediment yield contribution from gully erosion.

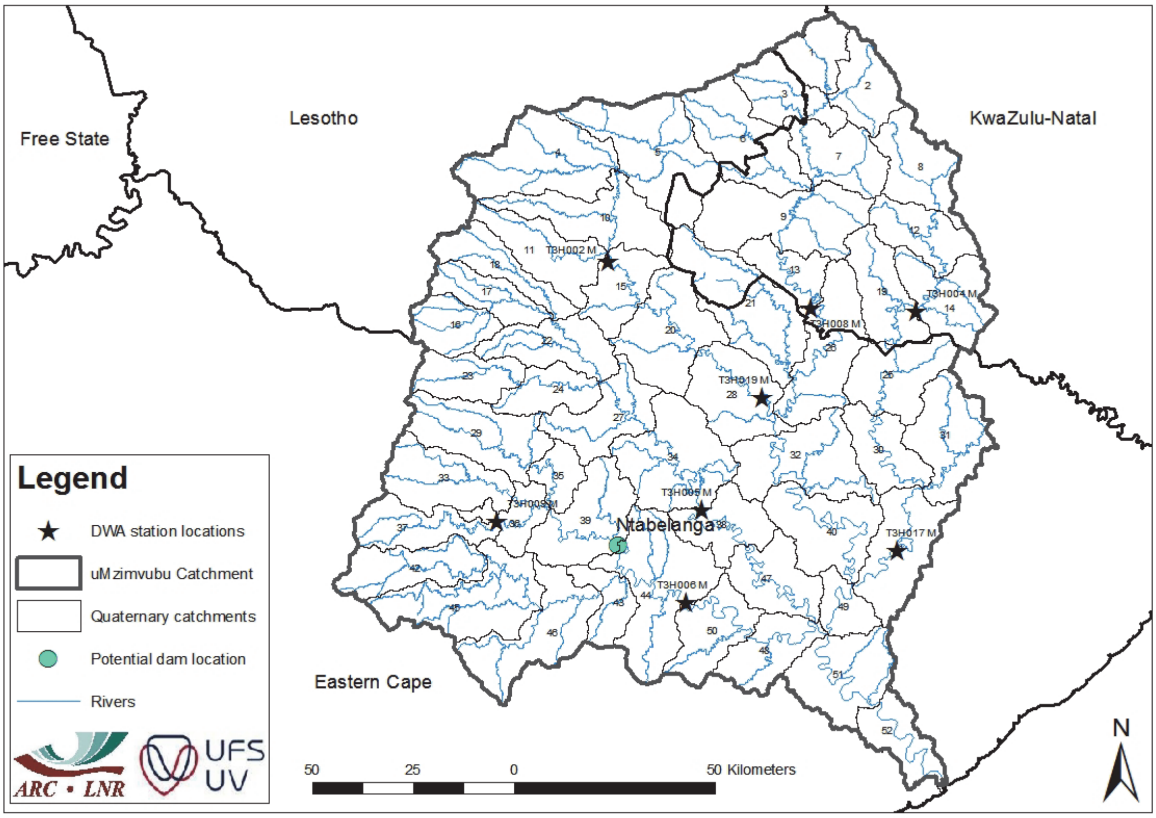

Figure 7: **Department of Water and Sanitation station locations in the Mzimvubu River Catchment.**

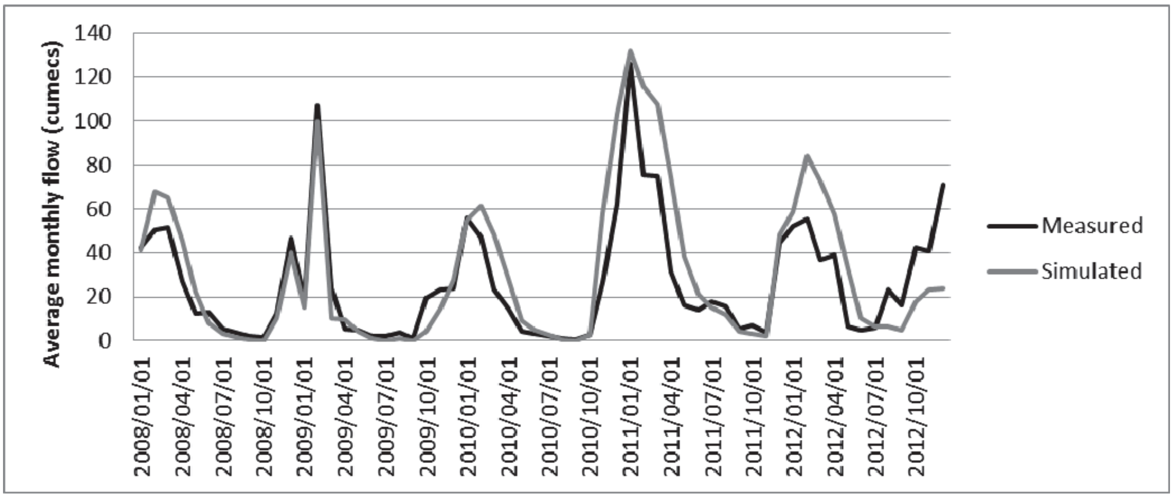

Figure 8: **Measured and simulated discharge from 2008 to 2012.**

4.2 Modelling the sediment yield contribution from gully erosion

Given the large number (>20,000) of gullies and size (19 826 km^2) of the catchment, it was not feasible to physically and representatively measure the sediment contribution from gully erosion in the field. The sediment yield contribution from gully erosion was assessed by means of remote sensing techniques in an integrated GIS approach that is semi-automatic and repeatable. This approach included gully digitizing, segmentation of SPOT 5 imagery, gully change detection, and developing a rule-based gully sediment yield model in a GIS. The specific reasons and techniques used are further described in Sub-sections 4.2.1 and 4.2.2 below. In order to create a catchment overview of sediment yield contribution from gully erosion, the gully location map created in 2007 was updated by digitising new and expanded gullies from SPOT 5 imagery acquired in 2012 (Section 4.2.1). These gullies were categorized into classes that, according to observations, uniquely influence sediment yield including gullies that are active or non-active (Section 4.2.2), gully depths (Section 4.2.3), and connected, partially connected, potentially connected or disconnected with the river network (Section 4.2.4). Finally, gully volumes and gully erosion rates were calculated (Section 4.2.5). The methodological flowchart for this approach is outlined in Figure 9.

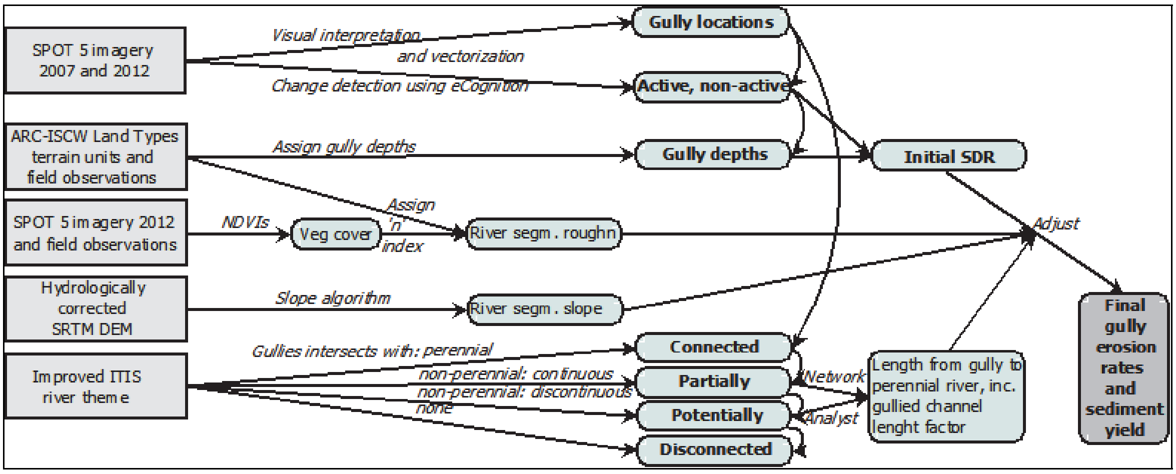

Figure 9: Methodology flow chart for modeling sediment yield contribution from gully erosion.

4.2.1 Updating the 2007 gully location map

The previous (2007) gully location map was first updated by manual vectorization of newly-developed gullies using SPOT 5 imagery acquired in 2012 at a scale of 1:10,000 (see Figure 10a). It is worth mentioning here that the initial plan was to also use the colour digital aerial imagery at 0.5 m resolution acquired from NGI in 2009 and 2012. However, the aerial imagery could not be used for change detection since the 2012 imagery is not available yet. SPOT 5 satellite imagery was utilized because the panchromatic sharpened images at 2.5

m resolution provides high resolution air photo-like quality for gully mapping (Taruvinga, 2008) and was acquired from government agencies for the whole country. Results of the accuracy analysis illustrate that 93% of all gullies were captured correctly (see Table 4).

Table 4: Number and percentage of gullies correctly captured/digitized.

Gullies observed	Gullies correctly captured	Accuracy
128	119	93%

Although vectorising gullies from SPOT 5 imagery by hand is subjective and exceedingly laborious, automated mapping techniques cannot express individual gullies with the required accuracy due to their spectral complexity over such a large area (Mararakanye and Le Roux, 2012). Spectral differences are caused by variances in soil moisture, organic matter, mineral content, shadow and illumination, and various land use types (Shruthi *et al*., 2011). Although the manually digitizing solves latter-mentioned problem, the digitized layer could not be used as it is. Gully polygons that were drawn by hand consist of additional fringe areas that do not precisely follow the real gully boundary. These additional fringe areas will not deliver accurate gully growth and subsequent sediment yield results. To render more objective and accurate results, both the 2007 and 2012 SPOT 5 images were segmented using eCognition® Developer 8 software.

4.2.2 Segmentation and change detection: identifying active and non-active gullies

Segmentation was performed on SPOT 5 imagery acquired in 2007 and 2012 to generate image objects with unique spectral and spatial characteristics (see Figure 10b). Segmentation can be defined as a process of partitioning an image into homogenous segments or image-objects on the basis of both spectral and spatial characteristics (Blaschke, 2010; Dey *et al*., 2010). Segmentation was performed because it is superior to conventional pixel-based classification, which is solely spectral (Benz *et al*., 2004). Furthermore, several approaches can be used in the segmentation process including homogeneity and shape analysis, region growing, pattern recognition, and rule-based segmentation (Bishop *et al*., 2012).

The ‘multi-resolution’ segmentation algorithm was used to subdivide SPOT 5 imagery of the entire catchment into smaller image objects. Each of the four image bands was given a weighting of 1 so that each band is equally represented in the segmentation process. By modifying the value of the so-called scale factor, you can vary the size of the resulting image objects, where a high scale parameter results in large objects and vice versa. Although it is recommended to use a scale factor that will create objects that are as large as possible and as fine as necessary, a scale factor of 10 was used in order to capture or represent all gullies (large and small). Scale factors larger than 10 did not delineate small discontinuous gullies with enough detail. As a result, small gullies were represented or captured by small objects whereas large gullies consisted of several objects that were later merged into single larger objects in a GIS. In addition, the homogeneity of objects can be set by two criteria namely colour and shape (compact or smooth). The colour and shape criteria parameters were set to 0.5 (which sums up to 1.0) and the compactness was set to 0.1, to create objects with relatively smooth shapes.

After segmentation, the second step includes the classification of objects into homogenous classes which involves computing the attributes of the object such as its location, size, shape, and its contextual relationships (distance and direction to all other objects on the landscape) across multiple scales (Bishop *et al.*, 2012). However, the spatial and spectral variability of the gullies in the catchment made it practically impossible and unfeasible to automate the gully classification process. Object-based gully feature extraction is challenged by not only the size, shape and distribution of gullies but also differences in soil moisture, organic matter, mineral content, shadow and illumination, and various land use types (Shruthi *et al*., 2011). Similar to the study of Wiegand *et al*. (2013), the boundary of several gully objects did not appear as a clear line but as a smooth transition to bare soil and/or grassland due to above-mentioned variability, as well as uncertainties related to the imagery (geometric and radiometric). Subsequently, the study could not use object-based modelling for change detection (the third step).

Singh (1989) defines change detection as the process of identifying differences in the state of an object or phenomenon by observing it at different times. Several change detection techniques exists e.g. perform segmentation of imagery into objects, followed by classification/extraction of objects, followed by detecting changes between objects from different dates. Besides the problem of object-based classification and extraction of gullies, automatic change detection was not utilized by this study because of the following reasons (Lu *et al*. 2004). First, the temporal, spatial, spectral and radiometric resolutions of the imagery itself have a significant impact on the success of a change detection project. In order to automate change detection analysis, several conditions must be satisfied including precise registration of multi-temporal images; precise radiometric and atmospheric calibration between multi-temporal images; and using images with anniversary or very near anniversary acquisition dates in order to eliminate the effects of external sources such as Sun angle and seasonal phenological differences. What's more, if the study area is mountainous such as the Mzimvubu River Catchment, topographic correction is required. Second, it is often difficult to distinguish true changed areas from the detected change areas since some techniques such as post-classification comparison can provide several change directions. Third, SPOT 5 imagery consists of huge datasets, which leads to excessive processing time and cost. In practice, change detection based on classification requires considerable effort including the use of several change detection techniques, whose results are then compared to identify the best product through visual assessment or quantitative accurate assessment (Lu *et al*. 2004). In order to avoid these problems in this study, it was decided to implement an integrated GIS approach as follows.

After exporting the image objects as shapefiles into a GIS, the 2007 and 2012 digitized gully location maps were refined by selecting only the objects with centroids within the digitized gullies (see Figure 10c). As mentioned above, the reason for using the objects this way is because the objects more accurately follow/overlap the real gully boundaries than the digitized polygons. Objects with centroids within the digitized gullies were then dissolved to create single gully polygons (see Figure 10d). As a result, both the 2007 and 2012 gully location maps that were digitized by hand were improved by excluding unwanted fringe areas.

Newly-developed gullies and gullies that expanded in spatial extent were determined by subtracting the 2007 gully extent layer from the 2012 gully extent layer (see Figure 10e). Gullies that expanded in spatial extent were categorised as active, whereas gullies that remained the same size were categorized as non-active. Although it is recognised that active gullies not only expand in length or sidewise but also incise in depth, multi-temporal analysis was not used to assess gully depth due to mainly one reason. The available imagery and methods applied here cannot express gully depths with the required accuracy due to their spectral complexity over such a large area. Furthermore, most gullies in this region deepens only until they reach the bedrock but keep expanding in length and sideways reaching lengths up to several kilometres and widths up to 100 m (Le Roux and Sumner, 2012).

4.2.3 Gully depth classification

Similar to the study of Grellier *et al*. (2012), we hypothesised that most gullies did not expand in depth in the last 5 years as gullies have almost all reached the bedrock. Gully depths were allocated by overlaying the most recent gully map with the depth classes for each Land Type (Land Type Survey Staff, 1972-2012) in the catchment, in conjunction with gully depth information that was obtained during ground truthing. Furthermore, soil and gully depth are highly correlated with terrain units, usually increasing downslope or towards the lower hillslope elements namely footslopes and valley floors (Le Roux and Sumner, 2012). Gully depth classes were therefore allocated in conjunction with terrain units that were created from the Hydrologically corrected SRTM DEM at 90 m resolution resampled to 30 m (Weepener *et al*., 2012). The same gully depths were used for both studied periods similar to the study of Grellier *et al*. (2012). Figure 11 illustrates the soil/gully depth map of the Mzimvubu River Catchment that was created.

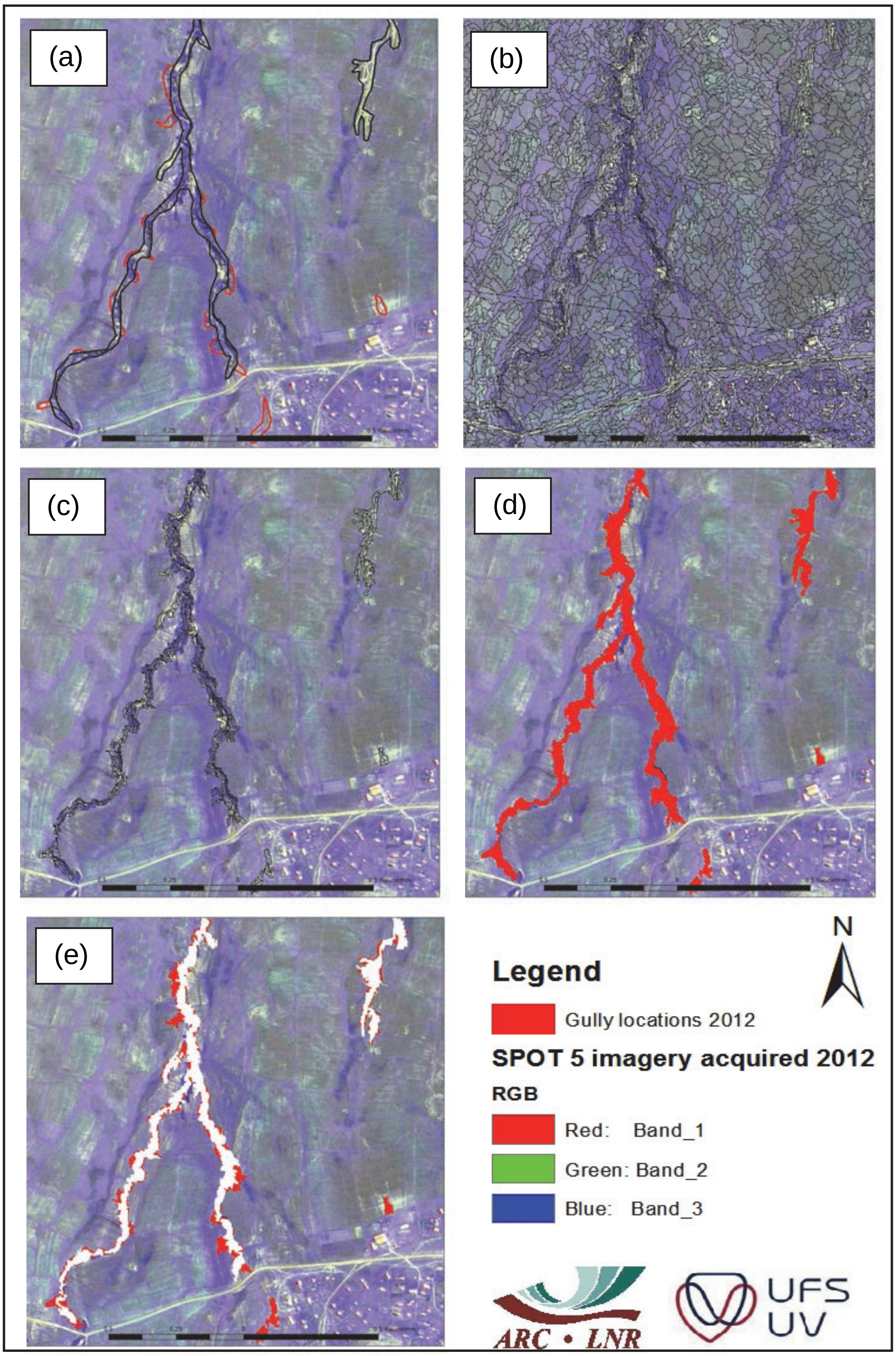

Figure 10: **Maps of a gully near Matatiele illustrating mapping techniques implemented including (a) manual vectorization of newly-developed gullies, (b) creation of image objects, (c) selection of image objects within gullies, (d) dissolved image objects to create single gully polygons, and (e) subtracting the 2007 gully extent layer from the 2012 layer.**

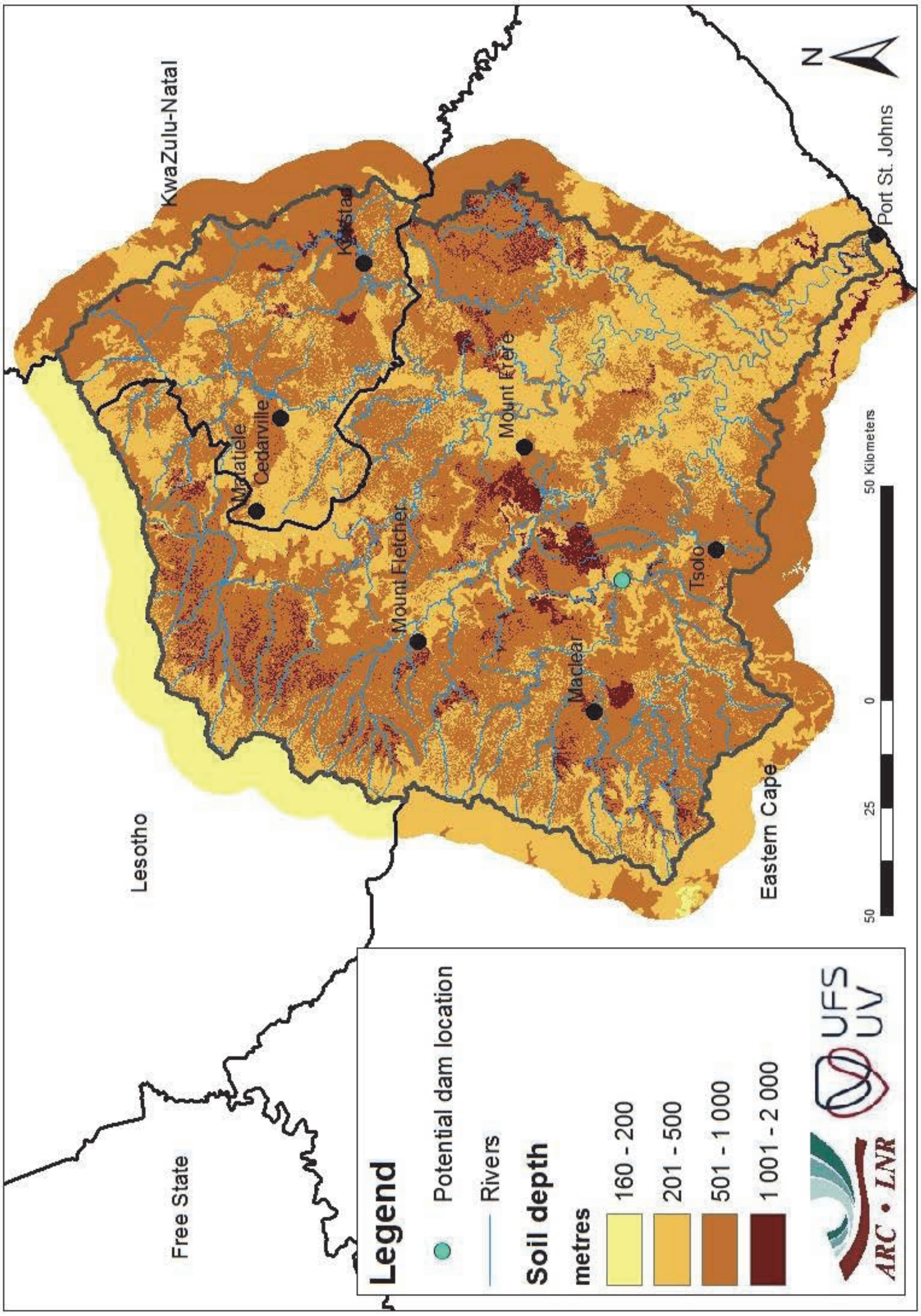

Figure 11: **Soil depth map of the Mzimvubu River Catchment.**

4.2.4 Gully connectivity classification

Gullies were further categorized into connectivity classes that, according to observations (see Figure 1 and Tables 4 and 5 in Appendix 1) uniquely influence sediment yield including connected, partially connected, potentially connected and disconnected with the river network. Gullies that are connected or disconnected with the river network were separated by means of overlay analysis of the gully map and river lines at 1:50,000 scale (NGI, 2013; Weepener *et al*., 2014). Gullies were categorised into 4 classes of (dis)connectivity as follows (Hooke, 2003):

- Fully connected (coarse sediment transfer during 'normal' flood events) – gullies that overlay or "touch" perennial rivers were assumed to be connected and all sediment generated from such gullies contribute to the sediment yield (see Figure 12a);
- Partially connected (transfer only in extreme flood events) – large continuous gullies that overlay and "touch" non-perennial rivers were assumed to be partially connected and only a fraction of the sediment generated from such a gully contributes to the sediment yield (see Figure 12b);
- Potentially connected (competence to transport but lack of supply) – small discontinuous gullies that overlay and "touch" non-perennial rivers were assumed to be potentially connected and only a fraction of the sediment generated from such a gully contributes to the sediment yield (see Figure 12c);
- Disconnected (sediment transfer is obstructed) – gullies that do not overlay and "touch" either perennial or non-perennial rivers were assumed to be disconnected and no sediment generated from such gullies contribute to the sediment yield (see Figure 12d).

Figure 13 illustrates a close-up view of the four gully connectivity categories for a gullied area near the future dam site at Ntabelanga. Streambank erosion was mapped in the same manner and categorised as such. The next step was to calculate the annual average rate at which gullies erode over a simulation period of 5 years between 2007 and 2012.

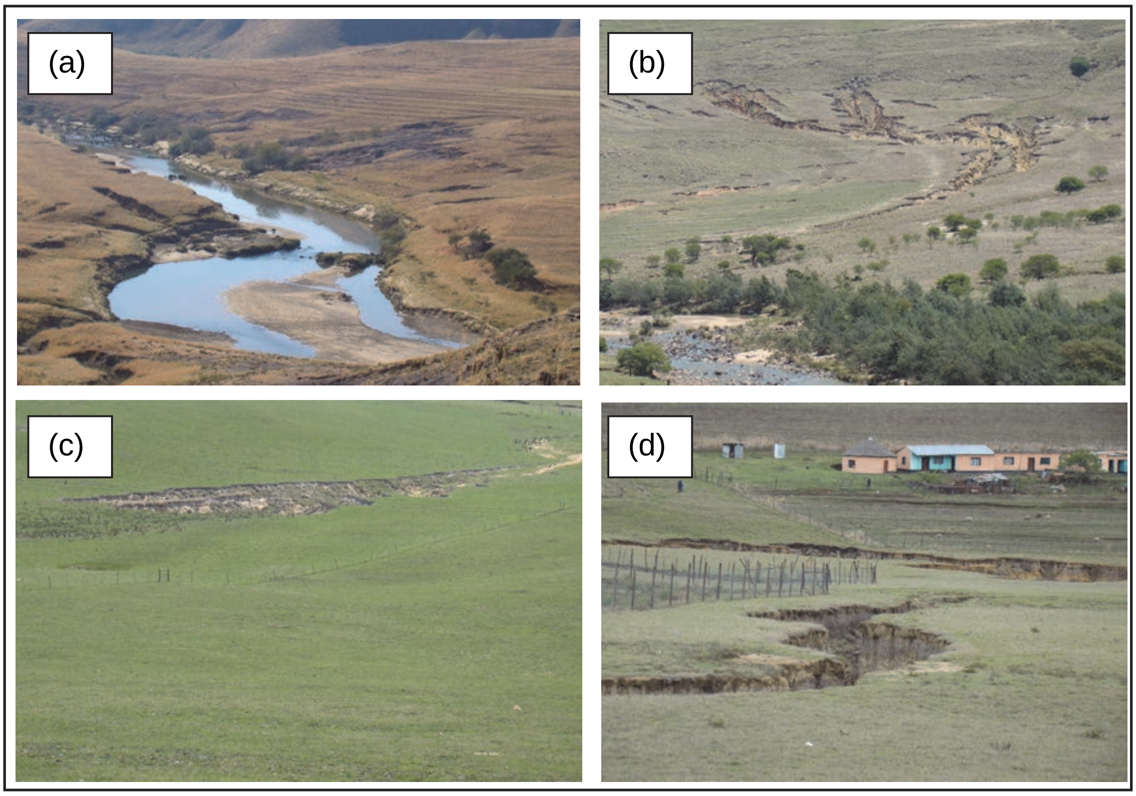

Figure 12: Photos of (a) gully connected with the Tsitsa River; (b) gully partially connected with the Inxu River, (c) gully potentially connected in a wetland near Tsolo, and (d) disconnected gully near Mount Frere.

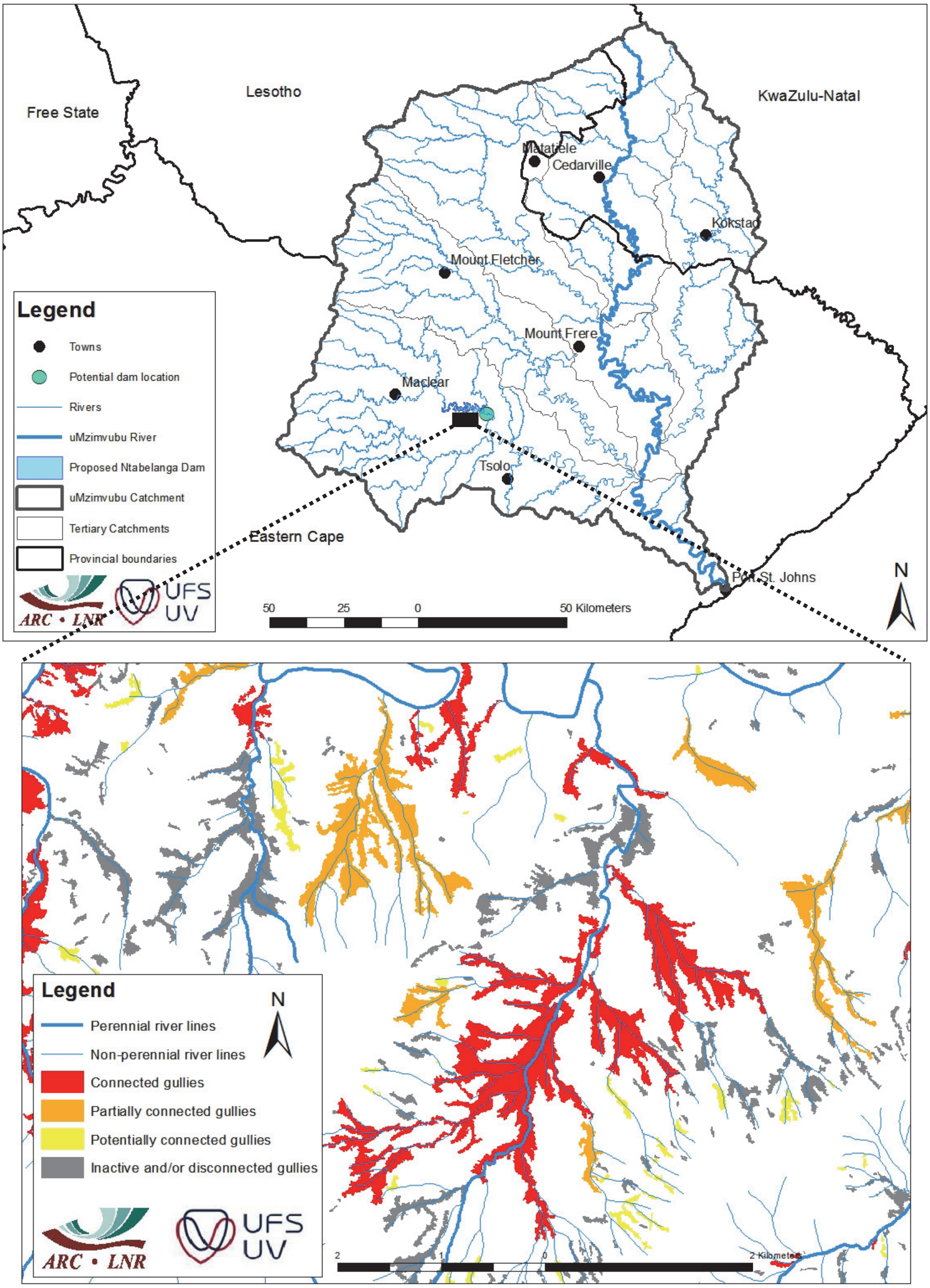

Figure 13: **A gullied area near future dam site illustrating four gully connectivity categories.**

4.2.5 Gully erosion rate assessment

A method similar to Grellier *et al*. (2012) was used to calculate gully volumes and gully erosion rates. Assuming an average bulk density of 1.6 g/cm^3 for the eroded material, the change detection results (in m^3) and gully depths (in m) were used to determine both initial gully volumes and end-volumes (in tonnes). The difference between these volumes provided the gully erosion rate during the simulation period of 5 years between 2007 and 2012. This rate at which soil in partially and potentially connected gullies erode, however, does not entirely contribute to the sediment yield; some of this eroded soil will be deposited somewhere between the gully sites and rivers depending on topography and land use-cover interactions (Rieke-Zapp and Nichols, 2011).

To account for these interactions, this study considered incorporation of the most important factors that could be readily derived for the whole catchment including the (*i*) slope or flow path lengths and (*ii*) slope steepness, as well as a (*iii*) roughness index. The methodology to derive these factors includes:

(*i) C*alculation of the flow path length from each partially and potentially connected gully outlet to the nearest perennial river. This was achieved by incorporating partially and potentially connected gullies into a Network Database in ArcMap® 10.2 (see Figure 14). A point shapefile was created, representing the outlet for each of these gullies. Another point shapefile was created, representing the junctions or destination points of each associated perennial river. In addition, the length of the gullied sections on the non-perennial river lines were calculated to account for the hypothesis that gullies act as a sediment conduit and connectivity increases within these gullied sections. This was achieved by creating gullied line features in the same Network Database representing the gullied sections along the non-perennial rivers (also shown Figure 14).

(*ii*) Calculation of the river slope for each non-perennial river line using automated routines in ArcMap 10.2® (see Figure 15).

(*iii*) Creation of a roughness index factor map to account for the hypothesis that connectivity decreases with increasing channel roughness (see Figure 16). The roughness index factor map was created by combining vegetation cover and rock content information. The vegetation cover map was created from 2012 SPOT 5 derived NDVIs (see Figure 17), whereas the rock factor information was obtained from the agricultural restriction/rock classes in the Land Type database of SA (Land Type Survey Staff, 1972-2012).

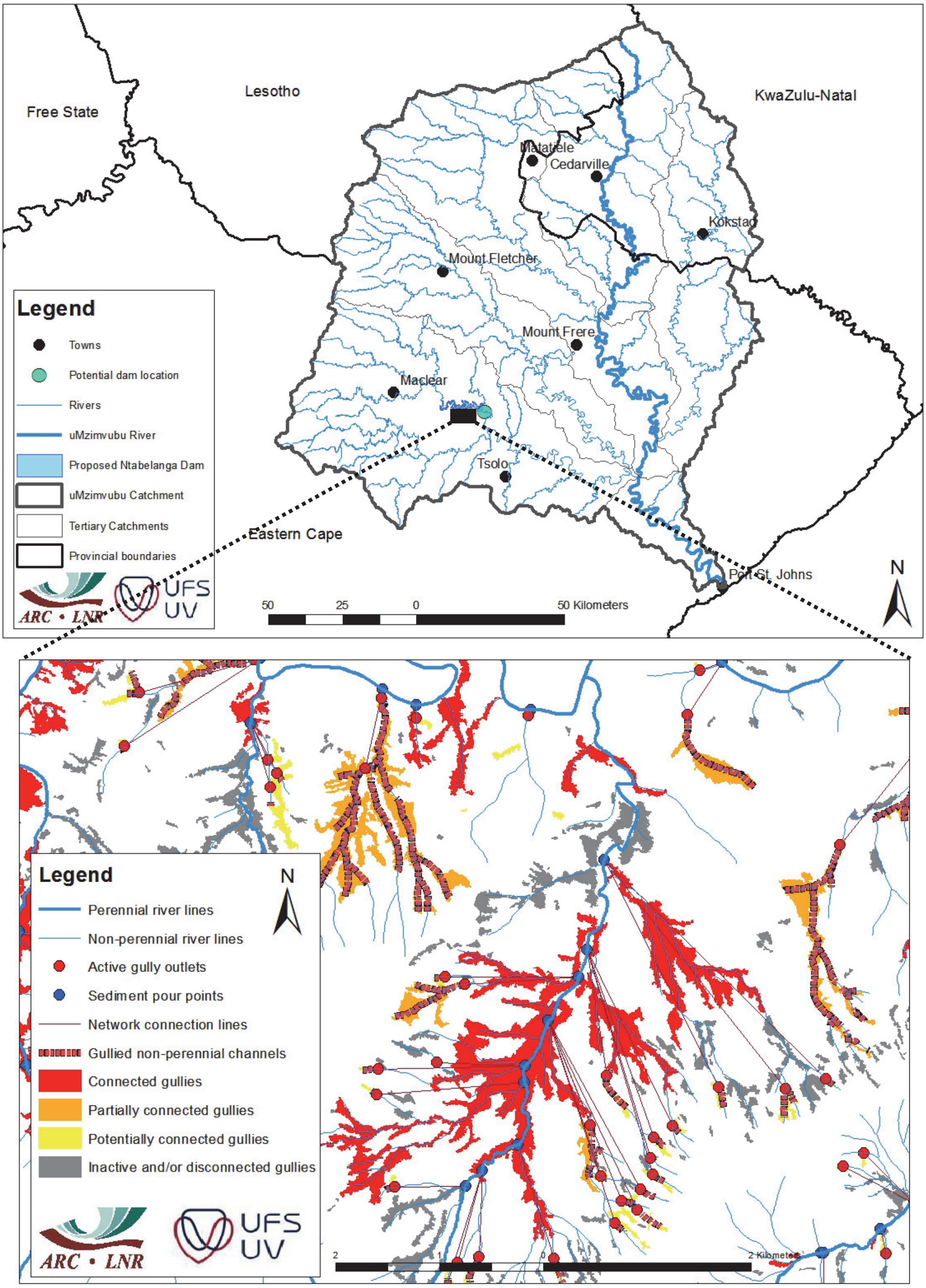

Figure 14: **A gullied area near future dam site illustrating four gully connectivity categories incorporated into a Data Network including gully outlet points, perennial river junctions or destination points, and gullied sections on the non-perennial river lines.**

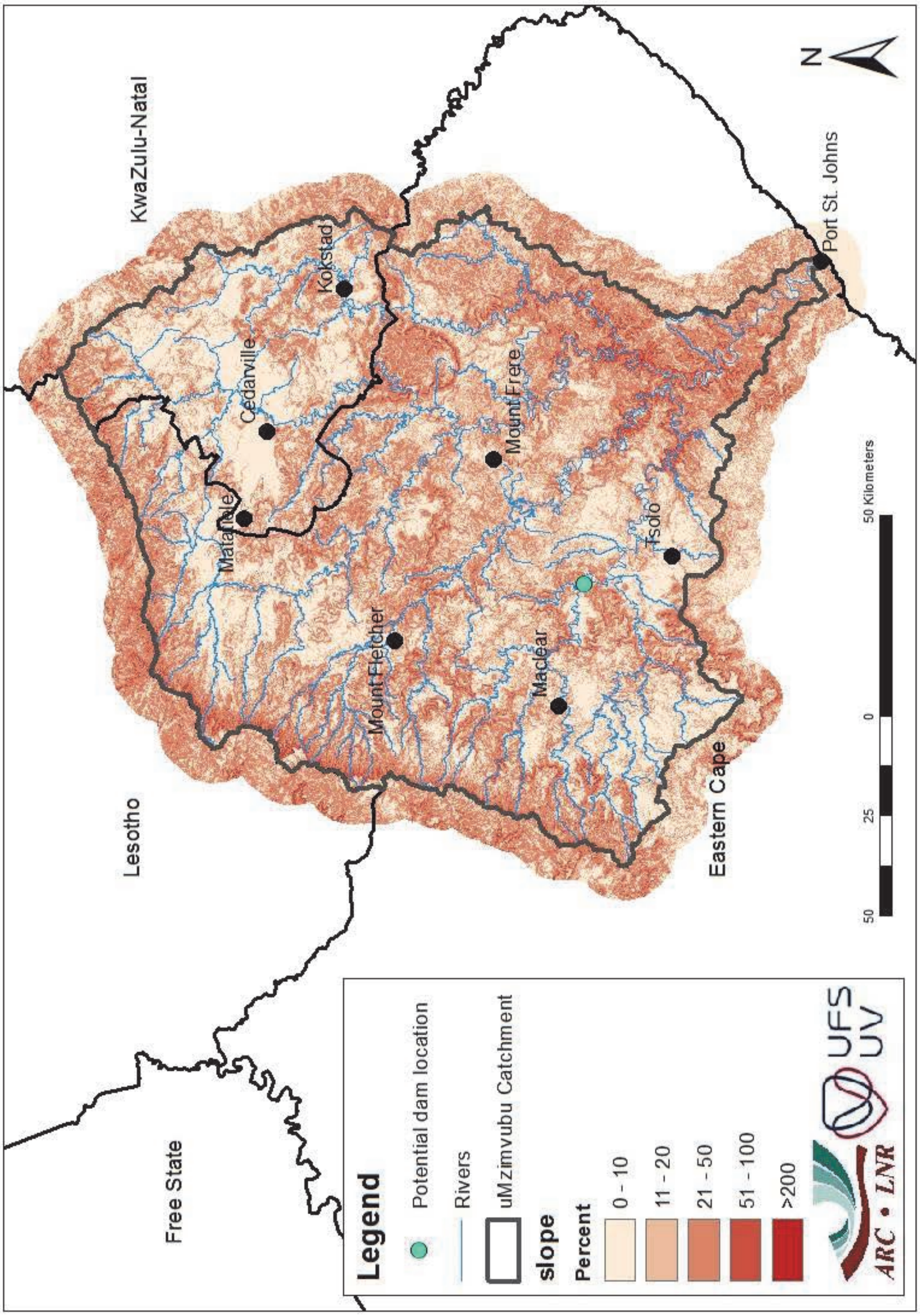

Figure 15: **Slope map of the Mzimvubu River Catchment.**

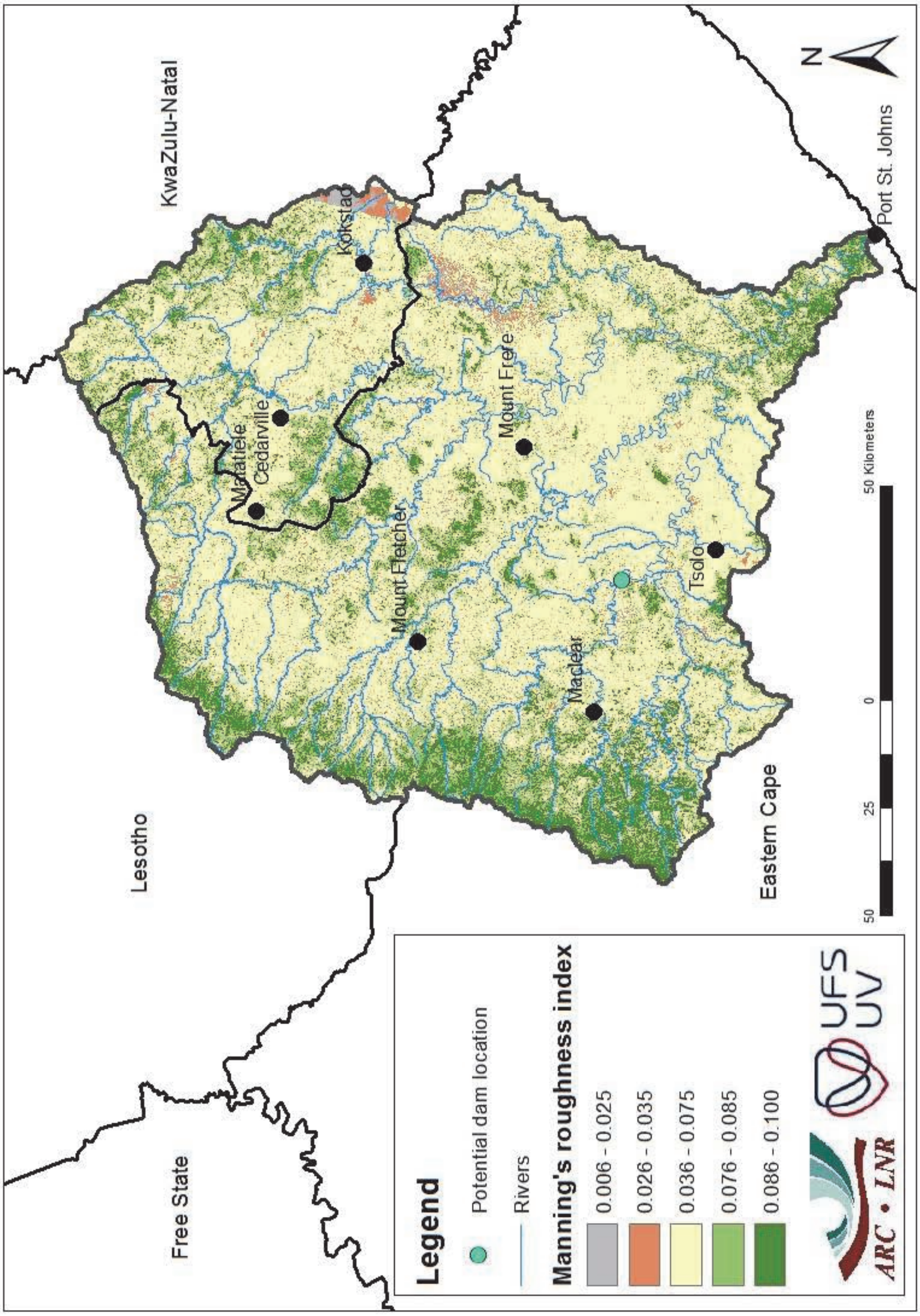

Figure 16: **Roughness index factor map of the Mzimvubu River Catchment.**

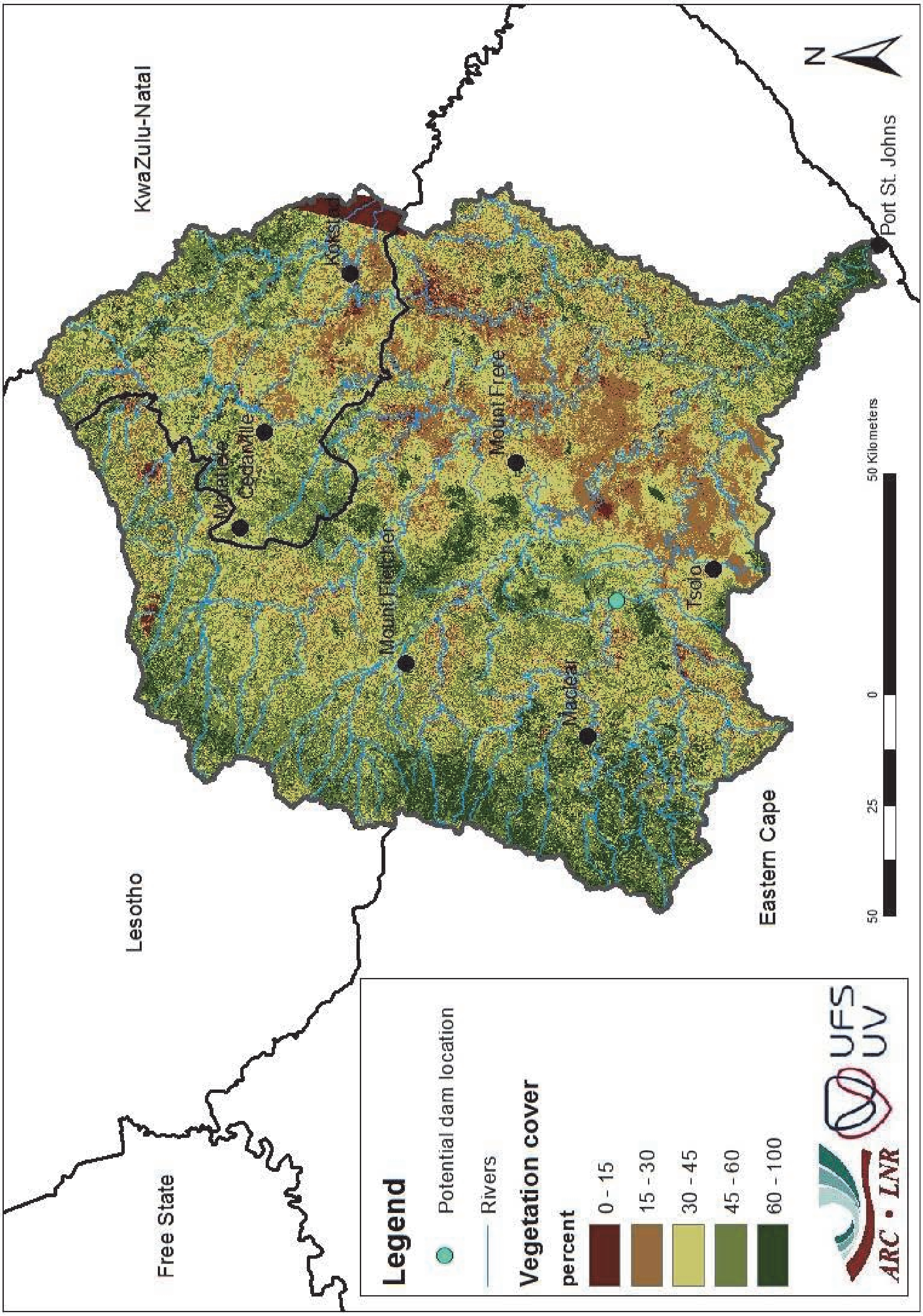

Figure 17: **Vegetation cover map of the Mzimvubu River Catchment.**

Subsequently, the fractions of sediment generated from the partially and potentially connected gullies were adjusted according to rules based on the (*i*) slope or flow path length and (*ii*) slope steepness, as well as a (*iii*) roughness index factor between each gully and perennial river line. The (*i*) flow path length were further adjusted (reduced by a scale-cost distance factor) according to the length of gullied sections. These rules are shown in Appendix 2. For example, a relatively large fraction of sediment reached a river and/or sub-catchment outlet if a gully is near the river and has a steep slope with low vegetation cover and/or roughness (between the gully and the river). In contrast, a relatively small fraction of sediment reached a river and/or sub-catchment outlet if a gully is far from the river and has a smooth slope with high vegetation cover and/or roughness (between the gully and the river).

Finally, an average annual sediment delivery rate was calculated for each mapped gully in the catchment. The average annual sediment delivery rate values were summed to provide the sediment yield contribution from gully erosion for all the sub-catchments and subsequently the whole catchment during the simulation period of 5 years. To compare these results with other studies, gully erosion rates (in tonnes) were divided by 5 years to get an average annual erosion rate, which was further converted to sediment yield (in t/ha·yr). The combination of results from approaches 1 and 2 provided the total sediment yield in the Mzimvubu River Catchment.

5. RESULTS AND DISCUSSION

A description of the sediment yield in the Mzimvubu River Catchment is provided with further detailed description for the Ntabelanga Dam Catchment. Results are displayed as a series of maps and graphs illustrating simulated flow and sediment yield as mean annual averages of the 5 year simulation period between 2008 and 2012 at a sub-catchment/quaternary catchment scale. The SWAT model results describe the sediment yield contribution from sheet and rill erosion in Section 5.1, whereas results from the remote sensing and integrated GIS approach describes the sediment yield contribution from gully erosion in Section 5.2. The total sediment yield, including sheet-rill and gully data integration is described in Section 5.3.

5.1 Sediment yield contribution from sheet and rill erosion

Model simulation was conducted over a period of 5 years (2008 to 2012) preceded by a one-year model “warm-up” initialization period (2007). Figure 18 illustrates (for each sub-catchment) the sediment yield contribution from sheet-rill erosion that is transported into river channels (in t/ha·yr).

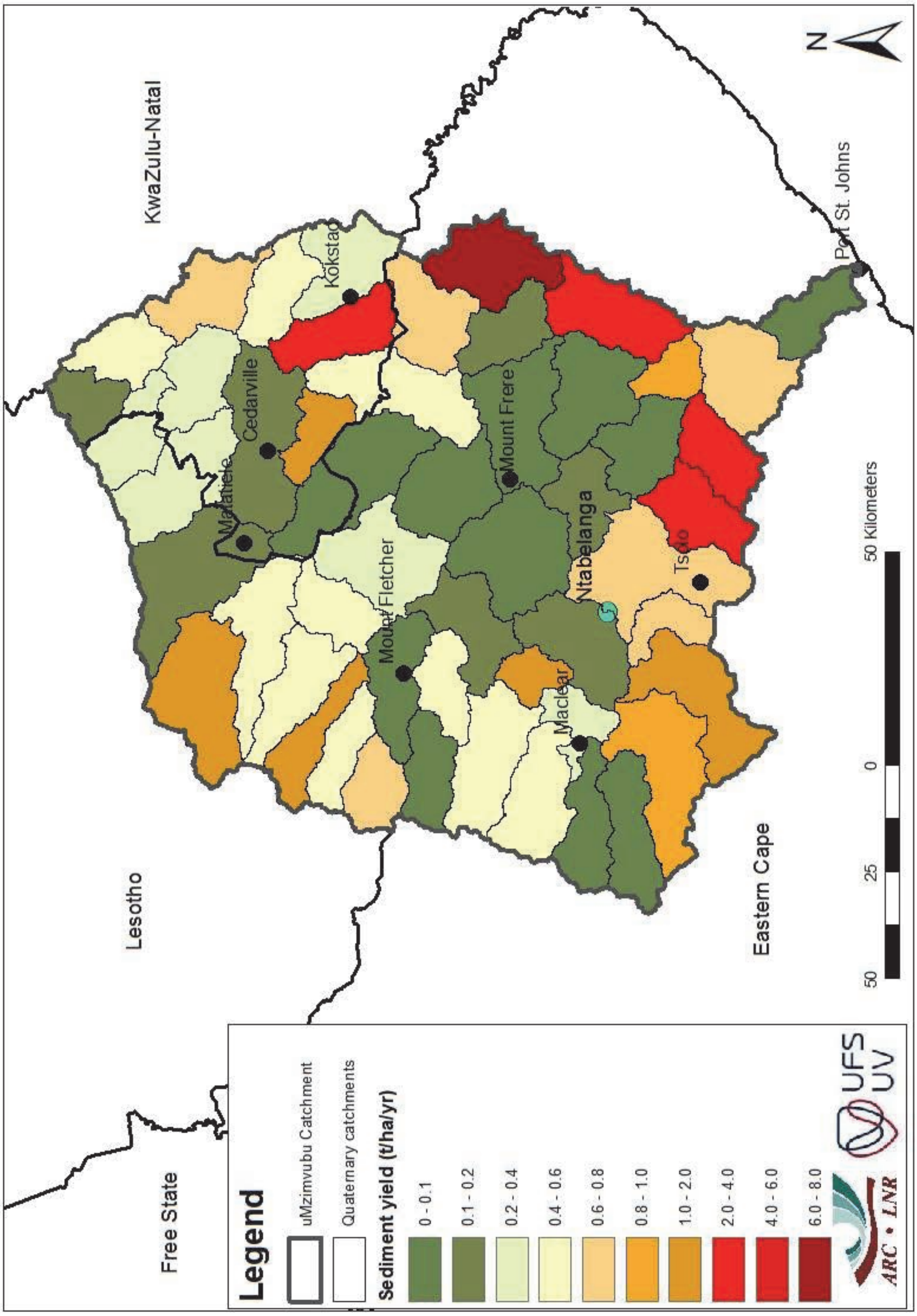

Figure 18: **Sediment yield map for the Mzimvubu River Catchment as simulated by ArcSWAT.**

The sediment yield contribution from sheet-rill erosion range between 0.1 to 8 t/ha·yr per sub-catchment with an overall average of approximately 1.0 t/ha·yr. The sediment yield contribution from sheet-rill erosion of the sub-catchment in which the future dam will be built at Ntabelanga is 0.1 t/ha·yr. According to ArcSWAT simulations, sub-catchments with the lowest sediment yield occur in the central part of the Mzimvubu River Catchment, whereas sub-catchments with the highest sediment yield occur on the periphery. One possible reason for this phenomenon is that USLE-based models such as ArcSWAT overestimates sediment yield in sub-catchments where steep slopes are prominent (Le Roux and Sumner, 2013). Sub-catchments on the periphery of the Mzimvubu River Catchment have steeper slopes compared to sub-catchments in the central part. It is also noteworthy that sub-catchments with relatively good vegetation cover (e.g. near the main catchment outlet in the south) have lower sediment yield than sub-catchments with less vegetation cover (e.g. cultivated areas north of Mount Fletcher). Furthermore, ArcSWAT utilizes the Modified USLE that models only the sheet and rill aspects of the erosion cycle and disregards gully erosion processes. Thus, ArcSWAT probably underestimates soil losses and subsequent sediment yield in the Mzimvubu River Catchment where gullies are prominent.

The following results illustrate the rates as simulated by ArcSWAT for 6 sub-catchment outlets of the future dam, as well as the main catchment outlet at Port St. Johns (see locations in Figure 19). Figures 20 to 22 illustrate the monthly average rates for these outlets including flow, sediment concentration and sediment output. Flow is defined as the average daily streamflow out of sub-catchment channel during the time step (cumecs). Sediment concentration is the concentration of sediment in the sub-catchment channel during the time step (mg/kg), whereas sediment output is the sediment transported with water out of the sub-catchment channel during the time step (tonnes). Figure 20 illustrates that the monthly average flow ranges between 0.5 (at upstream sub-catchments 29, 33 and 37 in the winter months) to over 250 cumecs (at the main catchment outlet in the summer months). Figure 21 illustrates that monthly average sediment concentration range between less than 1 (at upstream sub-catchments 29, 33 and 37 in the winter months) to nearly 150 mg/kg (at sub-catchment 36 in the summer months). Figure 22 illustrates that monthly sediment output range between less than 1 (at upstream sub-catchments 29, 33 and 37 in the winter months) to 110,000 tonnes (at the main catchment outlet in summer).

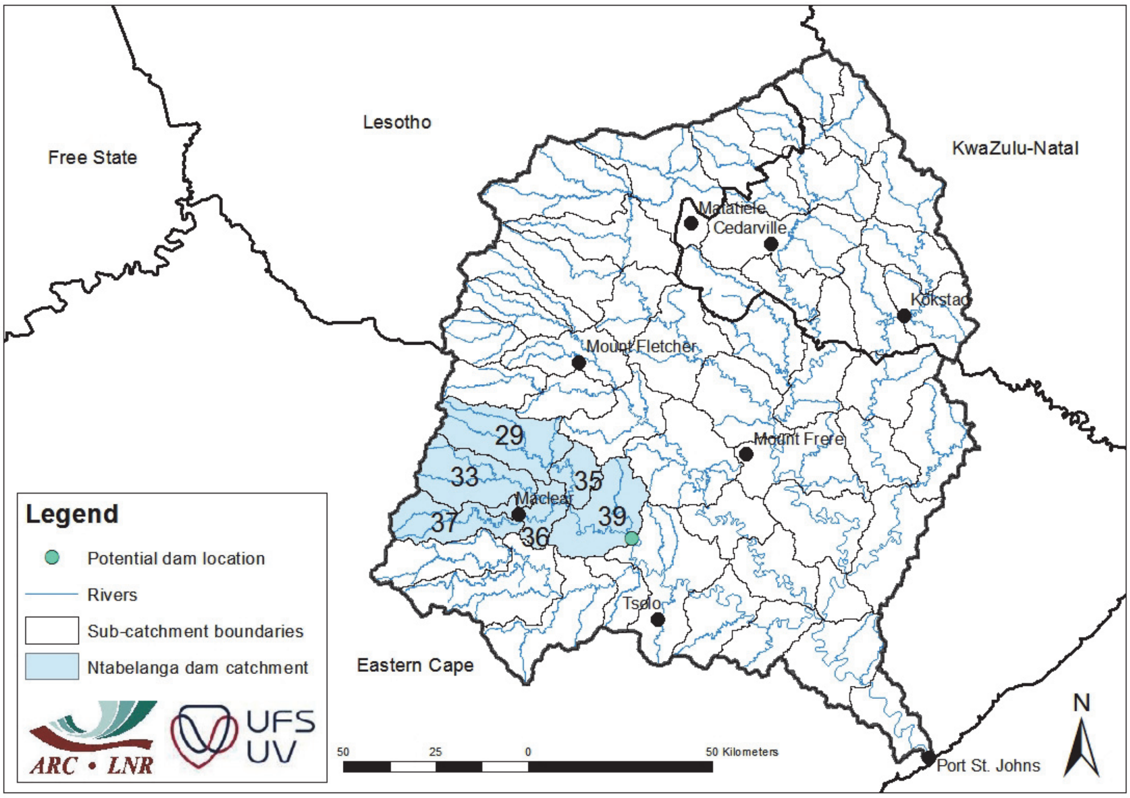

Figure 19: **Location of the sub-catchments of the future dam at Ntabelanga.**

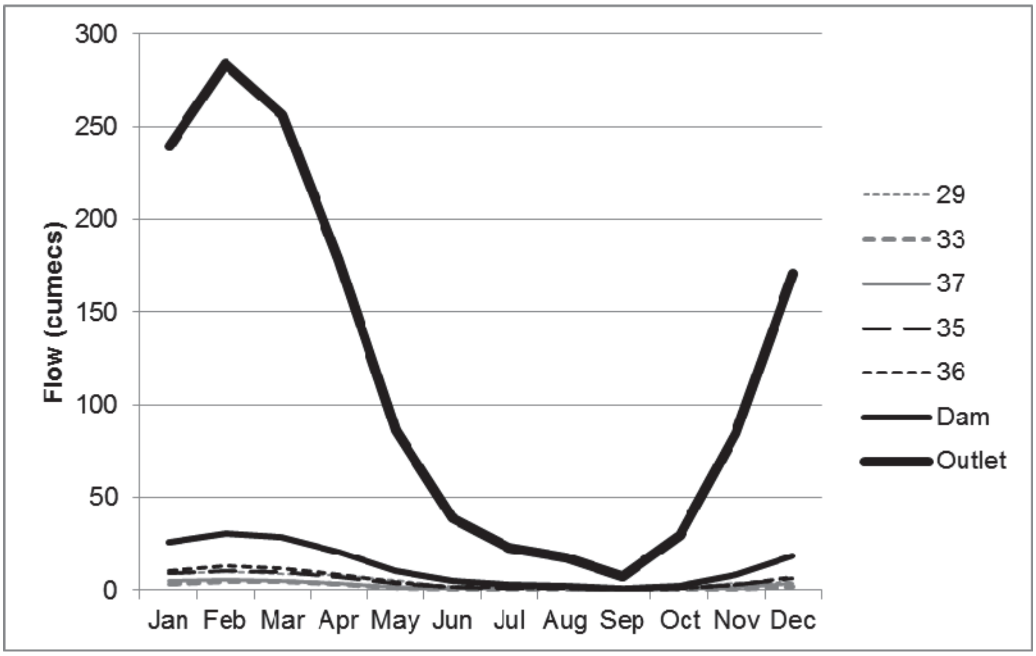

Figure 20: **Monthly average flow rates (cumecs) at 6 sub-catchment outlets of the future dam catchment, as well as the main catchment outlet for the 5 year simulation period between 2007 and 2012.**

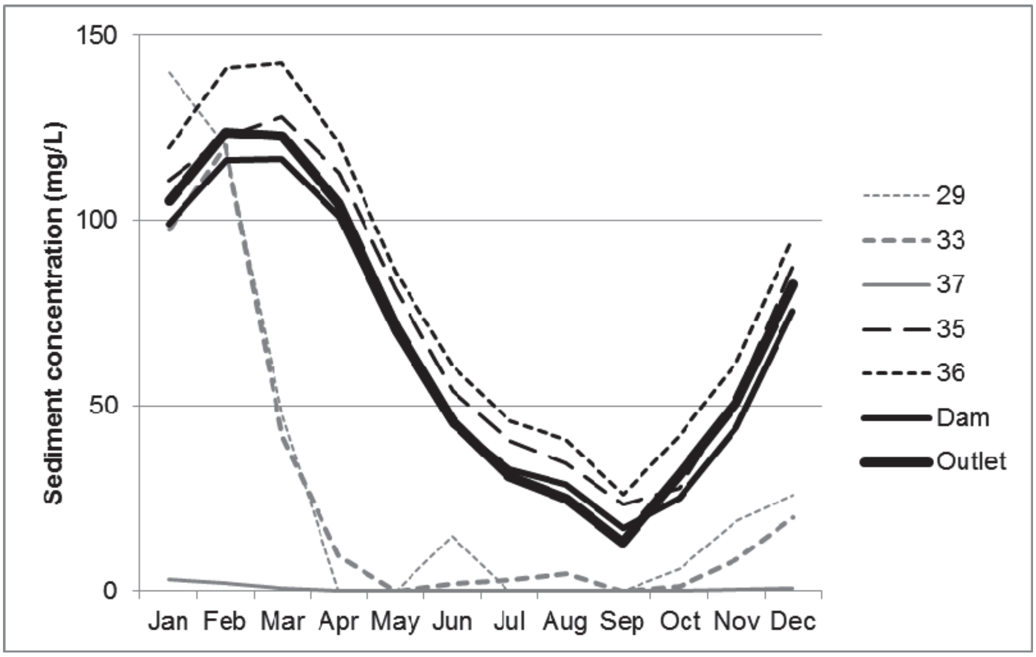

Figure 21: **Monthly average sediment concentration (mg/kg) contribution from sheet-rill erosion at 6 sub-catchment outlets of the future dam catchment, as well as the main catchment outlet for the 5 year simulation period between 2007 and 2012.**

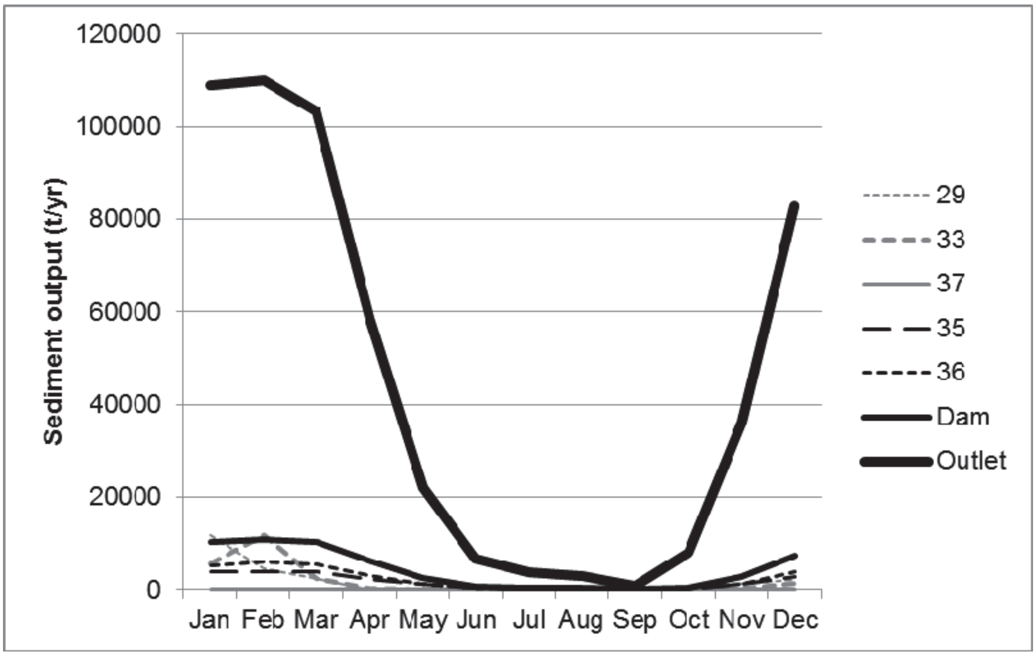

Figure 22: **Monthly average sediment output (tonnes) contribution from sheet-rill erosion at 6 sub-catchment outlets of the future dam catchment, as well as the main catchment outlet for the 5 year simulation period between 2007 and 2012.**

At the future dam site at Ntabelanga, the monthly average flow ranges between 1 (in the winter months) to 30 (in February) (see Figure 20). Monthly average sediment concentration ranges between 17 (in the winter months) to over 100 mg/kg (in the summer months) (see Figure 21). Monthly sediment output ranges between 80 (in the winter months) to over 10,000 tonnes (in February) (see Figure 22).

Figure 23 illustrates that in total, the annual average sediment output contribution from sheet-rill erosion range between 270 (at sub-catchment 37 upstream) to over 50,000 tonnes (at the future dam outlet). According to the results as simulated by ArcSWAT, the average sediment output at the main outlet at Port St. Johns exceeds 500,000 t/yr. It is noteworthy here that the sediment output contribution from sheet-rill erosion at the main outlet (as well as the future dam outlet) is not the sum of the sediment output from sub-catchments upstream. The reason is due to upstream deposition of sediment along the river channels.

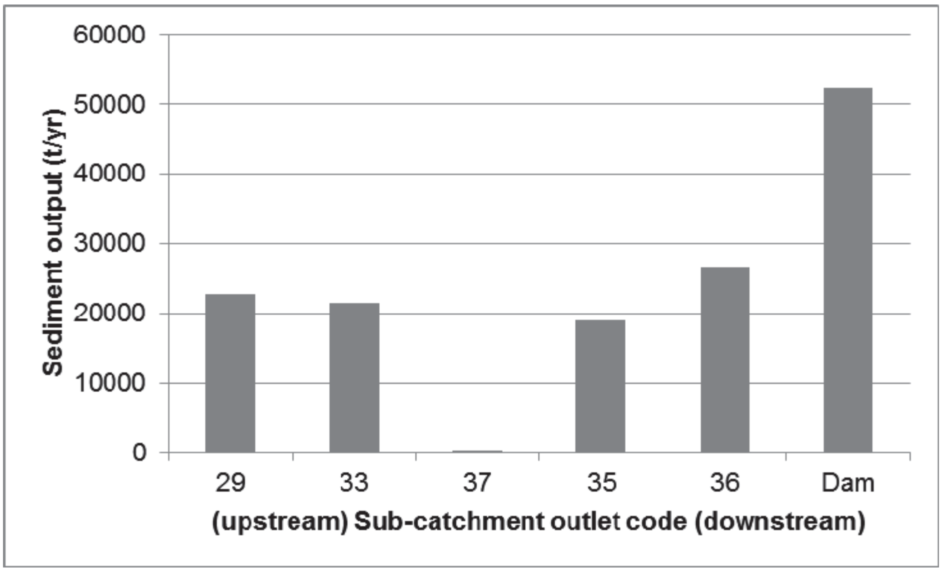

Figure 23: Annual average sediment output contribution from sheet-rill erosion at 6 sub-catchment outlets of the future dam catchment.

Model outputs substantiate several logical criteria regarding sediment dynamics. First, Figures 20 to 22 follow the same parabolic pattern which indicates that sediment output is controlled by the water flux. Second, results clearly illustrate a summer dominant erosion pattern which is mainly caused by intensive summer rainfall between October and April. According to simulations, nearly 80% of the average annual streamflow and 85% of the annual sediment output (approximately 400,000 metric t per annum) are concentrated in the rainy season. Third, sediment outputs increase downstream due to the cumulative contribution of runoff and sediment with increasing spatial scale (routed downstream from upper sub-catchment outlets to the main catchment outlet). Results indicate that sub-catchments with a relatively high sediment yield contribute to high sediment loadings in the river which are subsequently routed to an outlet further downstream as addressed by several other studies (e.g. De Vente *et al*., 2007; Lesschen *et al*., 2009; Le Roux *et al*., 2013). Lastly, results confirm our understanding of the links between source areas of erosion (e.g. steep slopes with poor crop cover) on one hand and areas of deposition on the other (e.g. level slopes with good vegetation cover). Results are consistent with other studies where vegetation cover and soil type of source zones have major influences on sediment generation (e.g. Medeiros *et al*., 2010), whereas good vegetation cover on level slopes serve as zones where sediment is deposited (e.g. Le Roux *et al*., 2013). The average sediment yield of 1.0 t/ha·yr is three times less than the sediment yield estimated by Tibebe and Bewket (2011) (4.3 t/ha·yr) in the Keleta Catchment in Ethiopia. The most probable reason is because 73% of the Keleta Catchment is under extensive cultivation whereas more than 70% of the Mzimvubu River Catchment is covered by natural vegetation and grassland used for grazing. Natural vegetation and pasture areas provide better protection to soil against erosion and reduces sediment delivery.

It is recognized that ArcSWAT probably underestimated the sediment yield contribution from sheet and rill erosion from overgrazed areas in the Mzimvubu River Catchment. However, as mentioned above the main problem is that ArcSWAT utilizes the Modified USLE that models only the sheet and rill erosion and disregards gully erosion processes. ArcSWAT underestimates soil losses and subsequent sediment yield in sub-catchments where gullies are prominent. Figure 24 illustrates the sediment yield map of the catchment as simulated by ArcSWAT superimposed by the gully locations. Section 5.2 describes the results from the remote sensing and integrated GIS approach, representing the sediment yield contribution from gully erosion.

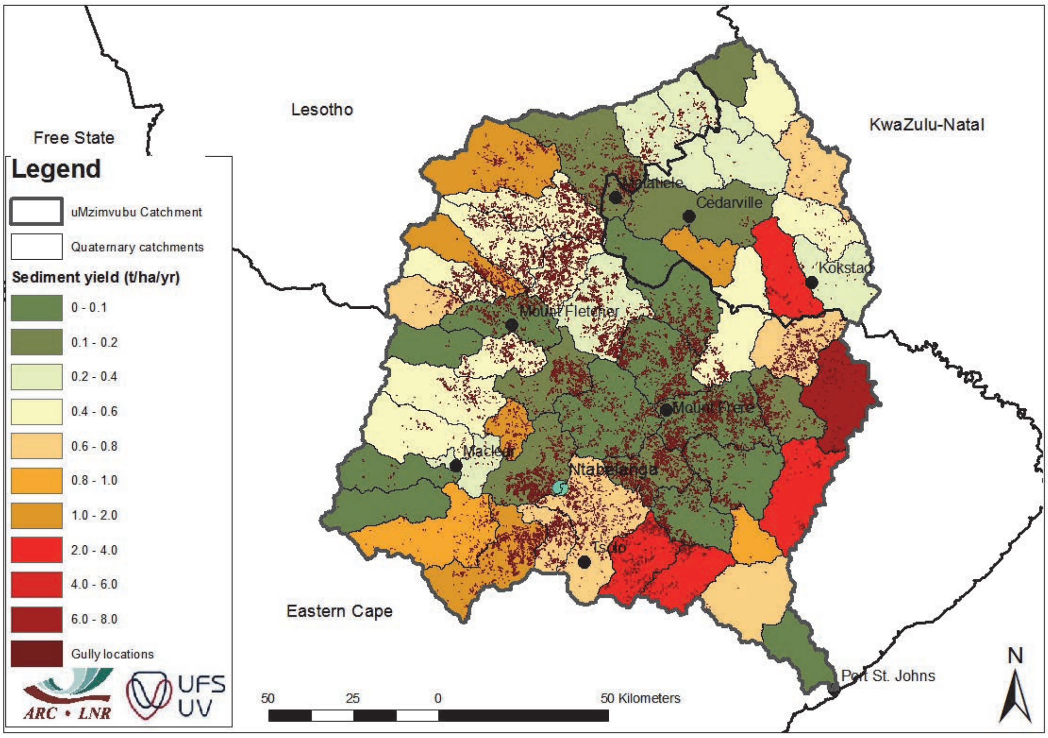

Figure 24: **Sediment yield map for the Mzimvubu River Catchment as simulated by ArcSWAT superimposed by the gully locations.**

5.2 Sediment yield contribution from gully erosion

The sediment yield contribution from gully erosion is presented as a series of maps and graphs over a period of 5 years between 2007 and 2012. Figures 25 and 26 illustrate the previous and updated gully location maps of the Mzimvubu River Catchment respectively. The previous gully location map illustrated in Figure 25 was produced by means of visual interpretation and vectorization from SPOT 5 satellite imagery acquired in 2007, whereas the updated gully location map illustrated in Figure 26 was produced from SPOT 5 satellite imagery acquired in 2012. Figure 27 best illustrates the location of newly gullied areas (active and new gullies) and Figure 28 illustrates a close-up view of newly gullied areas near the future dam site between Tsolo and Maclear. These maps clearly indicate that active gully erosion occurs throughout the catchment. The updated gully location map consists of 29 976 gullies, affecting an area of approximately 28 315 ha (see Table 5).

Compared to the first gully location map created from SPOT 5 imagery acquired in 2007, the updated gully location map consists of 12 265 new gullies, affecting an additional area of 3 970 ha since 2007. Furthermore, 11 643 gullies were active or expanded, affecting an additional area of 2 418 ha since 2007. Active gully expansion range from 10 to 12 840 m^2/yr and averages 1 140 m^2/yr. The number of gullies increased by 65% in the catchment after only 5 years and the surface area affected by gullies increased by 30%. This expansion rate compares well with the estimated total retreat area of 1 530 m^2/yr by Grellier *et al*. (2012) in the upper Thukela River Catchment.

Many gullies expanded sidewise (widen) but the majority expanded at gully heads similar to the findings of Johansen *et al*. (2012). Although most of the new gullies are still small and discontinuous, results indicate that gullied areas increased substantially. This is also evident in Figure 29 illustrating that 37 out of the 52 sub-catchments have a positive active/non-active gully ratio. Therefore, these 37 sub-catchments consist of more active gullies than stable gullies. Sub-catchments 29, 33 and 37 are especially a cause of concern in terms of sediment yield since they are located directly upstream of the future dam at Ntabelanga. These active and still expanding gullies could potentially contribute large amounts of sediment downstream and decrease the life expectancy of the future dam.

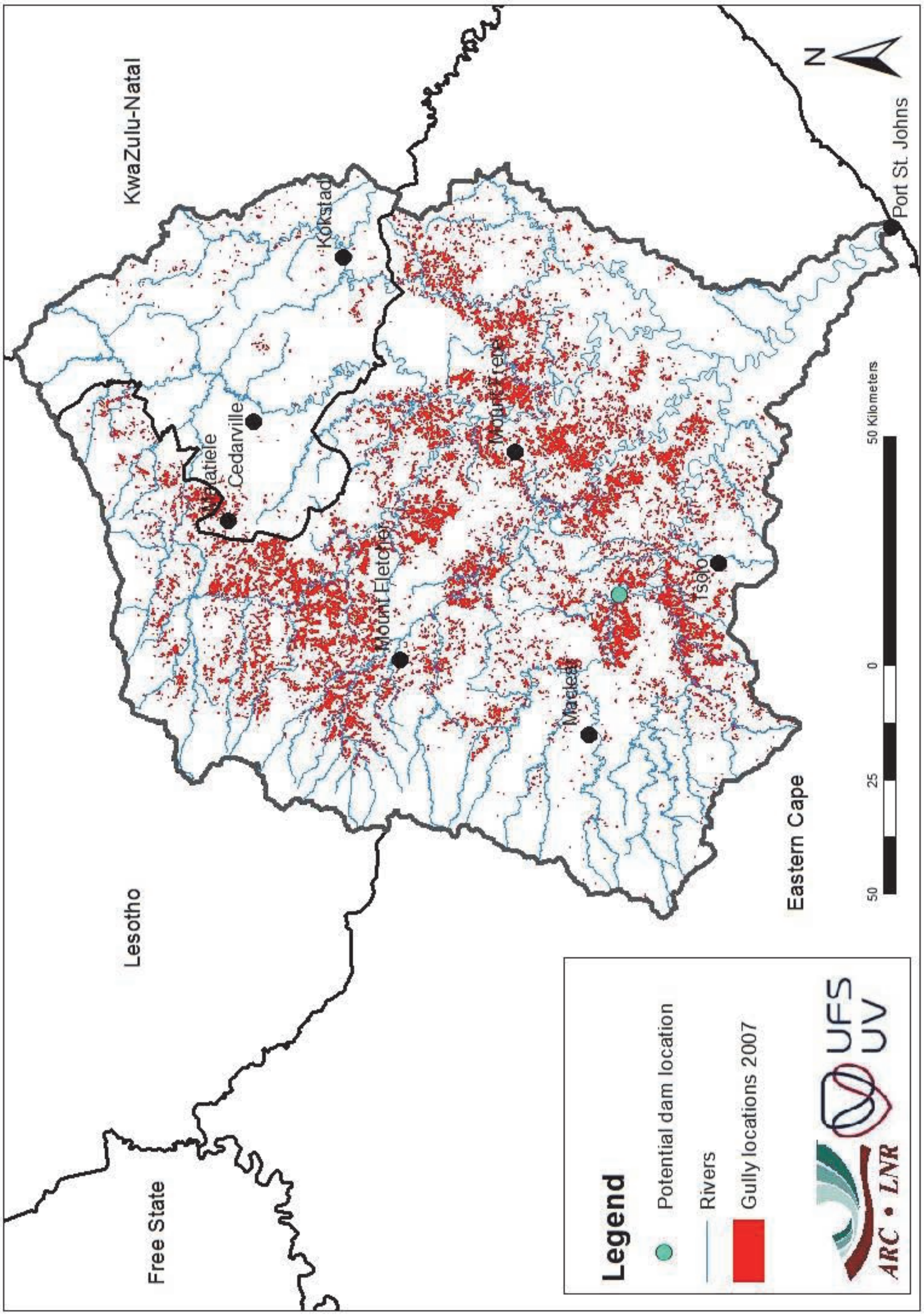

Figure 25: **Previous (2007) gully location map of the Mzimvubu River Catchment.**

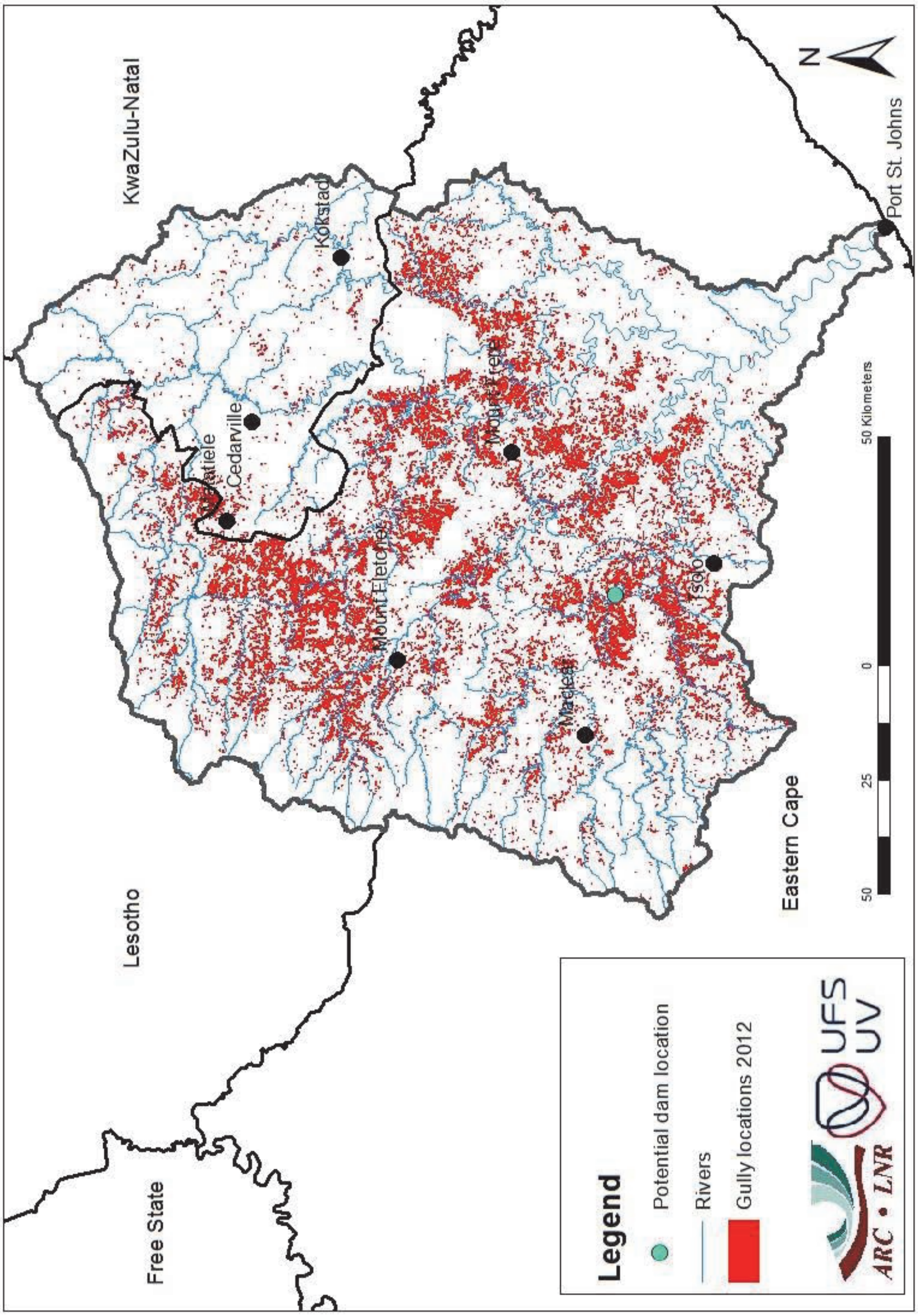

Figure 26: Updated (2012) gully location map of the Mzimvubu River Catchment.

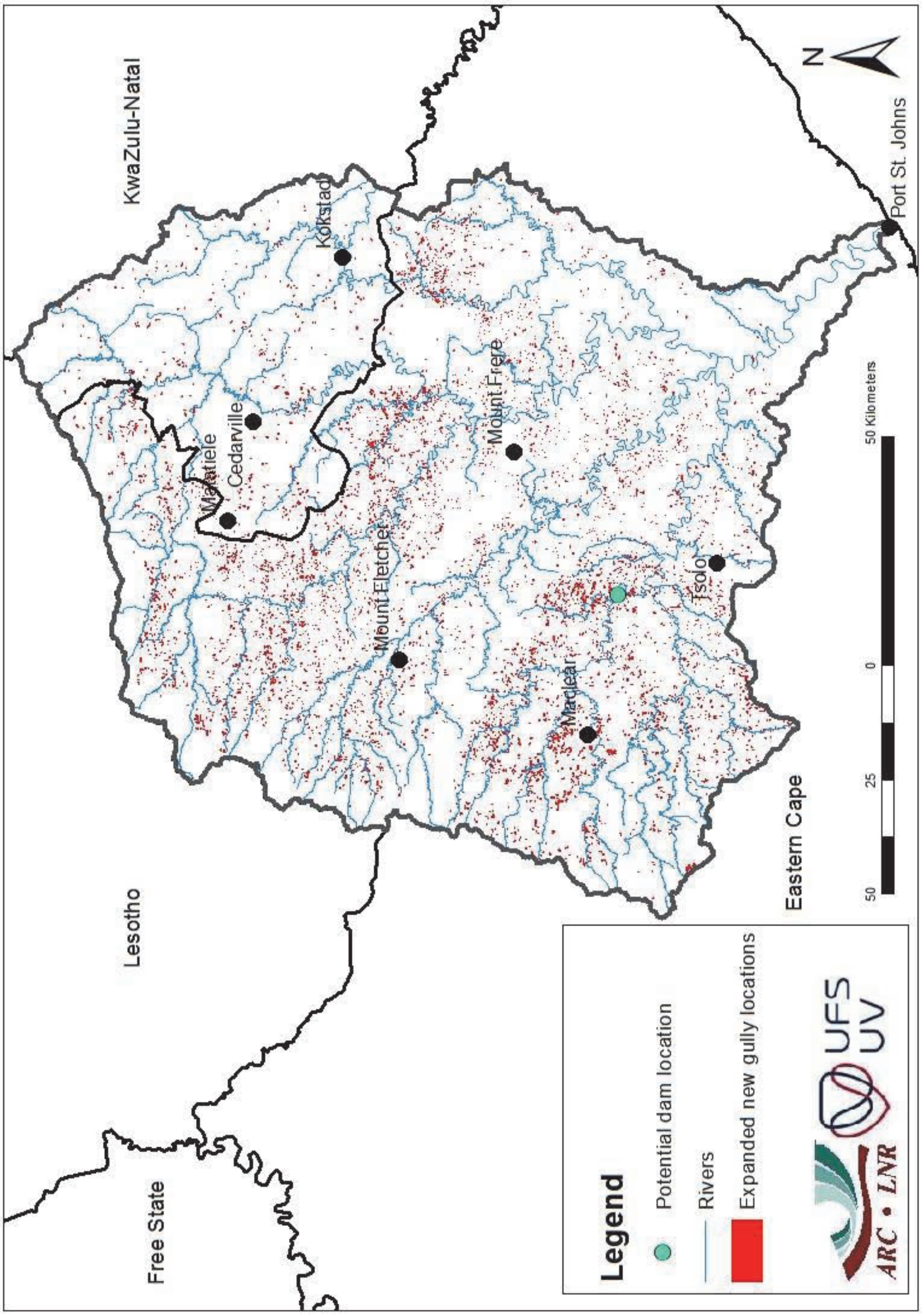

Figure 27: **Location of newly developed and active gullied areas in the Mzimvubu River Catchment.**

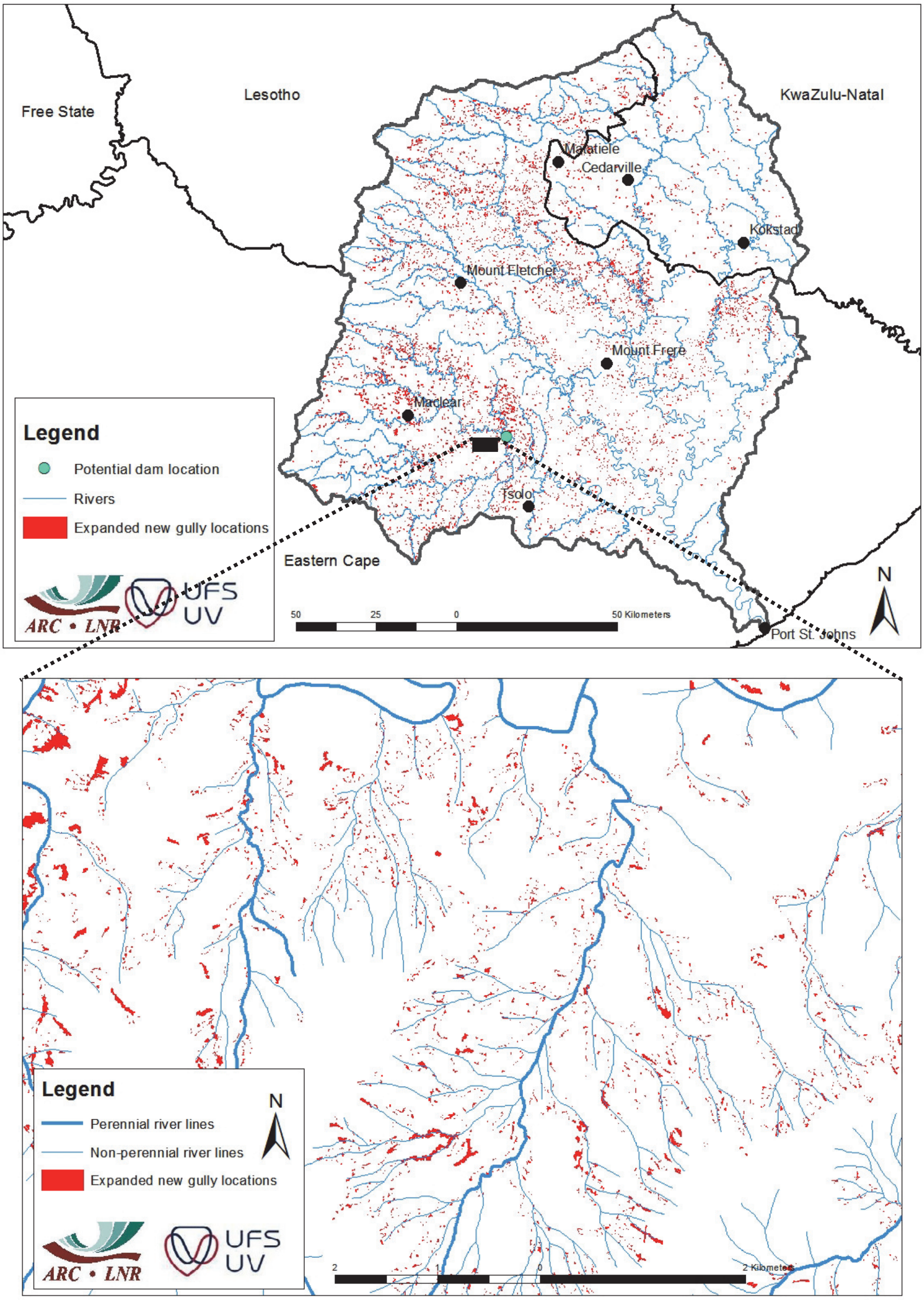

Figure 28: **Location of newly developed and active gullied areas for an area near the future dam.**

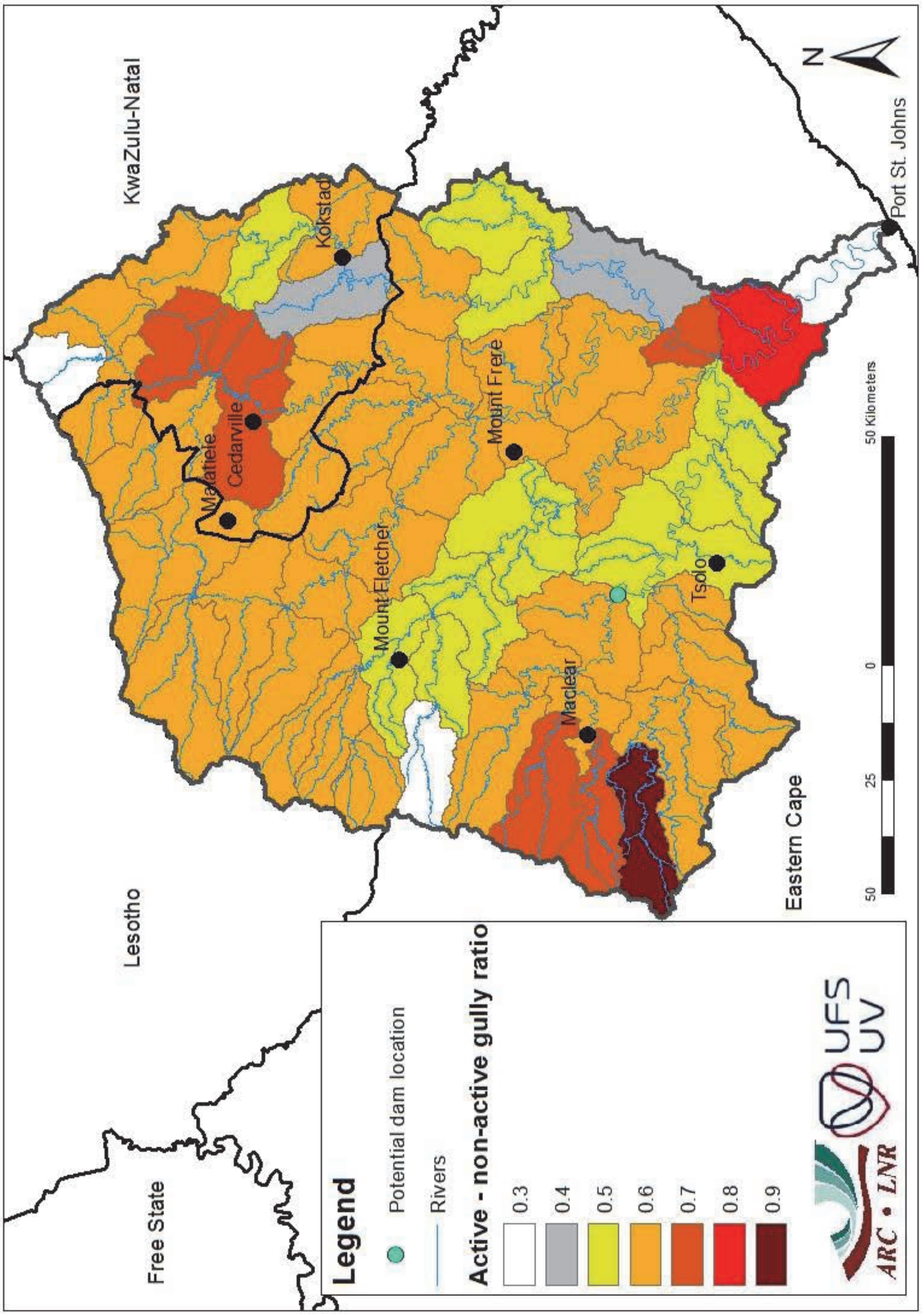

Figure 29: Ratio of active/non-active gullies in the Mzimvubu River Catchment.

Table 5: Summary of the number of new, expanding and connected gullies from 2007 to 2012.

Description	Number of gullies
New	12 265 (3 970 ha)
Expanded	11 643 (2 418 ha)
Connected with other gullies	1 391
Connected with perennial rivers	2 172 in 2007; 3 549 in 2012
Connected with non-perennial rivers	8 427 in 2007; 12 230 in 2012
Connected and active with perennial rivers	2 711
Partially connected (and active) with non-perennial rivers	2 297
Potentially connected (and active) with non-perennial rivers	6 665
Disconnected and/or inactive with all rivers	18 303

Figure 30 illustrates the location of gullies in terms of four categories of (dis)connectivity. Shown in Table 5 above, 2 711 active gullies are connected with perennial rivers, 2 297 active gullies are partially connected with non-perennial rivers, and 6 665 active gullies are partially connected with non-perennial rivers. The Mzimvubu River Catchment consists of 18 303 disconnected and/or inactive gullies.

Figure 31 illustrates the sediment yield map representing the sediment yield contribution from gully erosion. Results indicate that the sediment yield contribution from gully erosion ranges between 0 and 50 t/ha·yr per sub-catchment, with an overall average of approximately 5.0 t/ha·yr. The sediment yield contribution from gully erosion of the sub-catchment in which the future dam will be built at Ntabelanga is 22.4 t/ha·yr.

Figure 32 illustrates that gully erosion contributes over 90 million t/yr to the sediment output of the Mzimvubu River Catchment. Figure 32 also illustrates the annual average sediment output contribution proportionally from connected, partially connected, potentially connected and disconnected gullies. As expected, connected gullies make the largest contribution of more than 50 million t/yr, followed by partially and potentially connected gullies at approximately 20 million t/yr and 15 million t/yr respectively. For the Ntabelanga Dam Catchment, Figure 33 illustrates that the annual average sediment output contribution from gully erosion range between 236 109 (at sub-catchment 37 upstream) to nearly 10 million tonnes (at the future dam outlet). It is noteworthy here that the sediment output contribution from gully erosion at the future dam outlet is not the sum of the sediment output from sub-catchments upstream. The reason is due to large number of active and connected gullies in the sub-catchment where the dam will be built.

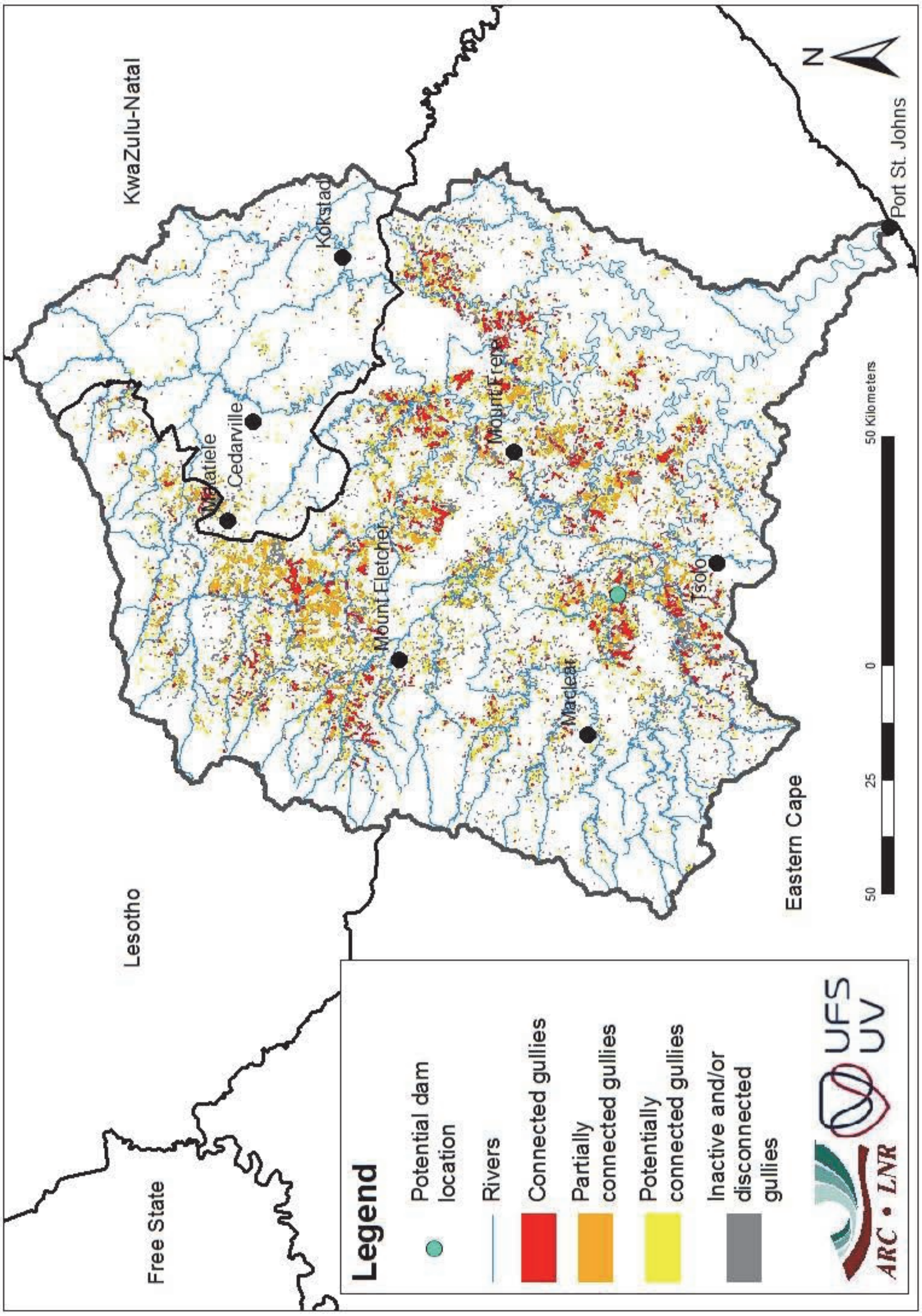

Figure 30: **Location of gullies in terms of four categories of (dis)connectivity in the Mzimvubu River Catchment.**

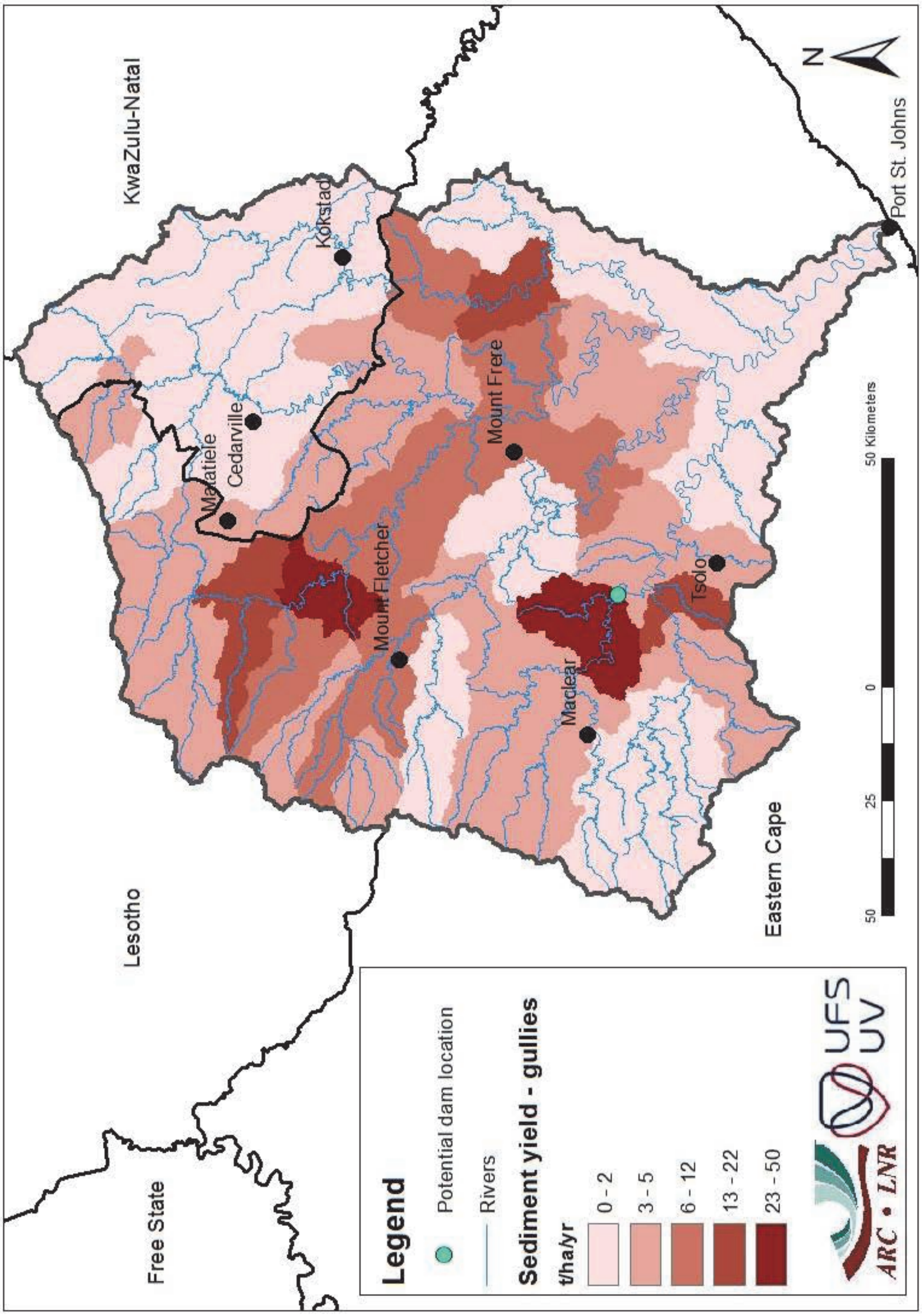

Figure 31: **Sediment yield map – contribution from gully erosion for the Mzimvubu River Catchment.**

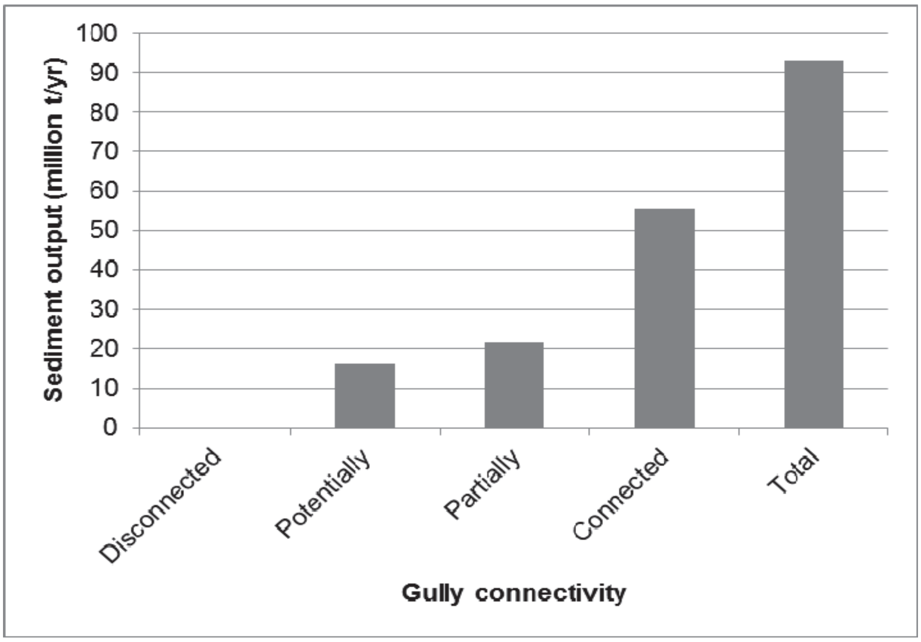

Figure 32: **Annual average sediment output contribution from connected, partially connected, potentially connected and disconnected gullies in the Mzimvubu River Catchment.**

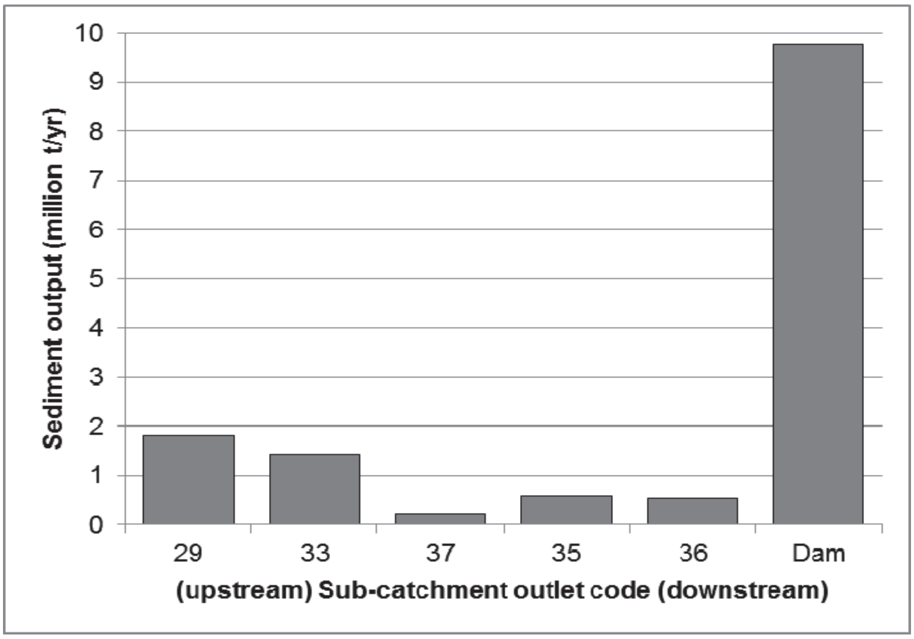

Figure 33: **Annual average sediment output contribution from gully erosion at 6 sub-catchment outlets of the future dam catchment.**

Model outputs indicate that gully erosion contributes significantly to the sediment yield in the Mzimvubu River Catchment. Although in reality not all the sediment generated by gullies will reach the future dam outlet, once the sediment reaches a perennial river the sediment can be rapidly transported downstream as suspended load (Podwojewski *et al*., 2011; Rieke-Zapp and Nichols, 2011). Grellier *et al*. (2012) observed in the upper Thukela River

Catchment that once gully erosion occurs, the sediment from the gully is exposed to rainfall and/or runoff and easily transported downstream. It is therefore hypothesised that the sediment yield estimated for perennial rivers will be exported relatively rapidly to sub-catchment outlets.

The sediment yield contribution from gully erosion compares well with gullied areas referenced in Poesen *et al*. (2003) ranging between 0.1 and 64.9 t/ha·yr. However, our estimated rate of 22.4 t/ha·yr in sub-catchment 39 where the future dam will be built is 9 times less than that (200 t/ha·yr) estimated by Grellier *et al*. (2012) in the upper Thukela River Catchment in South Africa. Although the study area of Grellier *et al*. (2012) has environmental similarities (sub-humid grassland) to the Mzimvubu River Catchment, aforementioned study area is only 2.5 km^2 including only one large continuous gully system. The Mzimvubu River Catchment is much larger including numerous continuous gullies with similar excessive rates. The sediment yield contribution from these numerous continuous gullies compares with the gully erosion rates of badlands in France (Descroix and Olivry, 2002), as well as badlands in the Barasona Catchment in Spain with erosion rates of 302-455 t/ha·yr (Martínez-Casasnovas and Poch, 1998 in Grellier *et al*., 2012). Although the approach to estimate sediment yield contribution from gully erosion could not be validated, it seems as if it produced realistic results.

5.3 Total sediment yield

Integration of the sheet-rill and gully results produced a total sediment yield map of the Mzimvubu River Catchment that is illustrated in Figure 34. Results indicate that the sediment yield ranges between 0 and 50 t/ha·yr per sub-catchment, averaging approximately 5.0 t/ha·yr. The highest sediment yield of 50 t/ha·yr is simulated for sub-catchment 15 north of Mount Fletcher, followed by 22.5 t/ha·yr for sub-catchment 39 at Ntabelanga where the future dam will be built. Sub-catchment 43 west of Tsolo has the third highest sediment yield of 20.4 t/ha·yr. Low sediment yield values between 0 and 1 t/ha·yr are simulated for sub-catchments east of Matatiele and for sub-catchments in the south near the main catchment outlet, as well as some sub-catchments in the Drakensberg Mountains in the west. These sub-catchments have relatively good vegetation cover and stable soils.

In the Ntabelanga Dam Catchment the sediment yield range between 1 t/ha·yr (at sub-catchment 37 upstream) to above-mentioned 22.5 t/ha·yr (at sub-catchment 39 downstream where the future dam will be built) (see Figure 35). Figure 36 illustrates that the annual average sediment output in the Ntabelanga Dam Catchment range between a quarter million t/yr (at sub-catchment 37 upstream) to nearly 10 million t/yr (at the future dam outlet). Results illustrate that gully erosion feed massive amounts of sediment into the river network, contributing approximately 20 times more to the sediment output than sheet-rill erosion.

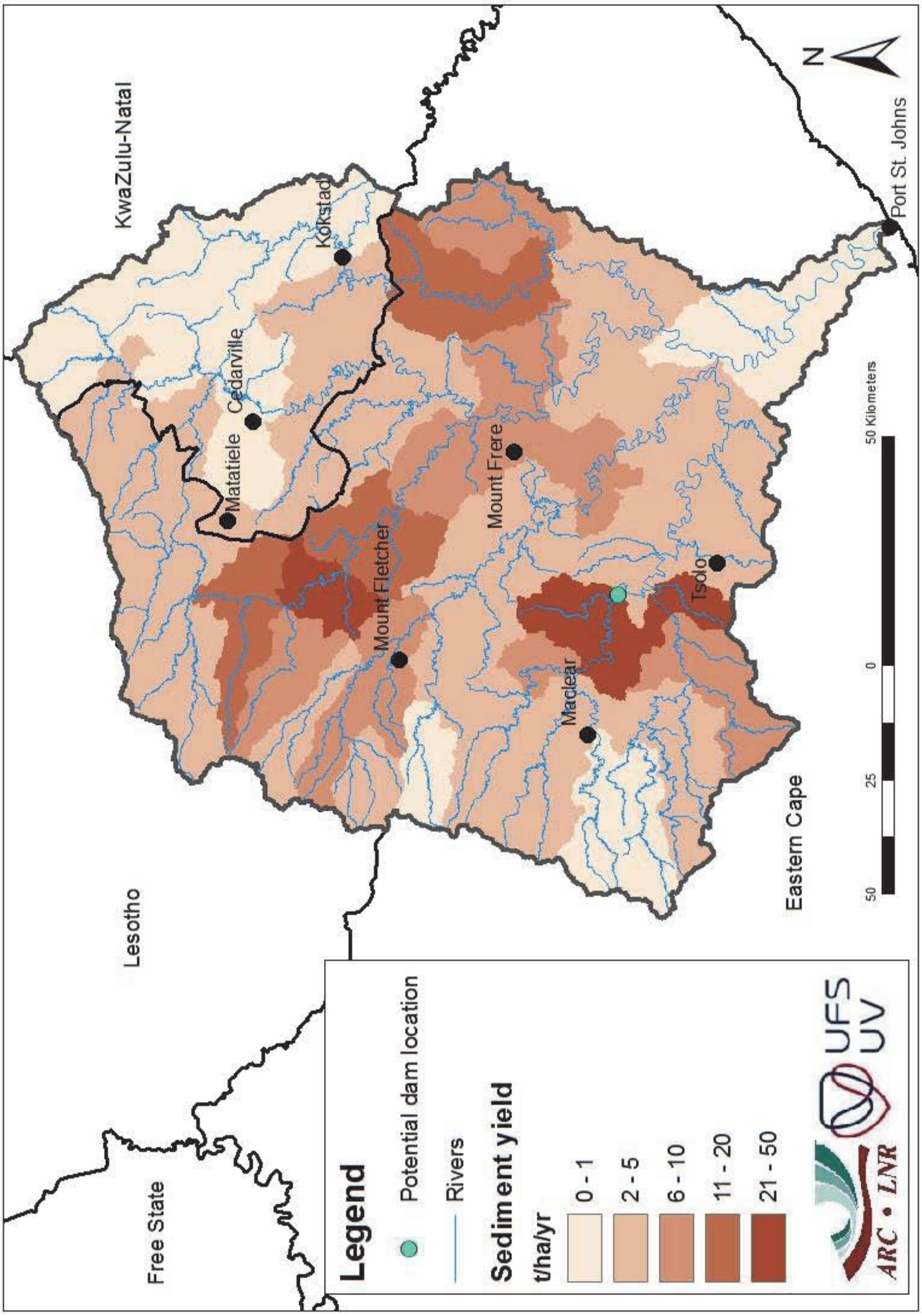

Figure 34: **Total sediment yield map of the Mzimvubu River Catchment.**

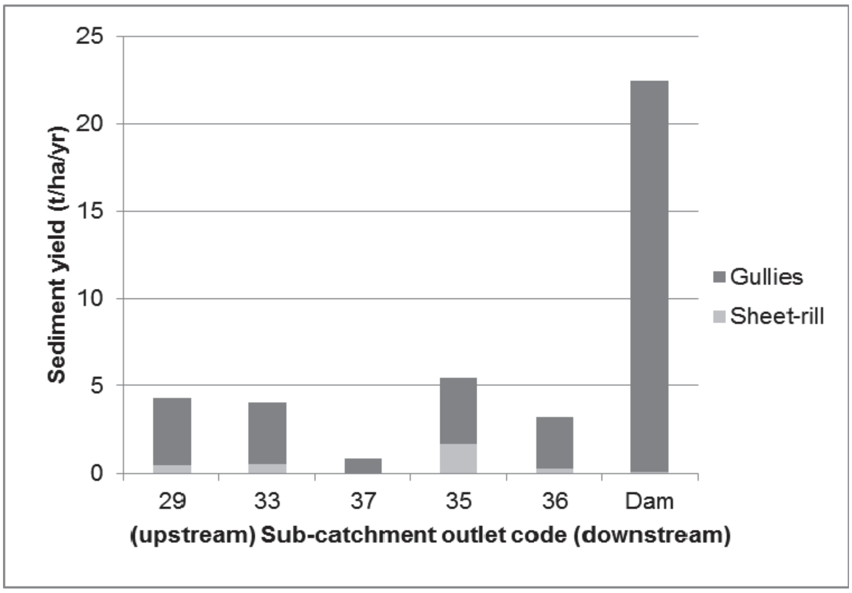

Figure 35: **Annual average sediment yield contribution from sheet-rill and gully erosion at 6 sub-catchment outlets of the future dam catchment.**

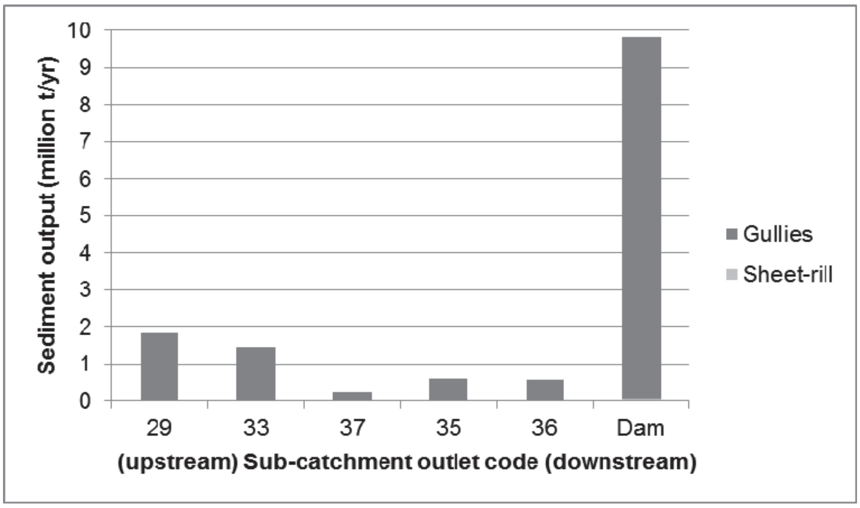

Figure 36: **Total annual average sediment output at 6 sub-catchment outlets of the future dam catchment.**

5.3.1 Causal factors

Although each sub-catchment has different processes and factors contributing to the sediment yield dynamics, gully erosion is the dominant process and sediment yield contributor. In general, factors leading to the development of gullies are gentle footslopes in zones of saturation along drainage paths with a large contributing area, erodible duplex soils derived from mudstones, and poor vegetation cover due to overgrazing (Le Roux and Sumner, 2012). A combination of overgrazing and erodible duplex soils derived susceptible mudstones proves to be key factors that determine the development of gullies in the catchment.

It should be noted that soils in the Ntabelanga Dam Catchment are underlain by Tarkastad, Elliot and Molteno Formations associated with duplex soils that are highly erodible with widespread gully erosion. Table 6 ranks the main geology types of the Ntabelanga Dam Catchment from highest to lowest in order of the percentage affected by gullies. Approximately 60% of gullies are situated on Tarkastad mudstones. Soils from these mudstones are notably different from other soils in the catchment. These soils have a marked increase in clay content from the topsoil to subsoil horizon and are therefore named duplex soils. Duplex soils have an abrupt transition between the topsoil and the subsoil with respect to texture, structure and consistence (Samadi *et al*., 2005; Van Zijl *et al*., 2013). These soils limit intrinsic permeability since water does not move readily into the subsurface matrix, which leads to increased subsurface flow causing tunnel erosion (Beckedahl, 1998; Van Zijl *et al*., 2013). In addition, several studies agree that soils prone to tunnel erosion are usually dispersive and easily lose aggregation as a result of high sodium absorption (e.g. Rienks *et al*., 2000; Valentin *et al*., 2005). However, due to the lack of spatial information at a regional scale, the correlation between gullies and sodic soils still needs further investigation.

Current observations further indicate that erosion sites occur commonly in susceptible geologies under subsistence farming areas. Many sub-catchments have high livestock concentrations. Consequently, overgrazing occurs which significantly contributes to high erosion rates. Furthermore, it seems as if gullies develop along pathways and livestock tracks. The adoption of conservation farming practices is required in these areas, especially in the Ntabelanga Dam Catchment.

Table 6: Geology types in the Ntabelanga Dam Catchment ranked in order of the percentage surface area affected by gully erosion.

Lithology description	Area (ha)	Area containing gullies (%)	Gullies inside geology (%)
Drakensberg basaltic lava	212 222 000	0.01	0.08
Drakensberg pyroclastic rocks	38 346 000	0.09	0.09
Clarens fine-grained sandstone, siltstone	212 320 000	0.17	0.93
Elliot red and greenish grey mudstone	778 576 000	0.18	3.70
Alluvium	63 153 200	0.21	0.34
Karoo dolerite network of dolerite sills, sheets and dykes	484 783 000	0.27	3.39
Adelaide mudrock, subordinate sandstone	317 100 000	0.69	3.78
Molteno Alternating sandstone, olive mudstone and dark grey shale	1 571 470 000	1.90	28.03
Tarkastad red and greenish-grey mudstone	1 203 560 000	0.79	59.21

Although it is postulated that large rainfall events play an important role in gully development, the manner in which event driven processes influence gully development and sediment generation still needs to be researched in the Mzimvubu River Catchment. The importance of rainfall erosivity or large rainfall events as a contributing factor needs to be assessed by comparing active gully development with rainfall event data. Results in Section 5.1 clearly illustrate a summer dominant sheet-rill erosion pattern which is mainly caused by intensive summer rainfall that possibly coincides with low vegetation cover. Nearly 80% of the average annual streamflow and 85% of the annual sediment output contribution from sheet-rill erosion are concentrated in the rainy season.

5.3.2 Dam life expectancy

Modelling of the sediment yield made it possible to estimate the dam life expectancy for the future dam at Ntabelanga on the Tsitsa River. Based on digital elevation data in a GIS, the future dam will have a surface area of approximately 21 742 176 m^2 and a volume of 302 017 955 m^3. The sediment output at the outlet of sub-catchment 39 where the irrigation dam will be built is estimated at nearly 10 million t/yr. Assuming an average bulk density value of 1.6 g/cm^3, the sediment volume that will be deposited in the dam equates to 6 138 097 m^3/yr. As a result, the life expectancy of the dam will be approximately 49 years without proper siltation prevention or design measures. This number, however, accounts for the sediment output in sub-catchment 39 alone and not the sediment output from the other sub-catchments upstream of the future dam (including 29, 33, 35, 36, 37 and 39). If the sediment output from the other sub-catchments upstream of the future dam is also taken into account (by summation of their sediment output), the life expectancy of the dam could be 34 years without proper siltation prevention or design measures. The future dam at Ntabelanga could therefore experience a similar fate as the Welbedacht Dam near Dewetsdorp in the Free State where the storage capacity reduced by more than 80% in just twenty years after completion (DWA, 2011).

The fact that soil erosion is naturally highly variable needs to be recognized (Lu *et al*., 2003), as well as the fact that results are partly based on a number of parameter values assigned by experts. Since results will vary by altering the parameters, the results should not be interpreted as absolute values. Furthermore, the sediment yield and dam life expectancy is based on a 5 year timeframe between 2007 and 2012 for which the most recent multi-temporal and high resolution imagery is available. The sediment yield prior and after this timeframe remains uncertain. Nevertheless, modelling the flow and sediment yield in the catchment made it possible to identify major soil erosion processes and sediment generating areas. Understanding these processes and factors will enable area-specific management intervention and erosion control measures. Lastly, estimation of the dam life expectancy could possibly aid in dam design.

6. CONCLUSION AND RECOMMENDATIONS

This study models the major soil erosion processes and sediment yield in the catchment by means off two approaches. These include (1) Model the sediment yield contribution from sheet-rill erosion using ArcSWAT, a graphical user interface for SWAT and ArcMap® software, and (2) Modelling the sediment yield contribution from gully erosion using remote sensing techniques in an integrated GIS approach. This approach included gully digitizing, segmentation of SPOT 5 imagery, gully change detection, and developing a rule-based gully sediment yield model in a GIS. The following conclusions can be drawn from the study:

1.1) The sediment yield and sediment output contribution from sheet-rill erosion for sub-catchments in the Mzimvubu River Catchment is relatively low, averaging approximately 1.0 t/ha·yr and 80,000 t/yr respectively. The average sediment output and sediment yield contribution from sheet-rill erosion in sub-catchment 39 where the future dam will be built is approximately 50,000 t/yr and 0.1 t/ha·yr respectively. ArcSWAT outputs substantiate several logical criteria regarding sediment dynamics. First, sediment output is controlled by the water flux. Second, results clearly illustrate a summer dominant erosion pattern which is mainly caused by intensive summer rainfall between October and April. Third, sub-catchments with a relatively high sediment yield contribute to high sediment loadings in the river which are subsequently routed to an outlet further downstream as addressed by several other studies (e.g. De Vente *et al*., 2007; Lesschen *et al*., 2009; Le Roux *et al*., 2013). Fourth, results are consistent with other studies where vegetation cover and soil type of source zones have major influences on sediment generation (e.g. Medeiros *et al*., 2010), whereas good vegetation cover on level slopes serves as zones where sediment is deposited (e.g. Le Roux *et al*., 2013).

1.2) ArcSWAT utilizes the Modified USLE that models only sheet and rill processes and disregards gully erosion in the central part of the catchment. Thus, ArcSWAT underestimates soil losses and subsequent sediment yield in the Mzimvubu River Catchment where gullies are prominent.

2.1) Gullied areas increased substantially since 2007 with 37 out of the 52 sub-catchments having a positive active/non-active gully ratio. The Mzimvubu River Catchment consists of 12 265 new gullies, affecting an additional area of 3 970; whereas 11 643 gullies were active or expanded, affecting an additional area of 2 418 ha. Active gully expansion range from 10 to 12 840 m^2/yr and averages 1 140 m^2/yr. This expansion rate compares well with the estimated total retreat area of 1 530 m^2/yr by Grellier *et al*. (2012) in the upper Thukela River Catchment. Furthermore, many gullies expanded sidewise (widen) but the majority expanded at gully heads similar to the findings of Johansen *et al*. (2012).

2.2) The sediment yield and sediment output contribution from gully erosion for sub-catchments in the Mzimvubu River Catchment is high, averaging approximately 5.0 t/ha·yr and 1 787 500 t/yr respectively. The average sediment output and sediment yield contribution from gully erosion in sub-catchment 39 where the future dam will be built is approximately 9.8 million t/yr and 22.4 t/ha·yr respectively. These results compare well with gullied areas referenced in Poesen *et al*. (2003), where rates range from 0.1 to 64.9 t/ha·yr.

3.1) Integration of the sheet-rill and gully results produced a total sediment yield map of the Mzimvubu River Catchment, with an average of 5.0 t/ha·yr. In the Ntabelanga Dam Catchment the sediment yield range between 1 t/ha·yr upstream to 22.5 t/ha·yr downstream at the future dam outlet. The annual average sediment output in the Ntabelanga Dam Catchment range between a quarter million t/yr upstream to nearly 10 million t/yr at the future dam outlet.

3.2) Gully erosion feed massive amounts of sediment into the river network, contributing approximately 20 times more to the sediment output than sheet-rill erosion. Although each sub-catchment has different processes and factors contributing to the sediment yield dynamics, gully erosion is the dominant process and sediment yield contributor in the Mzimvubu River Catchment. Overgrazing and erodible duplex soils derived susceptible mudstones are key factors that determine the development of gullies in the catchment (Le Roux and Sumner, 2012).

3.3) Based on digital elevation data in a GIS, the sediment volume that will be deposited in the future dam equates to 6 138 097 m^3/yr, indicating the life expectancy of the dam could be 49 years without proper siltation prevention or design measures. This number, however, accounts for the sediment output in sub-catchment 39 alone and not the sediment output from the other sub-catchments upstream of the future dam. If the sediment output from the other sub-catchments upstream of the future dam is also taken into account (by summation of their sediment output), the life expectancy of the dam could be 34 years without proper siltation prevention or design measures. The future dam at Ntabelanga could therefore experience a similar fate as the Welbedacht Dam near Dewetsdorp in the Free State where the storage capacity reduced by more than 80% in just twenty years after completion.

To prevent siltation of the future dam at Ntabelanga, it is recommended to identify vegetated and/or gully-free areas susceptible to gully development. The main reason that susceptible areas need to be identified and protected is because it is not financially feasible to rehabilitate large gullies with expensive structures at a catchment scale. Since prevention is better than cure, area-specific management and erosion control measures will be needed to prevent sedimentation of the future dam. Therefore, the next step will be to identify or map/model areas that are intrinsically susceptible to erosion before being extrinsically triggered or accelerated by land use and human-induced reduction of the vegetation cover.

It is further recommended to assess by means of scenario analysis how much sediment will be yielded from the susceptible areas (currently gully-free) if gully development should take place. In future it will also be useful to determine the relative impact of different land use and management scenarios, as well as scenarios under climate change. Soil erosion and sedimentation may get worse in the future due to population growth and potential climatic changes. It is often argued that climate change will increase future erosion rates, especially where increased rainfall intensity and/or extreme event frequency are predicted (Boardman, 2006). However, Boardman (2006) stresses that certain land use changes causing a reduction in the vegetation cover are likely to have greater impact on the erosion risk than any likely climate change.

Before gully susceptible areas and scenario analysis can be achieved, it is recommended to first determine gully factor dominance including topographical variables, parent material-soils interactions, rainfall erosivity and cover management. The manner in which event driven processes influence sediment generation in the catchment needs to be researched. This study indicates that nearly 80% of the average annual streamflow and 85% of the annual sediment output contribution from sheet-rill erosion are concentrated in the rainy season. However, the manner in which event driven processes influence gully development and sediment generation still needs to be researched in the Mzimvubu River Catchment. This can be achieved by comparing active gully development with rainfall event data. According to Bouchnak *et al*., (2009) gully erosion increases significantly with rainfall >40 mm per day, or >25 mm per hour (Rieke-Zapp and Nichols, 2011).

Further refinement will be possible given additional research including the following. Results still need to be validated over a long-term and wide range of conditions, including careful calibration of model components. There is a need for datasets comprising spatially distributed data of recorded flow and sedimentation, especially for calibration and validation (see also Van Zyl, 2007; Boardman, 2006). Sediment source fingerprinting can be used to assess the source, timing and controls dominant in the migration of sediments (see Lorentz *et al*., 2011). Studies using LiDAR (Light Detection and Ranging) highlights the potential of this technology to perform three dimensional gully monitoring (e.g. Eustace *et al*., 2011). Airborne LiDAR has the potential to create very accurate DEMs of gullies over time (Johansen *et al*., 2012), but ground-based sensors may provide better local resolution at lower cost (Perroy *et al*., 2010).

This study indicated that the proposed location for the Ntabelanga Dam is located in an area where sedimentation will be a huge risk. It is therefore important to take precautions such as the following:

- Design the dam in such a way that sediment will bypass the main dam;
- Include silt traps upstream of the dam;
- Manage catchment processes upstream of the dam to reduce erosion (this may include manage land use practices such as grazing, erect sediment fences below disturbed areas, establish vegetation communities to reduce runoff, create wetlands to reduce the speed of flow in drainage canals/rivers, rehabilitate eroded areas and gullies where possible – keeping in mind that the soils are susceptible to pipe forming and that the normal rehabilitation practices might not be sufficient/successful.
- Conduct a pilot study to find the best mitigation measures applicable to the larger area.

Finally and importantly, results should not be interpreted as absolute values. The fact that soil erosion is naturally highly variable needs to be recognized (Lu *et al*., 2003). Predictive models are far more useful as a comparative tool for planning, than as a quantitative tool. Nevertheless, modelling the flow and sediment yield in the catchment made it possible to identify major soil erosion processes and sediment generating areas. Understanding these processes and factors will enable area-specific management intervention and erosion control measures. Lastly, estimation of the dam life expectancy could possibly aid in dam design.

7. REFERENCES

AGES. 2009. *DWAF water resource study in support of the ASGISA EC Mzimvubu Development Project: groundwater assessment, volume 3 of 5. Unpublished AGES report No P WMA 12/000/00/3609*. Africa Geo-Environmental Engineering and Science, East London, South Africa.

Aplin P. 2004. Remote sensing: land cover. Progress in Physical Geography **28**(2): 283-293.

Arnold JG, Allen PM, Bernhardt G. 1993. A comprehensive surface-groundwater flow model. *Journal of Hydrology* **142**: 47-69.

Arnold JG, Srinivasan R, Muttiah RS, Williams JR. 1998. Large area hydrologic modeling and assessment part I: model development. *Journal of the American Water Resources Association* **34**(1): 73-89.

Arnold JG, Williams JR, Maidment DR. 1995. Continuous-time water and sediment-routing model for large basins. *Journal of Hydraulic Engineering* **121**(2): 171-183.

Arnold JG, Williams JR, Srinivasan R, King KW, Griggs RH. 1994. *SWAT-Soil Water Assessment Tool*. USDA Agricultural Research Service, Grassland, Soil and Water Research Laboratory: Temple, Texas.

Beckedahl HR. 1998. Aspects of subsurface erosion phenomena in eastern southern Africa. *Peterman's Geographische Mitteilungen (Supplement)* **245**: 213.

Benz UC, Hofmann P, Willhauck G, Lingenfelder I, Heynen M. 2004. Multi-resolution, object-oriented fuzzy analysis of remote sensing data for GIS-ready information. *ISPRS Journal of Photogrammetry and Remote Sensing* **58**: 239-258.

Bishop MP, James LA, Shroder Jr JF, Walsh SJ. 2012. Geospatial technologies and digital geomorphological mapping: Concepts, issues and research. *Geomorphology* **137**: 5-26.

Blaschke T. 2010. Object based image analysis for remote sensing. *ISPRS Journal of Photogrammetry and Remote Sensing* **65**: 2-16.

Boardman J. 2006. Soil erosion science: Reflections on the limitations of current approaches. *Catena* **68**: 73-86.

Bouchnak H, Felfoul MS, Boussema MR, Snane MH. 2009. Slope and rainfall effects on the volume of sediment yield by gully erosion in the Souar lithologic formation (Tunisia). *Catena* **78**: 170-177.

Bracken LJ, Croke J. 2007. The concept of hydrological connectivity and its contribution to understanding runoff-dominated geomorphic systems. *Hydrological Processes* **21**: 1749-1763.

Casalí J, Giménez R, Bennett S. 2009. Gully erosion processes: monitoring and modelling. *Earth Surface Processes and Landforms* **34**: 1839-1840.

Chen E, Mackay DS. 2004. Effects of distribution-based parameter aggregation on a spatially distributed agricultural nonpoint source pollution model. *Journal of Hydrology* **295**: 211-224.

Climatology Staff. 1978-2012. *ARC-ISCW Agrometeorology Weather Station Network Data for South Africa*, *Unpublished*. ARC-Institute for Soil, Climate and Water: Pretoria, South Africa.

Council for Geoscience. 2007. *Geological data 1:250 000*. Council for Geoscience: Pretoria, South Africa.

De Roo APJ, Jetten VG. 1999. Calibrating and validating the LISEM model for two datasets from the Netherlands and South Africa. *Catena* **37**: 477-493.

Descroix L, Olivry JC. 2002. Spatial and temporal factors of hydric erosion in black marls bad lands of the French southern Alps. *Hydrological Sciences Journal* **47**: 227-242.

De Vente J, Poesen J, Arabkhedri M. Verstraeten G. 2007. The sediment delivery problem revisited. *Progress in Physical Geography* **31**(2): 155-178.

Dey V, Zhang Y. Zhong M. 2010. A review on image segmentation techniques with remote sensing perspective. In: Wagner W. Székely B. (eds.) *ISPRS TC VII Symposium July 5-7, 2010* Vol. XXXVIII, Part 7A. IAPRS: Vienna.

Dickinson A, Collins R. 1998. Predicting erosion and sediment yield at the catchment scale. In: De Vries P. Agus F. Kerr J. (eds.) *Soil erosion at multiple scales, principles and methods for assessing causes and impacts*. CABI Publishing: New York. pp. 317-341.

DWA. 2011. *Dams in South Africa: Welbedacht Dam: Free State*. Department of Water Affairs: South Africa. http://www.ewisa.co.za/misc/damfswelbedacht. Accessed on 07 February 2011.

DWA. 2012. Department of Water Affairs: South Africa. http://www.dwaf.gov.za/Documents/RSP.aspx. Accessed on 17 June 2012.

Dwivedi RS, Kumar AB, Tewari KN. 1997. The utility of multisensor data for mapping eroded lands. *International Journal of Remote Sensing* **18**(11): 2303-2318.

Elwell HA. 1976. *Natal Agricultural Research Bulletin No 7, Soil Loss Estimator for Southern Africa*. Department of Agricultural Technical Services: Natal, South Africa.

Eustace AH, Pringle MJ, Denham RJ. 2011. A risk map for gully locations in central Queensland, Australia. *European Journal of Soil Science* **62**: 431-441.

Flügel W, Märker M, Moretti S, Rodolfi G, Sidrochuk A. 2003. Integrating geographical information systems, remote sensing, ground truthing and modeling approaches for regional erosion classification of semi-arid catchments in South Africa. *Hydrological Processes* **17**: 929-942.

Gassman PW, Reyes MR, Green CH, Arnold JG. 2007. The Soil and Water Assessment Tool: historical development, applications, and future research directions. *Transactions of the ASABE* **50**(4): 1211-1250.

Gau P. 2008. Understanding watershed suspended sediment transport. *Progress in Physical Geography* **32**(3): 243-263.

Gómez Gutiérrez A, Schnabel S, Felicísimo AM. 2009. Modelling the occurrence of gullies in rangelands of southwest Spain. *Earth Surface Processes and Landforms* **34**: 1894-1902.

Grellier S, Kemp J, Janeau JL, Florsch N, Ward D, Barot S, Podwojewski P, Lorentz S. Valentin C. 2012. The indirect impact of encroaching trees on gully extension: A 64 year study in a sub-humid grassland of South Africa. *Catena* **98**: 110-119.

Hochschild V, Märker M, Rodolfi G, Staudenrausch H. 2003. Delineation of erosion classes in semi-arid southern African grasslands using vegetation indices from optical remote sensing data. *Hydrological Processes* **17**: 917-928.

Hochschild V, Herold M. 2001. Hydrological analysis of high resolution multifrequent, multipolarimetric and interferometric airborne SAR data. In: Owe M, Brubaker K, Ritchie J, Rango A. (eds.) *Remote Sensing and Hydrology 2000, International Association of Hydrological Sciences Publication No. 267*. International Association of Hydrological Sciences Press: Wallingford, UK. pp. 349-353.

Hook J. 2003. Coarse sediment connectivity in river channel systems: a conceptual framework and methodology. *Geomorphology* **56**: 79-94.

Jakeman AJ, Green TR, Beavis SG, Zhang L, Dietrich CR, Crapper PF. 1999: Modelling upland and in-stream erosion, sediment and phosphorus transport in a large catchment. *Hydrological Processes* **13**(5): 745-752.

Jetten V, Govers G, Hessel R. 2003. Erosion models: quality of spatial patterns. *Hydrological Processes* **17**: 887-900.

Johansen K, Taiheib S, Tindalla D, Phinn S. 2012. Object-based monitoring of gully extent and volume in north Australia using LiDAR data. *Proceedings of the 4th GEOBIA, May 7-9, 2012*. Rio de Janeiro. pp.168-173.

King C, Baghdadi N, Lemote V, Cerdan O. 2005. The application of remote-sensing data to monitoring and modelling of soil erosion. *Catena* **62**: 79-93.

Knight J, Spencer J, Brooks A, Phinn S. 2007. *Large-area, high-resolution remote sensing based mapping of alluvial gully erosion in Australia's tropical rivers. Proceedings of the 5th Australian Stream Management Conference: Australian Rivers: Making a Difference*. Charles Sturt University: New South Wales. pp. 199-204.

Land Type Survey Staff. 1972-2012. *Land Types of South Africa: Digital Map (1:250,000 scale) and Soil Inventory Databases*. ARC-Institute for Soil, Climate and Water: Pretoria, South Africa.

Lenhart T, Van Rompaey A, Steegen A, Fohrer N, Frede H, Govers G. 2005. Considering spatial distribution and deposition of sediment in lumped and semi-distributed models. *Hydrological Processes* **19**: 785-794.

Le Roux JJ, Morgenthal TL, Malherbe J, Sumner PD, Pretorius DJ. 2008. Water erosion prediction at a national scale for South Africa. *Water SA* **34**(3): 305-314.

Le Roux JJ, Sumner PD. 2012. Factors controlling gully development: comparing continuous and discontinuous gullies. *Land Degradation and Development* **23**: 440-449.

Le Roux JJ, Sumner PD. 2013. Water erosion risk assessment in South Africa: a proposed methodological framework. *Geografiska Annaler: Series A, Physical Geography* **95**: 323-336.

Le Roux JJ, Sumner PD, Lorentz SA, Germishuyse T. 2013. Connectivity Aspects in Sediment Migration Modelling Using the Soil and Water Assessment Tool. *Geosciences* **3**(1): 1-12.

Lesschen JP, Schoorl JM, Cammeraat LH. 2009. Modelling runoff and erosion for a semi-arid catchment using a multi-scale approach based on hydrological connectivity. *Geomorphology* **109**: 174-183.

Lorentz SA, Miller J, Lechler P, Mackin G, Lord M, Kollongei JK, Pretorius J, Ngeleka K, Zondi N, Le Roux JJ. 2011. *Definition of process zones and connectivity in catchment scale NPS processes, WRC report 1808/1/11*. Water Research Commission: Pretoria, South Africa.

Lu D, Mausel P, Brondízio E, Moran E. 2004. Change detection techniques. *International Journal of Remote Sensing* **25**(12): 2365-2401.

Lu H, Prosser IP, Moran CJ, Gallant JC, Priestley G, Stevenson JG. 2003. Predicting sheetwash and rill erosion over the Australian continent. *Australian Journal of Soil Research* **41**: 1037-1062.

Mararakanye N, Nethengwe NS. 2012. Gully Features Extraction Using Remote Sensing Techniques. *South African Journal of Geomatics* **1**(2): 109-118.

Mararakanye N. Le Roux JJ. 2012. Gully erosion mapping at a national scale for South Africa. *South African Geographical Journal* **94**(2): 208-218.

Martinec J, Rango A. 1989. Merits of statistical criteria for the performance of hydrological models. *Water Resources Bulletin* **25**: 421-432.

Martinez-Casasnovas JA. 2003. A spatial information technology approach for the mapping and quantification of gully erosion. *Catena* **50**: 293-308.

Martínez-Casasnovas JA. Poch RM. 1998. Study of soil conservation of the Joaquín Costa watershed. *Limnetica* **14**: 83-91.

Medeiros PHA, Güntner A, Francke T, Mamede GL, De Araújo JC. 2010. Modelling spatio-temporal patterns of sediment yield and connectivity in a semi-arid catchment with the WASA-SED model. *Hydrological Sciences Journal* **55**(4): 636-648.

Metternicht GI, Zinck JA. 1998. Evaluating the information content of JERS-1 SAR and Landsat TM data for discrimination of soil erosion features. *ISPRS Journal of Photogrammetry and Remote Sensing* **53**(3): 143-153.

Merritt WS, Letcher RA, Jakeman AJ. 2003. A review of erosion and sediment transport models. *Environmental Modelling and Software* **18**: 761-799.

Midgley DC, Pitman WV, Middleton BJ. 1990. *Surface Water Resources of South Africa. WRC Report No 298/5.1/94. Volume V*. Water Research Commission: Pretoria, South Africa.

Msadala V, Gibson L, Le Roux JJ, Rooseboom A, Basson GR. 2010. *Sediment Yield Prediction for South Africa: 2010 Edition, WRC report 1765/1/10*. Water Research Commission: Pretoria, South Africa.

Mucina L, Rutherford MC. 2006. *The vegetation of South Africa, Lesotho and Swaziland*. *Strelitzia* **19**. South African National Biodiversity Institute, Pretoria, South Africa.

Nash JE, Sutcliffe JV. 1970. River flow forecasting through conceptual models. *Journal of Hydrology* **10**: 282-290.

National Land Cover. 2000. *National Land Cover 2000*, *Unpublished*. ARC-Institute for Soil, Climate and Water; Council for Scientific and Industrial research: Pretoria, South Africa.

Ndomba PM, Mtalo F, Killingtveit A. 2009. Estimating gully erosion contribution to large catchment sediment yield rate in Tanzania. *Physics and Chemistry of the Earth* **34**: 741-748.

Nearing MA, Foster GR, Lane LJ, Finkler SC. 1989. A process-based soil erosion model for USDA-Water Erosion Prediction Project technology. *Transactions of the ASABE* **32**: 1587-1593.

Neitsch SL, Arnold JG, Kiniry JR, Williams JR. 2011. *Soil and Water Assessment Tool Theoretical Documentation, Version 2009*. USDA Agriculture Research Service, Blackland Research Center, Texas Agricultural Experiment Station: Texas, USA.

NGI. 2013. *What is ITIS Portal*. Chief Directorate – National Geo-spatial Information: Cape Town, South Africa. Available from: http://www.ngi.gov.za/index.php/online-shop/what-is-itis-portal [Accessed 14 October 2013].

Parsons AJ. 2012. How useful are catchment sediment budgets? *Progress in Physical Geography*, In press. DOI: 10.1177/0309133311424591.

Pegram GC, Görgens AHM. 2001. *A Guide to Non-point Source Assessment: To Support Water Quality Management of Surface Water Resources in South Africa, WRC Report No. TT 142/01*. Water Research Commission: Pretoria, South Africa.

Perroy RL, Bookhagen B, Asner GP, Chadwick OA. 2010. Comparison of gully erosion estimates using airborne and ground-based LiDAR on Santa Cruz Island, California. *Geomorphology* **118**: 288-300.

Podwojewski P, Janeau JL, Grellier S, Valentin C, Lorentz S, Chaplot V. 2011. Influence of vegetal soil cover on water runoff and soil detachment in a sub-humid South African degraded rangeland. *Earth Surface Processes and Landforms* **36**: 911-922.

Poesen J, Nachtergaele J, Verstraeten G, Valentin C. 2003. Gully erosion and environmental change: importance and research needs. *Catena* **50**: 91-133.

Price KP. 1993. Detection of soil erosion within pinyon-juniper woodlands using Thematic Mapper (TM) data. *Remote Sensing of Environment* **45**(3): 233-248.

Renard KG, Foster GR, Weesies GA, McCool DK, Yoder DC. 1994. *RUSLE Users Guide. Predicting Soil Erosion by Water: A Guide to Conservation Planning with the Revised Universal Soil Loss Equation. USDA, Agriculture Handbook No. 703*. USDA: Washington DC, USA.

Rieke-Zapp DH, Nichols MH. 2011. Headcut retreat in a semiarid watershed in the southeastern United States since 1935. *Catena* **87**: 1-10.

Rienks SM, Botha GA, Hughes JC. 2000. Some physical and chemical properties of sediments exposed in a gully (donga) in northern KwaZulu-Natal, South Africa and their relationship to the erodibility of the colluvial layers. *Catena* **39**: 11-31.

Ritchie JC. 2000. Soil erosion. In: Schultz GA, Engman ET. (eds.) *Remote sensing in hydrology and water management*. Springer: Berlin, Germany.

Samadi M, Germishuyse T, Van der Walt M. 2005. *Understanding South African Soils*. ARC – Institute for Soil, Climate and Water: Pretoria, South Africa.

Schulze RE. 1995. Hydrology and Agrohydrology: A text to accompany the ACRU 3.00 Agrohydrological Modelling System, WRC report no TT69/95. Water Research Commission: Pretoria, South Africa.

Schulze RE. 2007. *South African Atlas of Climatology and Agrohydrology, WRC Report 1489/1/06*. Water Research Commission: Pretoria, South Africa.

Servenay A, Prat C. 2003. Erosion extension of indurated volcanic soils of Mexico by aerial photographs and remote sensing analysis. *Geoderma* **117**(3-4): 367-375.

Shruthi RBV, Kerle N, Jetten V. 2011. Object-based gully feature extraction using high spatial resolution imagery. Geomorphology **134**: 260-268.

Singh A. 1989. Digital change detection techniques using remotely sensed data. *International Journal of Remote Sensing* **10**: 989-1003.

Smith MJ, Pain CF. 2009. Applications of remote sensing in Geomorphology. *Progress in Physical Geography* **33**(4): 568-582.

Symeonakis E, Drake N. 2004. Monitoring desertification and land degradation over sub-Saharan Africa. *International Journal of Remote Sensing* **25**(3): 573-592.

Srinivasan R, Ramanarayanan TS, Arnold JG, Bednarz ST. 1998. Large area hydrologic modeling and assessment part II: model application. *Journal of the American Water Resources Association* **34**: 91-101.

Srinivasan R, Zhang X, Arnold J. 2010. SWAT ungauged: hydrological budget and crop yield predictions in the upper Mississippi river basin. *Transactions of the ASABE* **53**(5): 1533-1546.

Stroosnijder L. 2005. Measurement of erosion: Is it possible? *Catena* **64**: 162-173.

Taruvinga K. 2008. Gully mapping using remote sensing: Case study in KwaZulu-Natal, South Africa. MSc Dissertation. Waterloo University: Canada.

Tibebe D, Bewket W. 2011. Surface runoff and soil erosion estimation using the SWAT model in the Keleta watershed, Ethiopia. *Land Degradation and Development* **22**(6): 551-564.

USDA SCS. 1972. *National Engineering Handbook, Section 4 Hydrology*. USDA Agricultural Conservation Service: USA.

Valentin C, Poesen J, Li Y. 2005. Gully erosion: Impacts, factors and control. *Catena* **63**: 132-153.

Vanmaercke M, Poesen J, Verstraeten G, De Vente J, Ocakoglu F. 2011. Sediment yield in Europe: Spatial patterns and scale dependency. *Geomorphology* **130**(3-4): 142-161.

Van Zijl GM, Ellis F, Rozanov DA. 2013. Emphasising the soil factor in geomorphological studies of gully erosion: a case study in Maphutseng, Lesotho. *South African Geographical Journal* **95**(2): 205-216.

Van Zyl AJ. 2007. A knowledge gap analysis on multi-scale predictive ability for agriculturally derived sediments under South African conditions. *Water Science and Technology* **55**(3): 107-114.

Van Zyl AJ, Lorentz S. 2003. *Predicting the impact of farming systems on sediment yield in the context of integrated catchment management, WRC report no 1059/1/03*. Water Research Commission: Pretoria, South Africa.

Vrieling A. 2006. Satellite remote sensing for water erosion assessment: A review. *Catena* **65**: 2-18.

Vrieling A, Rodrigues SC, Bartholomeus H, Sterk G. 2007. Automatic identification of erosion gullies with ASTER imagery in the Brazilian Cerrados. *International Journal of Remote Sensing* **28**(12): 2723-2738.

Wang T, He F, Zhang A, Gu L, Wen Y, Jiang W, Shao H. 2014. A Quantitative Study of Gully Erosion Based on Object-Oriented Analysis Techniques: A Case Study in Beiyanzikou Catchment of Qixia, Shandong, China. The Scientific World Journal **2014**: 1-11.

Weepener HL, Van den Berg HM, Metz M, Hamandawana H. 2012. The development of a hydrologically improved Digital Elevation Model and derived products for South Africa based on the SRTM DEM. WRC report k5/1908. Water Research Commission: Pretoria, South Africa.

Weepener HL, Le Roux JJ, Van den Berg EC, Tswai DR. 2014. *A methodology to create a South African river network with hydraulic intelligence*, *WRC report*. in prep. Water Research Commission: Pretoria, South Africa.

Wheater HS, Jakeman AJ, Beaven KJ. 1993. Progress and directions in rainfall-runoff modelling. In: Jakeman AJ. Beck MB. McAleer MJ. (Eds.) *Modelling change in environmental systems*. John Wiley and Sons: Chichester, pp. 101-132.

Wiegand C, Rutzinger M, Heinrich K, Geitner C. 2013. Automated Extraction of Shallow Erosion Areas Based on Multi-Temporal Ortho-Imagery. *Remote Sensing* **5**: 2292-2307.

Williams JR. 1969. Flood routing with variable travel time or variable storage coefficients. *Transactions of the ASABE* **12**(1):100-103.

Williams JR. 1975. Sediment-yield prediction with universal equation using runoff energy factor. In *Present and Prospective Technology for predicting sediment yield and sources. ARS.S-40*, US Gov. Print. Office: Washington, DC; 244-252.

Williams JR, Brendt HD. 1977. Sediment yield based on watershed hydrology. *Transactions of the American Society of Agricultural Engineers* **20**: 1100-1104.

Wischmeier WH, Smith DD. 1978. *Predicting Rainfall Erosion Losses, a Guide to Conservation Planning. USDA Agriculture Handbook No. 537*. USDA: Washington DC, USA.

Woolhiser DA, Smith RE, Goodrich DC. 1990. *KINEROS, a kinematic runoff and erosion model: Documentation and user manual, ARS-77, SWRC reference No. 703*. USDA: Washington DC, USA.

APPENDIX 1: FIELD OBSERVATION DATA

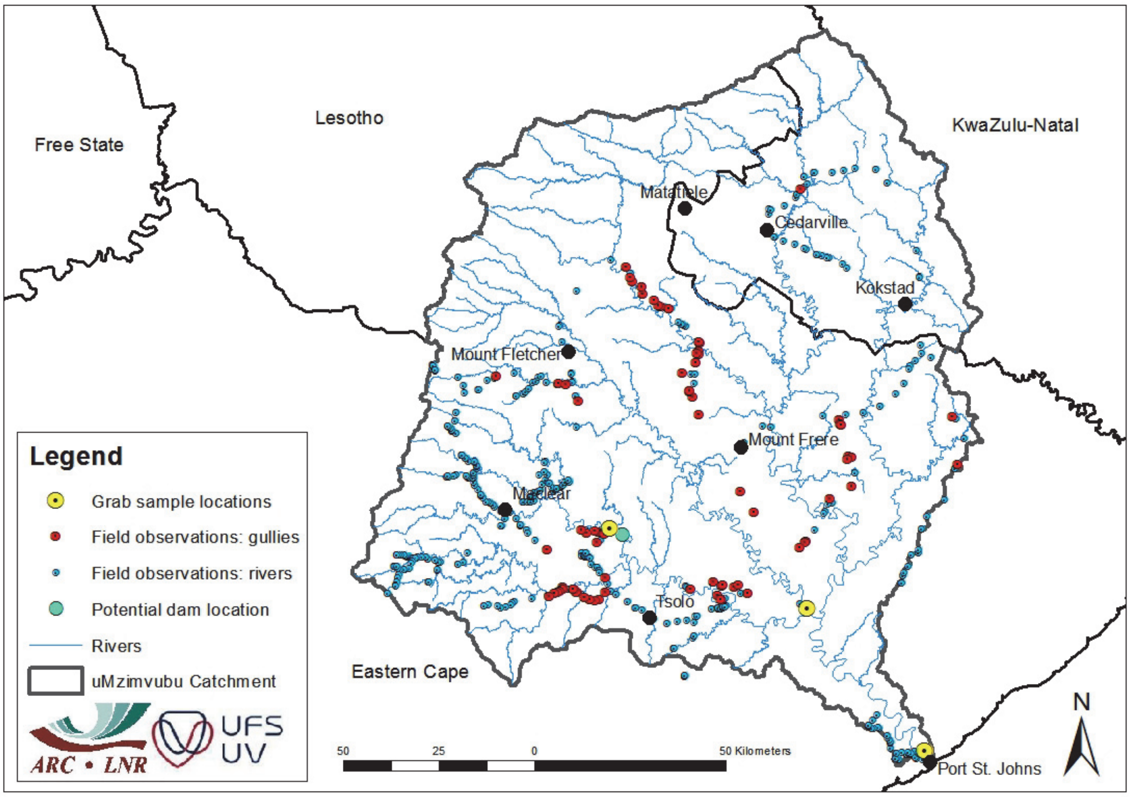

Figure 1: **Field observation points and location where grab samples were taken.**

Table 1: **Field observation data captured for land cover map verification and channel properties.**

#	Photo[1]	Landcover[2]	Channel depth (m)	Channel's roughness coefficient[3]
1	44; 50-51	6		1
2	45	6	2	4
3	46;	6	2	4
4	47-51	6	1.5	5
5	52; 63	6		5
6	54	6	2	5
7	55-56	6	>3	4
8	80	6		5
9	89	18		3
10	103; 77	18		2
11	104	18		4
12	105; 78-79	18	2	3
13	106; 83-85	18	>3	2
14	107; 86	18	1	3
15	108; 87	6		3
16	111; 88-89	18	0.5	2
17	113; 90	18		3
18	117; 91	5	2-3	4
19	121; 97	18	1.5	2
19	124; 98	18	3	3

20	121-122	18	2	5
20	125; 99	18	1.5	4
21	126; 100-101	18	1-3	3
22	157; 103	8		3
23	159; 105	8	1.5	4
24	117-178; 110	18		2
25	179; 111	18	1.5	2
26	180; 112	18		2
27	181; 113-114	18		3
28	184?; 116-120	18		2
29	184?; 123	18		2
30	188; 124	18		2
31	189; 126	6	>3	2
32	189; 127	6		4
33	190; 128	18		3
34	191; 129	18		3
35	193; 130	18	1.5-3	4
36	194; 131	18	1.5-3	4
37	194; 132	18		4
39	?	18		4
40	?	18		4
41	200	18	1	5
42	202	18	3	2
43	203; 133	18		4
44	207; 134	18		4
45	208; 135	18		3
46	209; 136	18		2
47	210;137	18		3
48	212; 138	18	>3	5
49	213; 139	18	>3	2
50	215; 140-141	18		2
51	217; 142-143	18		2
52	258	8	1	5
53	261	8	0.5	4
54	262; 151	8		5
55	239	8	3	4
56	234	8	1.5	4
57	232	8	1	4
58	264	8	1	3
59	265	8	2.5	4
60	231	8	2	5
61	269	8	5	5
62	271; 153	18		4
63	272	6	1.5-3	4
64	228	6	2	4
65	276	6	2	4
66	275	6		4
67	277	6	2.5	4
68	279; 158	3 and 8	1.5-3	3
69	279; 159-160	18	>3	4
70	281; 163	18	>3	2
71	284-285	18	1	4
72	286-287; 164-172	18	>3	3
73	288-289; 173-175	14 or 18	>3	2
74	290; 178-179	14 or 18	>3	3
75	293; 180-181	14 or 18	>3	2
76	294; 182	18	>3	2

77	255; 183	18	1.5-3	3
78	297; 184	18	2	4
79	298; 185	18		4
80	299; 187-188	18	>3	2
81	299; 187-188	18	2	4
82	?;189	18	1.5-3	2
83	300; 190	6	2.5	3
84	301;191	6	2	5
85	302-304; 192-194	18	2.5	2
86	305; 195	18	1.5	2
87	306	18	1	2
88	306	18	1.5	4
89	307	18	2	3
90	308; 196	18	1	2
91	309; 197	18	2.5	1
92	312; 198	18	2.5	1
93	313; 199	18	2.5	3
94	314	18	1.5	5
95	315-316	18	>3	5
96	317; 201	18	1.5-3	3
97	318; 202	18	1.5-3	2
98	319; 203	18	1.5-3	2
99	319; 204	18	1.5-3	2
100	322; 206	18	>3	4
101	323; 207	18	1	4
102	324	18	1.5-3	3
103	325	18	2	4
104	325; 209	18	1.5-3	3

1. Photo numbers of photos that was taken (GPS camera; and second camera) in the field but not shown here.

2. Land cover classes:

2	open water
3	wetlands
4	forest/plantations
5	cultivation sub. cultivated
6	cultivation sub. grazing
7	cultivation com. cultivated
8	cultivation com. grazing
9	cultivation sugarcane
10	cultivation orchards
11	urban high density
12	urban low density (rural)
13	bare rock/soil (erosion)
14	degraded natural veld
15	bushland/woodland
16	Tea
17	Sugargane
18	Overgrazed.

3. Channel's roughness coefficient: Manning's roughness coefficient for channels:

For channels or gullies	Median	Range
14. Earth, straight and uniform	0.025	0.016-0.033
15. Earth, winding and sluggish	0.035	0.023-0.050
16. Not maintained, weeds and brush	0.075	0.040-0.140
17. Few trees, stones or brush	0.050	0.025-0.065
18. Heavy timber and brush	0.100	0.050-0.150

Table 2: Total suspended solids (mg/L) of grab samples taken in November 2013.

Grab sample number	Location	Total suspended solids (mg/L)
1	Mzimvubu River Mouth 1	574.2
2	Mzimvubu River Mouth 1	689.4
3	Tsitsa-Tina River Confluence (Tsitsa side)	3131.6
4	Tsitsa-Tina River Confluence (Tina side)	688.0

Table 3: Total suspended solids (mg/L) of grab samples taken in June 2014.

Grab sample number	Location	Total suspended solids (mg/L)
1	Tsitsa Bridge near dam site	0.0
2	Tsitsa Bridge near dam site	48.0
3	Tsitsa Bridge near dam site	0.6
4	Tsitsa-Tina River Confluence (Tsitsa side)	0.0
5	Tsitsa-Tina River Confluence (Tina side)	0.4

Table 4: Field observation data captured in November 2013 for gully erosion classification and verification.

#	Photo[1]	Map[2]	Scale[3]	Active[4]	Continuity[5]	Depth[6] (s, d, vd)	Veg-cover Internal/ external[7]	Manning internal/ external[8]	Connectivity (c, cs, p1, p2, d)[9]
1	44; 50-51	Yes/ No	Hillslope	Yes	c	d	<30 / >60	1 / n.a.	c
2	45	Yes	Hillslope	Yes	c	d	<30 / >60	4 / n.a.	cs
3	46	Yes	Hillslope	Yes	c	d	<30 / >60	4 / n.a.	cs
4	48-50?	No	Hillslope	Yes	d	d	<30 / >60	5 / n.a.	cs
5	52; 63	Yes	Hillslope	No	d	s	>60 / >60	5 / n.a.	c
6	54	Yes	Hillslope	Yes	c	d	<30 / >60	5 / n.a.	cs
7	55-56	Yes	Hillslope	Yes	c	vd	<30 / >60	4 / n.a.	cs
8	80	No	Hillslope	Yes	d	s	<30 / >60	5 / 12	d
9	89	No	Hillslope	Yes	c	s	<30 / >60	3 / 3	p1
10	103; 77	Yes	Hillslope	Yes	d	d	<30 / >60	2 / 12	d
11	104	No	Hillslope	Yes	d	s	<30 / >60	4 / 12	d
12	105; 78-79	Yes/ No	Catchm.	Yes	c	d	<30 / 30-60	3 / n.a.	c
13	106; 83-85	Yes	Hillslope	Yes	c	vd	<30 / 30-60	2 / n.a.	c
14	107; 86	Yes	Hillslope	Yes	c	s	<30 / <30	3 / n.a.	c
15	108; 87	Yes	Hillslope	Yes	d	s	<30 / >60	3 / 12	d
16	111; 88-89	Yes	Hillslope	Yes	c	s	<30 / >60	2 / 2	p1
17	113; 90	Yes	Hillslope	Yes	d	s	<30 / >60	3 / 12	d
19	121; 97	Yes	Hillslope	Yes	c	d	<30 / 30-60	2 / n.a.	cs
19	124; 98	Yes	Hillslope	Yes	c	vd	<30 / 30-60	3 / n.a.	c
20	122	No	Hillslope	Yes	c	d	<30 / 30-60	5 / n.a.	cs
20	125; 99	Yes	Hillslope	Yes	c	d	<30 / >60	4 / n.a.	cs
21	126; 100-101	Yes	Catchm.	Yes	c	d	<30 / 30-60	3 / n.a.	cs
22	157; 103	No	Hillslope	Yes	d	d	<30 / >60	3 / 12	d
24	177-178; 110	Yes/ No	Hillslope	Yes	d	s	<30 / >60	2 / 12	d
25	179; 111	Yes	Hillslope	Yes	c	d	<30 / >60	2 / n.a.	c

26	180; 112	Yes	Hillslope	Yes	c	vd	<30 / 30-60	2 / n.a.	cs
27	181; 113-114	Yes/ No	Hillslope	Yes	c	vd	<30 / >60	3 / n.a.	c
28	184?; 116-120	Yes	Hillslope	Yes	c	vd	<30 / 30-60	2 / n.a.	c
29	184?; 123	Yes	Hillslope	Yes	c	vd	<30 / 30-60	2 / n.a.	c
30	188; 124	Yes	Hillslope	Yes	d	d	<30 / 30-60	2 / 10	p1
31	189; 126	Yes/ No	Hillslope	Yes	c	vd	<30 / >60	2 / n.a.	c
32	189; 127	Yes/ No	Hillslope	Yes	c	d	<30 / >60	4 / 12	p1
33	190; 128	Yes	Hillslope	Yes	c	vd	<30 / <30	3 / n.a.	c
34	191; 129	Yes	Hillslope	Yes	c	vd	<30 / <30	3 / n.a.	c
35	193; 130	Yes	Hillslope	Yes	c	d	<30 / 30-60	4 / n.a.	cs
36	194; 131	Yes	Hillslope	Yes	c	d	<30 / >60	4 / n.a.	cs
37	194; 132	Yes	Hillslope	Yes	c	d	<30 / <30	4 / n.a.	c
39	?	No	Hillslope	No	d	s	>60 / >60	4 / 12	d
40	?	No	Hillslope	No	d	s	>60 / >60	4 / 12	d
43	203; 133	Yes/ No	Hillslope	Yes	c	d	<30 / <30	4 / n.a.	c
44	207; 134	Yes/ No	Hillslope	Yes	c	d	<30 / 30-60	4 / n.a.	c
45	208; 135	Yes/ No	Hillslope	Yes	c	d	<30 / 30-60	3 / n.a.	c
46	209; 136	Yes/ No	Hillslope	Yes	c	d	<30 / 30-60	2 / n.a.	c
47	210;137	Yes	Hillslope	Yes	c	d	<30 / <30	3 / n.a.	c!
48	212; 138	Yes	Hillslope	Yes	c	vd	<30 / 30-60	5 / n.a.	cs
49	213; 139	Yes	Hillslope	Yes	c	vd	<30 / >60	2 / n.a.	cs
50	215; 140-141	Yes	Hillslope	Yes	c	vd	<30 / 30-60	2 / n.a.	c
51	217; 142-143	Yes	Catchm.	Yes	c	vd	<30 / <30	2 / n.a.	c
54	262; 151	Yes	Hillslope	No	d	d	<30 / 30-60	5 / 12	d
62	271; 153	Yes	Hillslope	No	c	vd	<30 / 30-60	4 / 12	d
63	272	Yes/ No	Hillslope	Yes	c	d	<30 / >60	4 / n.a.	cs
66	275	Yes/ No	Hillslope	No	d	d	<30 / 30-60	4 / n.a.	d
68	279; 158	Yes	Hillslope	Yes	d	d	<30 / >60	3 / 12	p1
69	279; 159-160	Yes	Catchm.	Yes	c	vd	<30 / 30-60	4 / n.a.	c
70	281; 163	Yes	Hillslope	Yes	c	vd!	<30 / 30-60	2 / n.a.	c
72	286-287; 164-172	Yes	Hillslope	Yes	c	d	30-60 / >60	3 / n.a.	c
73	288-289; 173-175	Yes/ No	Hillslope	Yes	c	vd	<30 / >60	2 / n.a.	cs
74	290; 178-179	Yes	Hillslope	Yes	c	vd	<30 / >60	3 / n.a.	cs
75	293; 180-181	Yes/ No	Hillslope	Yes	c	vd	<30 / >60	2 / n.a.	cs
76	294; 182	No	Hillslope	Yes	c	vd	<30 / >60	2 / n.a.	cs
77	295; 183	Yes	Hillslope	Yes	c	d	<30 / >60	3 / n.a.	cs
79	298; 185	Yes/ No	Hillslope	Yes	d	s	<30 / >60	4 / n.a.	c!
80	299; 187-188	Yes	Hillslope	Yes	c	vd	<30 / 30-60	2 / n.a.	c!
82	?;189	Yes	Catchm.	Yes	c	vd	<30 / >60	2 / n.a.	cs!
83	300; 190	Yes	Hillslope	Yes	c	vd	<30 / >60	3 / n.a.	c
84	301;191	No	Hillslope	No	d	d	>60 / >60	5 / n.a.	d
85	302-304; 192-194	Yes	Hillslope	Yes	c	vd	<30 / >60	2 / n.a.	c
86	305; 195	Yes	Hillslope	Yes	c	v	<30 / >60	2 / n.a.	c
87	306	Yes	Hillslope	Yes	d	s	<30 / 30-60	2 / n.a.	c!
90	308; 196	Yes	Hillslope	Yes	c	s	<30 / 30-60	2 / n.a.	c
91	309; 197	Yes	Hillslope	Yes	c	d	<30 / 30-60	1 / n.a.	cs

92	312; 198	Yes	Hillslope	Yes	c	d	<30 / >60	1 / n.a.	cs
93	313; 199	Yes	Catchm.	Yes	c	d	<30 / 30-60	3 / n.a.	c
96	317; 201	Yes/ No	Hillslope	Yes	c	d	<30 / 30-60	3 / n.a.	c!
97	318; 202	Yes	Hillslope	Yes	c	d	<30 / <30	2 / n.a.	c!
98	319; 203	Yes	Hillslope	Yes	c	d	<30 / <30	2 / n.a.	c!
99	319; 204	Yes/ No	Hillslope	Yes	c	d	<30 / >60	2 / n.a.	c!
100	322; 206	Yes	Hillslope	Yes	c	vd	<30 / 30-60	4 / n.a.	c!
101	323; 207	Yes/ No	Hillslope	Yes	c	s	<30 / 30-60	4 / n.a.	c!
102	324	Yes	Hillslope	Yes	c	d	<30 / >60	3 / n.a.	c!
104	325; 209	Yes	Hillslope	Yes	c	d	<30 / >60	3 / n.a.	cs

Table 5: Field observation data captured in June 2014 for gully erosion classification and verification.

#	Photo[1]	Map[2]	Scale[3]	Active[4]	Continuity[5]	Depth[6] (s, d, vd)	Veg-cover Internal/ external[7]	Manning internal/ external[8]	Connectivity (c, cs, p1, p2, d)[9]
1	28	Yes	Hillslope	Yes	c	d	<30 / >60	2/12	c
2	31	Yes	Catchm.	Yes	c	vd	30-60 / >60	2/12	c
3		Yes	Catchm.	Yes	c	vd	<30 / >60	2/12	c
4	33	Yes	Hillslope	Yes	c	vd	<30 / >60	2/12	p
5		Yes	Hillslope	Yes	d	d	>60 / >60	3/10	c
6	34	Yes	Hillslope	Yes	c	vd/d	<30 / >60	2/12	p
7	35	Yes	Hillslope	Yes	d	vd	30-60 / >60	3/12	p
8	36	Yes	Hillslope	Yes	d	vd	<30 / >60	2/12	p
9	37	Yes	Hillslope	Yes	d	d	30-60 / >60	3/12	d
10	38	Yes	Hillslope	Yes	c	vd	30-60 / >60	3/12	c
11	43	Yes	Hillslope	Yes	d	S	<30 / >60	1/12	d
12	44	Yes	Hillslope	Yes	c	d	<30 / >60	4/12	p
13	45	Yes	Hillslope	Yes	c	d	30-60 / >60	3/12	c
14	46	Yes	Hillslope	Yes	c	vd	30-60 / >60	4/12	c
15	48	Yes	Hillslope	Yes	c	d	30-60 / >60	3/12	p
16	49	Yes	Catchm.	Yes	c	vd	<30 / >60	2/12	c
17	50	Yes	Hillslope	Yes	c	d	30-60 / >60	4/12	c
18	51	Yes	Hillslope	Yes	d	d	<30 / >60	3/12	d
19	52	Yes	Catchm.	Yes	c	d	<30 / >60	2/12	d
20	53	Yes	Hillslope	Yes	d	s	<30 / >60	1/12	d
21	54	Yes	Hillslope	Yes	d	s	<30 / >60	1/12	c
22	55	Yes	Hillslope	Yes	d	s	30-60 / >60	2/12	c
23	56	Yes	Hillslope	Yes	c	d	>60 / >60	3/12	c
24	57	Yes	Hillslope	Yes	d	d	30-60 / >60	3/12	p

1. Photo numbers of photos that was taken (GPS camera; and second camera) in the field but not shown here.

2. Ground-truthing of vectorised gullies (yes, or no, or yes/no = partially mapped).

3. Hillslope scale typically extends from upslope/crest areas to a stream channel with varying topography, soil and land management (Van Zyl, 2007); whereas a catchment is a land surface which contributes water and sediment to any given stream network (Rowntree and Wadeson, 1999), including smaller (sub)catchments (<10 km^2) to a very large catchment (>10 km^2).

4. Active gullies contribute to or deliver sediments in a catchment, whereas non-active stable gullies have none.

5. c = continuous gullies have a branching network that discharges into a stream/river at the base of a slope; and d = small discontinuous fade out into a depositional zone.

6. s = shallow (< 1.5 m); d = deep (1.5 to 3 m); and vd = very deep (>3 m).

7. Vegetation cover in percentage inside of gully and externally i.e. between gully and river.

8. Manning's roughness coefficient considering both inside channels/gullies and externally i.e. overland flow between gully and river as follows:

For channels or gullies	Median	Range
1. Earth, straight and uniform	0.025	0.016-0.033
2. Earth, winding and sluggish	0.035	0.023-0.050
3. Not maintained, weeds and brush	0.075	0.040-0.140
4. Few trees, stones or brush	0.050	0.025-0.065
5. Heavy timber and brush	0.100	0.050-0.150

For overland flow	Median	Range
1. Fallow, no residue	0.010	0.008-0.012
2. Conventional tillage, no residue	0.090	0.060-0.120
3. Conventional tillage, residue	0.190	0.160-0.220
4. Chisel plow, no residue	0.090	0.060-0.120
5. Chisel plow, residue	0.130	0.100-0.160
6. Fall disking, residue	0.400	0.300-0.500
7. No till, no residue	0.070	0.040-0.100
8. No till, 0.5-1 t/ha residue	0.120	0.070-0.170
9. No till, 2-9 t/ha residue	0.300	0.170-0.470
10. Rangeland, 20% cover	0.600	
11. Short grass prairie	0.150	0.100-0.200
12. Dense grass	0.240	0.170-0.300
13. Bermudagrass	0.410	0.300-0.480

9. c = connected (coarse sediment transfer during 'normal' flood events); cs = connected streambank erosion; p1 = partially connected (transfer only in extreme flood events); p2 = potentially connected (competence to transport but lack of supply); d = disconnected (transfer is obstructed) (Hooke, 2003).

References

Hooke J. 2003. Coarse sediment connectivity in river channel systems: a conceptual framework and methodology. *Geomorphology* **56**: 79-94.

Rowntree KM, Wadeson RA. 1999. *A hierarchical geomorphological model for the classification of selected South African rivers. WRC Report no 497/1/99*. Water Research Commission: Pretoria, South Africa.

Van Zyl AJ. 2007. A knowledge gap analysis on multi-scale predictive ability for agriculturally derived sediments under South African conditions. *Water Science and Technology* **55**(3): 107-114.

APPENDIX 2: RULES APPLIED TO MODEL THE SEDIMENT YIELD CONTRIBUTION FROM PARTIALLY AND POTENTIALLY CONNECTED GULLIES

Table 1: (*i*) Distance rules applied to partially and potentially connected gullies when calculating sediment delivery rates.

Distance from gully to perennial river (m)*	Fraction sediment reaching perennial river junction (%)
100 m	95
300 m	80
600 m	70
1200 m	60
2000 m	50
3000 m	40
4000 m	30
6000 m	20
10000 m	10
20000 m	5

* If a channel (non-perennial river line) is gullied, the flow path length was reduced by a scale-cost distance factor of 0.5. For example, if the distance from a partially or potentially connected gully to a perennial junction is 100 m, and 50 m of latter channel is gullied, then a new scale-cost distance of 75 m was used.

Table 2: (*ii*) Slope rules applied to partially and potentially connected gullies when calculating sediment delivery rates.

Slope steepness (%)	Fraction sediment reaching perennial river junction (%)
>15	100
10-15	95
5-10	85
0-5	75

Table 3: (*iii*) Roughness rules applied to partially and potentially connected gullies when calculating sediment delivery rates.

Roughness index	Fraction sediment reaching perennial river junction (%)
<=0.05	100%
0.06	90%
0.07	80%
0.08	70%
0.09	60%
0.10	50%